AN EXTENDED MASS SPECTRAL STUDY OF N-SUBSTITUTED 2-PYRIMIDINONES AND 2-PYRIMIDINTHIONES

Eva Maria Kazdan

A Thesis
in
The Department
of
Chemistry

Presented in Partial Fulfillment of the Requirements
for the degree of Doctor of Philosophy at
Concordia University
Montreal, Québec, Canada

February, 1980

ABSTRACT

AN EXTENDED MASS SPECTRAL STUDY OF N-SUBSTITUTED 2-PYRIMIDINONES AND 2-PYRIMIDINTHIONES

Eva M. Kazdan, Ph.D.
Concordia University, 1980

Fragmentation patterns were obtained for the title compounds bearing on N_1 the substituents R=H, D, CH_3, CD_3, CH_2CH_3, CD_2CD_3, CH_2CD_3, CD_2CH_3, $CH(CH_3)_2$, $CD(CH_3)_2$, $CH(CD)_3$, $PhCH_2$, $PhCD_2$, Ph and Ph-2,4,6-d_3. The primary fragmentation pathways for both (O and S) series involve loss of CS (X=O or S) and loss of HCN. The main difference between the series is that whereas loss of SH* is significant for the thiones, loss of OH* from the oxygen analogues is not apparent. With increasing complex R the primary fragmentation pathways diminish in importance as other modes leading to more stable fragments become possible. For all compounds M-1 ions are significant. Studies based upon deuterium labelling and metastable transitions in the FFFR showed that the molecular ions of both series of compounds lose H* partly from the 4 or 6 postion of the pyrimidine ring and partly from the N-substituent. Intensities of those M-1 ions that originate by expulsion of H* from the N-substituent depend upon R and the heteroatom (S or O). Attention has been given to the M-1 ion of 1-ethyl-2-pyrimidinthione. It has been revealed that

the molecular ion expels hydrogen atom from three sites, namely from the pyrimidine ring, the methylene group and the methyl group. The approach to obtain more information about the postulated thiazolium ring structure which could result when the methyl group is affected by the loss, has been outlined. On the basis of the experimental measurements and literature study the problems associated with possible future research work are discussed.

TO THE MEMORY OF MY MOTHER AND MY FATHER

ACKNOWLEDGEMENTS

I wish to express my sincere gratitude to Dr. R.T. Rye for his instructions, help and guidance throughout the course of this study.

I would like to thank Dr. O.S. Tee for initiating this project as well as for his continued interest in this investigation and for the financial aid I recieved in the latter part of my studies.

Further I wish to thank Dr. J.L. Holmes for access to the MS-902 S mass spectrometer at the University of Ottawa and Dr. J. Krause for the technical assistance in the metastable peak measurements.

Finally I appreciate Dr. T.J. Adley's help and friendly approach to my problems at the beginning of my graduate studies.

TABLE OF CONTENTS

INTRODUCTION

Many substituted pyrimidines occur in nature and several of these play vital roles in the metabolism of living cells. Uracil(1), thymine(2), cytosine(3) and 5-hydroxymethylcytosine form part of some nucleosides. Ribotides of orotic acid(uracil-6-carboxylic acid) and dihydroorotic acid, are known to be intermediates in the biosynthesis of uracil[1].

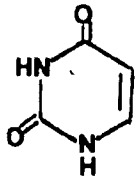

(1)

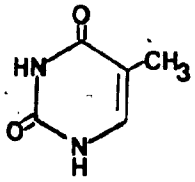

(2)

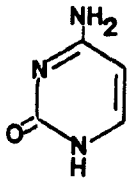

(3)

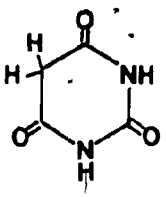

(4)

Some pyrimidines are biologically active and are widely used in medicine. For example, the barbiturates, which are derivatives of barbituric acid(4), are used as hypnotics. 2-Thiouracil was found to produce transient improvement in chronic granulocytic leukemia and its 6-alkyl derivatives are used to treat over-activity of the thyroid gland. The highly successful antimalarial agent, pyrimethamine, is 2,4-diamino-6-ethyl-5-p-chlorophenyl-pyrimidine, and the powerful oral diuretic, aminometradine, is 1-allyl-3-ethyl-6-aminouracil[1].

Undoubtedly, the biological importance of the substituted pyrimidines stimulated the wide spread attempt

of many chemists to obtain more information about their structure and reactivity[2].

Nucleosides are base-sugar units of nucleic acids, where the bases contain pyrimidine and purine ring system. The chemistry of nucleic acids is highly complex. It is not exactly known how many different nucleic acids there are, or in what sequences the pyrimidines and purines are arranged.

The mass spectra of substituted pyrimidines can serve as useful models with which the spectra of chemically or biologically altered pyrimidines can be compared to assist in the structure elucidation.

I - REVIEW OF PERTINENT LITERATURE

Mass spectra of compounds containing the pyrimidine ring were first obtained by Bieman and McCloskey[3], who studied the naturally occurring nucleosides by time of flight mass spectroscopy. The main fragmentation occurs at the bond between the heterocyclic base and the sugar moiety with accompanying transfer of one or two hydrogens to the base. These hydrogen atoms appear to originate from the hydroxyl hydrogens of the sugar, judging from mass spectra of the deuterated compounds. Peaks occur also at m/z values corresponding to (base + 30) and $(M^{+\cdot} - 89)$. The fragmentation pattern of uridine(I-5) is a typical example for this class of compounds(Scheme I-1).

The mass spectra of the important pyrimidine derivatives uracil(I-1), thymine(I-2), cytosine(I-3) and some N-methyl-uracils have been determined by Rice et al.[4]. The main fragmentation pathway of uracil is loss of HNCO by "retro-Diels-Alder" cleavage, followed by expulsion of HCN to form a ketene odd electron ion at m/z 42:

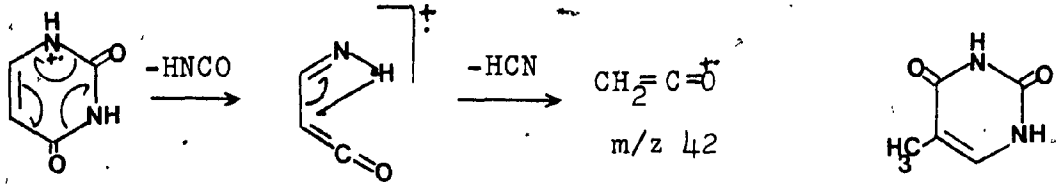

(I-1) (I-2)

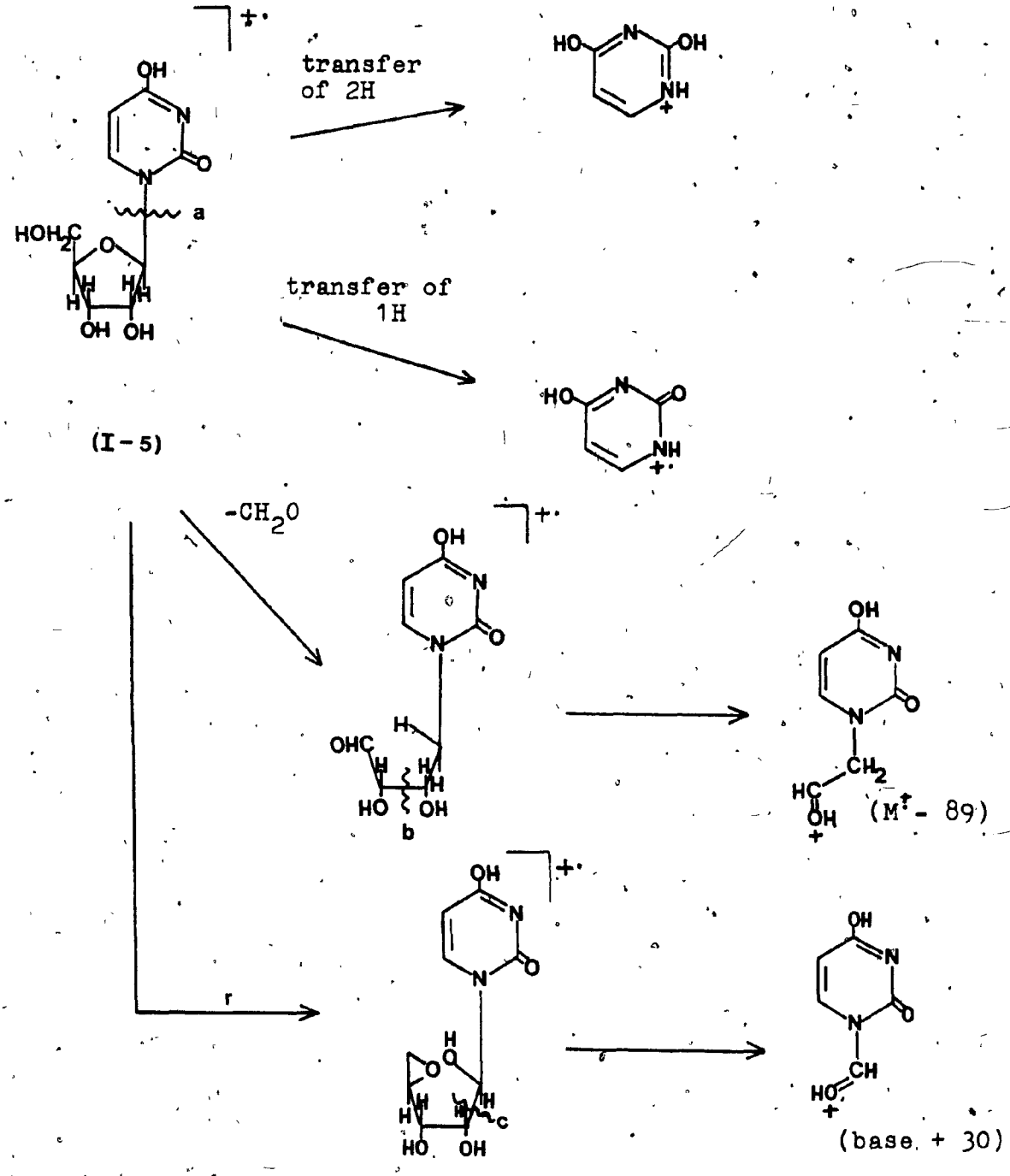

Scheme I-1

Thymine follows the same fragmentation pattern, while the mass spectrum of cytosine is much more complex. It is characterized by three distinct fragmentation pathways, namely loss of NH_2 radical, loss of CO and loss of HNCO from the parent ion. Of interest is the expulsion of carbon monoxide from the molecular ion, which does not occur significantly with the two dioxygenated compounds:

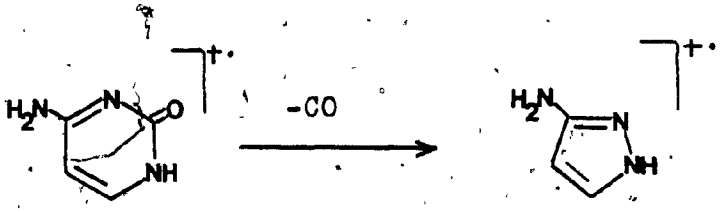

(I-3)

The spectrum of 1,3 -dimethyl-uracil is characterized by a molecular ion peak at m/z 140 and intense fragment ion peaks at m/z 83,55, and 42 corresponding to loss of CH_3NCO, CO and ketene radical according to the following scheme:

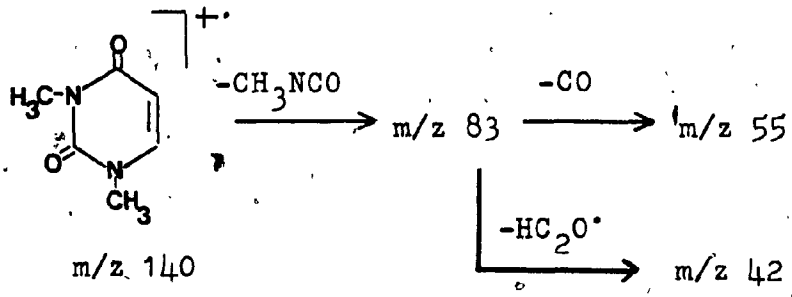

Kato et al.[5] studied the mass spectra of alkyl, phenyl, and chloropyrimidines and showed that prior to further fragmentation there are two intermediate ions (a and b), formed by α-cleavage:

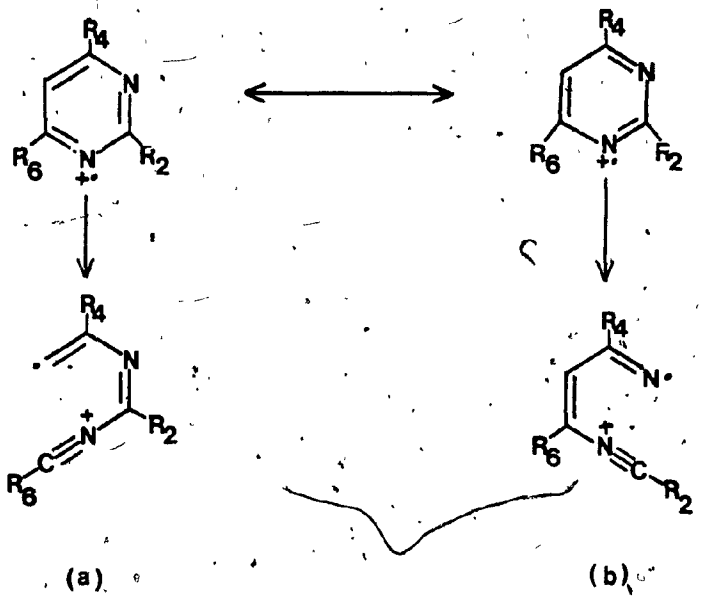

(a) (b)

The authors investigated mass spectra of eleven related compounds, having chloro, alkyl, and phenyl groups substituted for R_2, R_4 and R_6 in various combinations. It was observed that further fragmentation of the intermediates depends on their structures and on the character and position of the substituents.

Nishiwaki et al.[6] studied the mass spectrum of 2-amino-4-phenyl-6-methylpyrimidine(I-4). The molecular ion at m/z 185, which is the base peak and amounts to 32% of the total ion current, loses hydrogen, giving rise to a very intense ion at m/z 184. This is an unexpected feature since for 2-amino-4,6-dimethylpyrimidine the two main fragments are due to loss of HCN and probably CH_3CN from the molecular ion[6]. The fact that the spectrum of N, N,5-d_3-2-amino-4-phenyl-6-methylpyrimidine also displays a very prominent M-1 ion signifies that the phenyl ring is

involved in loss of the hydrogen. A hydrogen in the methyl group will not be affected in view of the behaviour of 2-ethylpyridine[7]. The particular M-1 ion may well be the following cyclic ion(I-4a), the formation of which would be an example of cleavage γ to a heterocyclic nitrogen:

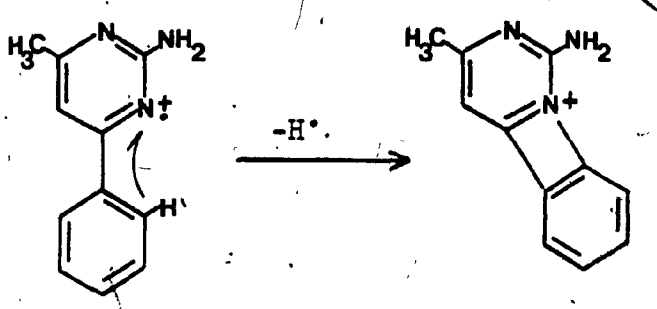

m/z 185 m/z 184

(I-4) (I-4a)

The only previous study of hydroxy-pyrimidines seems to be that of 4-hydroxy-6-methylpyrimidine(I-6). The mass spectrum of this compound showed little loss of HCN from the molecular ion but marked loss of CO[8]. This is most conveniently formalized as arising from the keto form of the molecular ion, and the resultant species(m/z 82) can be written as the open-chain ion or the imidazole ion. Loss of 40 mass units from m/z 82 produces the intense ion at m/z 42, and it has been suggested that the neutral fragment is methylacetylene:

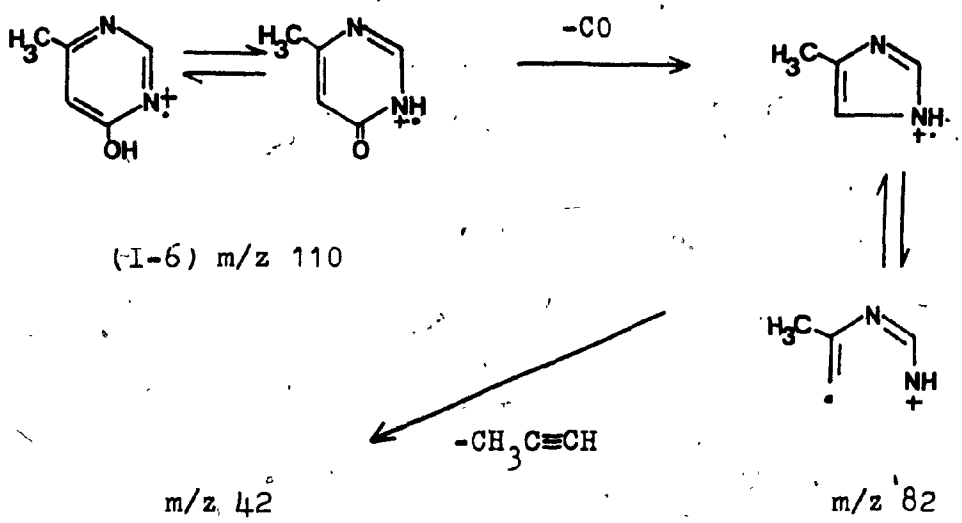

(I-6) m/z 110

m/z 42

m/z 82

Hvistendahl et al.[9] studied mass spectra of some dihydrothiazolopyrimidinium salts and zwitterions. The investigated compounds undergo structural or electronic rearrangement prior to evaporation in the mass spectrometer to become covalent. Of some interest to our study is the spectrum of I-7, where thermal decarboxylation first occurs with

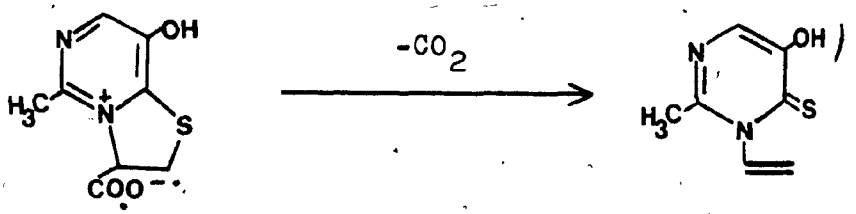

(I-7)

(I-7a)

ring opening to form the N-vinylthione(I-7a), which forms the molecular ion at m/z 168. The ion expels hydrogen to yield a thiazolopyrimidinium cation at m/z 167, which is the base peak. The second fragmentation pathway is loss of acetylene from the molecular ion to form a peak at m/z 142, which probably proceeds via McLafferty rearrangement:

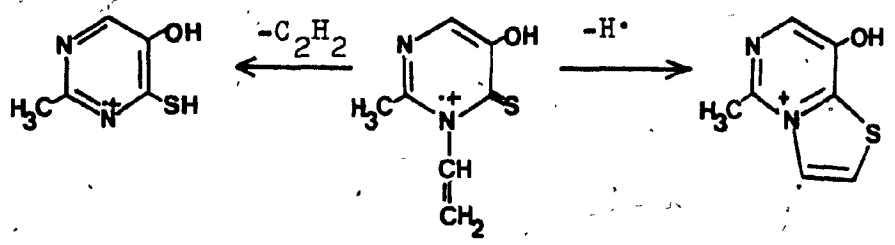

m/z 142 m/z 168 m/z 167

Another interesting spectrum is that of I-8, where first nucleophilic substitution by the anion takes place with opening of the thiazoline ring to form I-8a:

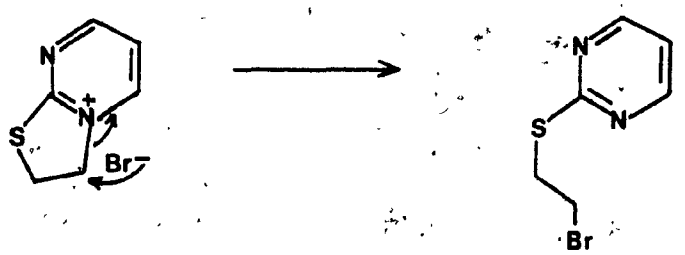

(I-8) (I-8a)

The molecule I-8a, upon electron impact, fragments as shown in the scheme below.

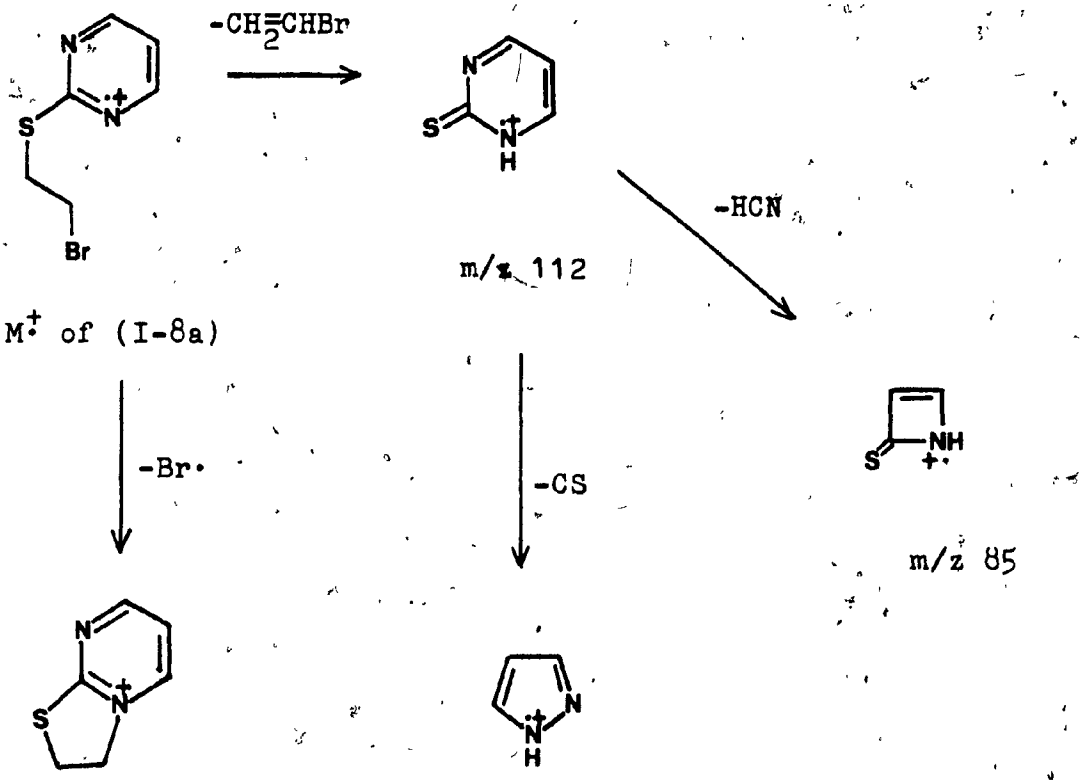

Substituted alkylthio-uracils were investigated by Wyrzykiewicz et al.[10]. Fragmentation pattern of twelve derivatives of I-9 was determined with different combinations of R substituents. It has been found that on the basis of the fragmentation patterns the position of uracil ring thiation may be deduced. The major fragmentation

is due to the cleavage of the $C_{sp^3}-C_{sp^3}$ and $S-C_{sp^3}$ bonds of the S-alkyl groups.

$\underline{R_3}$ and $\underline{R_4}$ = $\underline{S\text{-}i\text{-}C_3H_7}$, $\underline{S\text{-}n\text{-}C_4H_8}$ or $\underline{OH}$

$\underline{R_1}$ and $\underline{R_2}$ = $\underline{CH_3}$ or $\underline{H}$

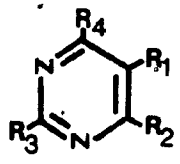

(I-9)

II - STATEMENT OF OBJECTIVE OF THE PRESENT WORK

The present work investigates the electron impact fragmentation of another important series of pyrimidines, the N-substituted 2-pyrimidinones(II-1) and their 2-thio-homologues(II-2).

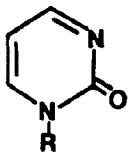

(II-1)

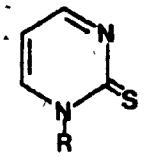

(II-2)

R =	
	H
	CH_3
	CH_2CH_3
	$CH(CH_3)_2$
	CH_2Ph
	Ph

R =	
	H
	CH_3
	CH_2CH_3
	-
	-
	Ph

The compounds were chosen in order to study influence of the various N-substituents on the fragmentation of the oxo- or thio- pyrimidine ring and to investigate possible correlations between the behaviour of the oxygen and sulfur analogues.

Their fragmentation patterns have been outlined in the author's M.Sc. thesis[11]. However, the processes proposed therein were very often based on mere intuition. To identify more closely the origin of the major fragments, the following labelled compounds were synthesized and their mass spectral fragmentation compared with that of unlabelled homologues.

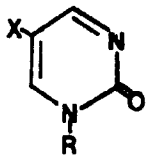

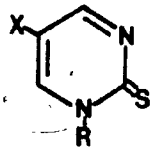

X = H	X = D	X = H	X = D
R= D	R= H	R= D	R= H
CD_3	CH_3	CD_3	CH_3
CD_2CD_3		CD_2CD_3	
$CH(CD_3)_2$		CH_2CD_3	
$CD(CH_3)_2$		CD_2CH_3	
$PhCD_2$			
Ph-2,4,6-d_3		Ph-2,4,6-d_3	

Only the main fragmentation processes giving rise to the ions in high m/z region were examined. The corresponding dissociations in the first field free region were investigated using the techniques described in the experimental section.

Attention is given to justify the proposed structures of the M-1 ions. In order to do this, the appropriate metastable processes were analyzed and kinetic energy releases were measured from the metastable peak shapes. Attempts to obtain ΔH_f of the M-1 ions were made on the basis of their appearance energy measurements.

The previously unknown 2(1H)-pyrimidinselenone

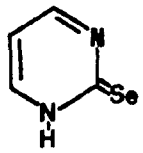

was made in order to compare the behaviour of selenium with the same group elements oxygen and sulphur, under the same circumstances.

III - THEORY SECTION

Basic theory of the mass spectrometry with ion fragmentation mechanism and interpretation of the mass spectra was explained in the previous study[11]. This section deals with the theory relevant to a metastable transition and ion structure determination[12].

THE MAIN ION BEAM

In the ionization chamber of a mass spectrometer ions are produced from a compound by bombarding the molecules of the compound with a mono-energetic beam of electrons. The mass spectrometer then separates these ions according to their mass-to-charge ratios by the action of electric and magnetic fields. The ions leave the ionization chamber under influence of the repeller electrodes and have relatively little kinetic energy, ~1eV. Outside the ionization chamber they are accelerated by the action of a strong electric field, corresponding to a potential drop of several thousand volts over a distance of the order of 1cm. In order to keep the relatively small energy spread of the original ion beam, high accelerating voltages, up to 10kV are used, so that the kinetic energy of all ions will be the same. The kinetic energy of an ion of mass m and charge e accelerated through a potential drop V is given by

equation (1), where v is the terminal velocity. The beam of

$$mv^2/2 = eV \qquad (1)$$

ions that have a kinetic energy equal to the full accelerating energy is known as the main ion beam.

If the energy of the bombarding electrons is just sufficient to ionize the molecule, only the molecular ion appears in the spectrum. If the electron-beam energy is increased the molecular ion can be formed with excess electronic and vibrational energy which can be high enough to enable fragmentation of the molecular ion.

METASTABLE IONS IN NORMAL MASS SPECTRA

Not all fragmentation processes take place in the source of a mass spectrometer. Some ions, called metastable ions, will decompose during passage between the source and the collector units in the spectrometer. Of special interest are the ions that decompose in the field-free region in front of the magnetic sector and those that decompose in front of the electric sector of a double-focusing mass spectrometer(Fig. III-1) in the so called first field free region. Hipple et al.[13] have shown that for the process

$$m_1^+ \longrightarrow m_2^+ + \text{neutral fragment},$$

the metastable peak is observed at mass m^* which is related

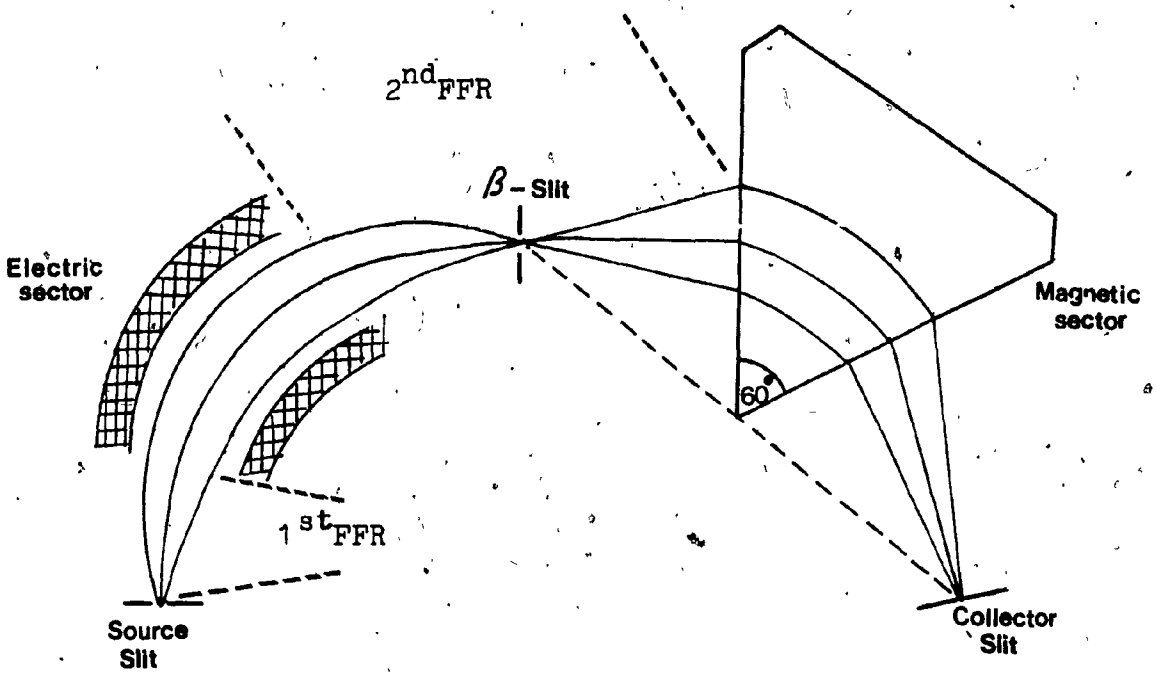

Fig. III-1

to m_1 and m_2 by the equation (2).

$$m^* = m_2^2/m_1 \qquad (2)$$

The velocity of the metastable ion m_1 entering the second field-free region is given by eqn, (1) as

$$v = (2eV/m_1)^{1/2} \qquad (3)$$

After the metastable transition, the product ion m_2 will have momentum

$$m_2 v = m_2(2eV/m_1)^{1/2} \qquad (4)$$

The radius followed by these ions in the magnetic sector is given by equation (5), where B is the magnetic field strength

$$r = m_2 v/Be \qquad (5)$$

After substitution for velocity from equation (3)

$$r = \frac{m_2}{Be} (2eV/m_1)^{1/2}$$

Thus

$$m_2^2/m_1 e = m^*/e = B^2 r^2/2V \qquad (6)$$

The daughter ions m_2^+ are transmitted through the magnetic sector with an apparent mass m^*, equal to m_2^2/m_1, eqn.(2).

FRAGMENTATION IN THE FIRST FIELD FREE REGION (FFFR)

Ions that decompose in front of the electric sector will not be observed in a conventional mass spectrum. Under normal operating conditions, only ions having the full acceleration energy will be transmitted through the electric sector. Decomposition in the FFFR can be detected by special defocusing methods that involve scanning either the electric sector voltage or the accelerating voltage.

The kinetic energy of the ions transmitted along the central path through the electric sector is

proportional to the electric sector voltage. The daughter ions m_2^+ arising from fragmentations ocurring in the FFFR will be unable to pass through the electric sector of the double focusing mass spectrometer. They will have lower kinetic energy, since upon fragmentation the initial kinetic energy of the main beam, $\frac{1}{2} m_1 v^2$, will be shared between the ionic and neutral fragments. In order to detect the ions m_2, it is necessary to lower the voltage across the electric sector by a fraction m_2/m_1 of the value at which ions that carry the full accelerating energy are transmitted. If E_1 is the voltage at which the daughter ions m_2 of the metastable transition are to be seen and E is the voltage corresponding to the main beam, then

$$E_1 = m_2 E/m_1 \qquad (7)$$

The other method, by which the above m_2 ions can be transmitted through the electric sector, is to keep the electric sector voltage fixed at the normal value E but to increase the main accelerating voltage from its normal value V to a new value V_1 and thus bring the m_2 ions to a kinetic energy equal to the full accelerating energy of the main beam. The daughter ion m_2^+ will pass through the electric sector if

$$V_1 = V m_1/m_2 \qquad (8)$$

KINETICS OF THE FRAGMENTATION

Figure III-2 illustrates the time scale of the mass spectrometer, an essential consideration in ion kinetics. Data refer to ions of mass 100 in the Hitachi RMH-2 mass spectrometer operating at an ion-accelerating voltage of 10 kV[14].

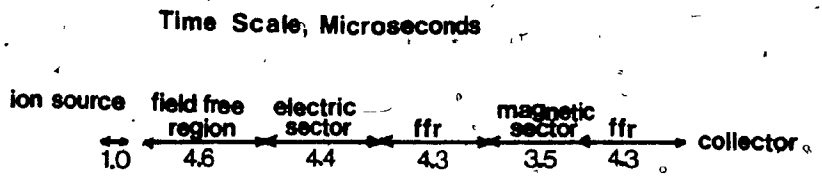

Fig. III-2

The fragmentation processes occurring in most analytical mass spectrometers follow first order kinetics. Such unimolecular decompositions require first, the formation of the activated complex(Fig. III-3),which is the result of the accumulation of sufficient energy in the appropriate vibrational and rotational modes and, secondly, the achievement of the appropriate geometry. The condition for an ion $ABCD^{+\bullet}$ to form an activated complex is that the ion possesses at least the activation energy for the process in question. The greater the internal energy the greater the probability that it will be correctly distributed for the decomposition and the faster the unimolecular reaction. The second condition for activated complex formation, appropriate geometry, requires time. In general the more similar the reactant and transition state geometries, the faster the reaction. Therefore simple bond cleavage will

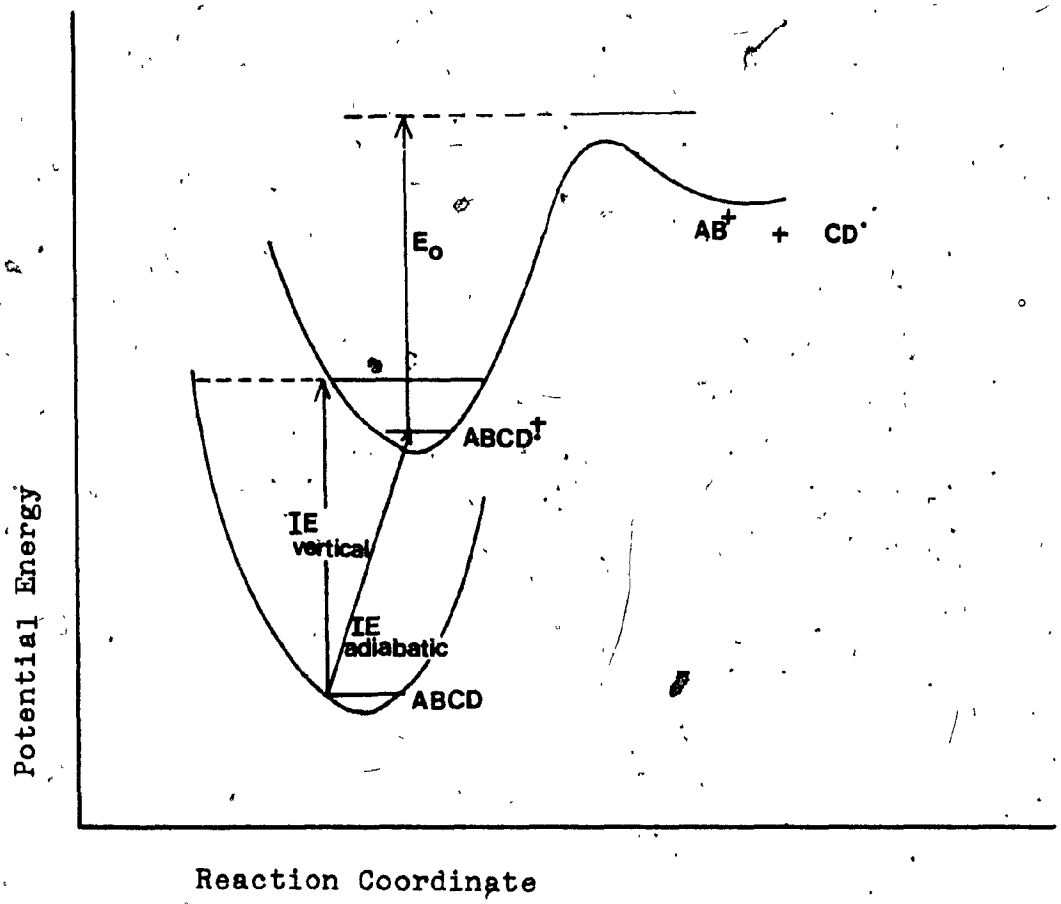

E_o .....activation energy

IE .....ionization energy

Appearance energy of $AB^+(AE) = IE_{adiabatic} + E_o$

Fig. III-3

proceed faster than elimination or rearrangement reactions or other processes of comparable energies. The slow reactions that give rise to the metastable peaks are more often due to rearrangement processes. The abundance of a fragment ion and a metastable ion formed from a molecular ion in a mass spectrmeter depends on the rate constant for the unimolecular reaction K(e), and on the probability of the internal energy distribution P(e). Metastable ions that decompose in a field free region of the mass spectrometer arise from reactions having rate constants approximately 10^5 to 10^6 sec^{-1}. The approximate formula for the calculation of the constant K(e) is the following[15]:

$$K(e) = \nu(E-E_o/E)^{s-1} \qquad (9)$$

ν .....frequency factor

E .....internal energy of the reacting ion

E_o .....activation energy

s .....number of vibrational degrees of freedom

If the molecules ABCD(Fig. III-3) are submitted to 70eV electron bombardment, the produced molecular ions $ABCD^{\cdot+}$ will have a variety of internal energy values. The probability function P(e) is a description of the internal distribution of a reacting ion, in this case, molecular ion $ABCD^{\cdot+}$.

RELEASE OF KINETIC ENERGY

The internal energy of the ionized molecule may be classified as either "fixed" or "non-fixed" in the activated complex. Figure III-4 illustrates the relationship between these quantities. The non-fixed energy $E^{\ddagger}$ corresponds to the difference between the internal energy E and the forward activation energy E_o. The term kinetic shift refers to a particular value of $E^{\ddagger}$ which is just sufficient to cause detectable fragmentation in the ion source (see Fig. III-2). It is thus some excess energy above the activation energy E_o necessary for a molecular ion $M^{+\cdot}$ to produce detectable fragment ions in a conventional mass spectrum.

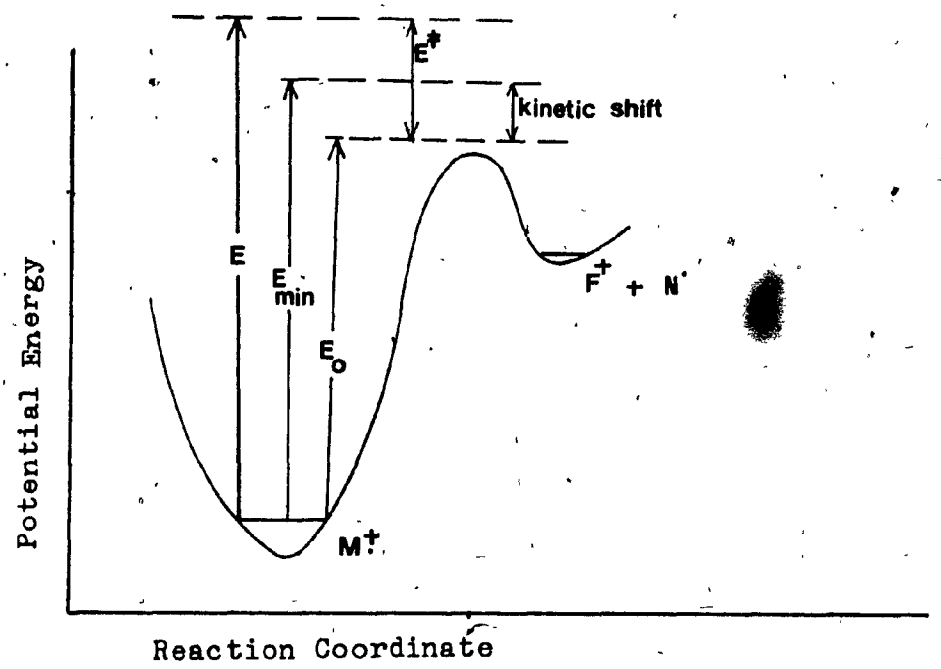

Fig. III-4

Kinetic shift is of importance to metastable ion decomposition since the average nonfixed internal energy of a metastable ion is not much in excess of E_o, that is, E^* is small.

As pointed out before, metastable peaks are diffuse. The diffuse nature of the peaks is due almost entirely to conversion of internal energy into kinetic energy of separation of the fragments. The kinetic energy T, released in the decomposition of a metastable ion, can arise from two separate sources(Fig. III-5). The excess

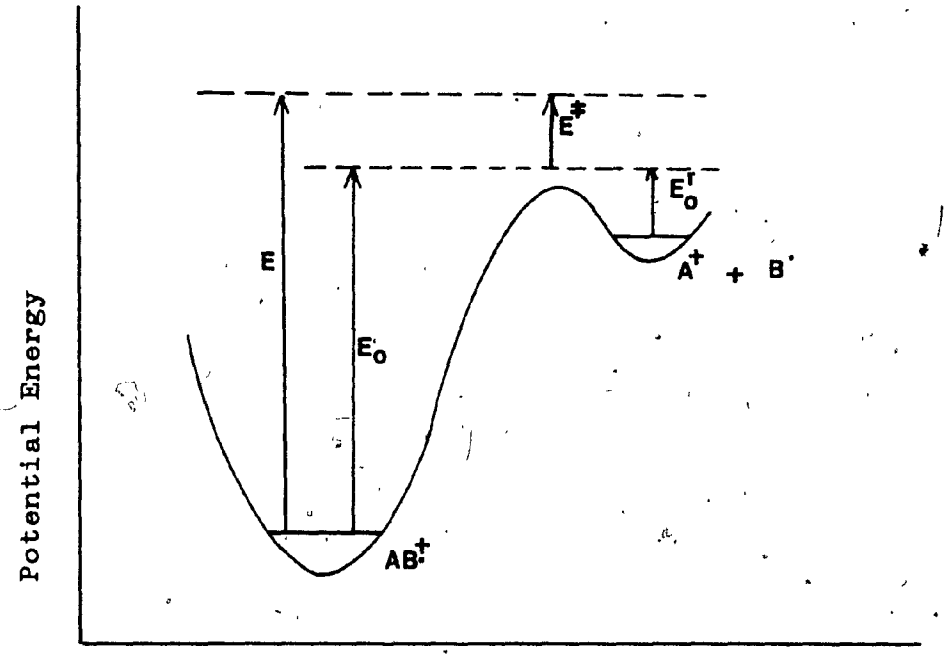

Fig. III-5

energy E^* of the activated complex which is available for statistical partitioning between the internal energies of the products and translational energy of their separation, and the reverse activation energy E_o^r which is also partitioned but not equipartitioned between the dissociation mode and other degrees of freedom.

Knowledge of the kinetic energy release is significant in the consideration of an ion structure characteristic. In the present work the accelerating voltage scan method was used, to determine the release of kinetic energy, T, occurring in the field-free region between the source and the electrostatic analyser. The calculation of T considers a metastable ion of mass m_1, carrying x charges, that fragments to give a fragment m_2, carrying y charges and a neutral fragment of mass m_3. The relationship between kinetic energy release T and peak width, ΔV, in an accelerating voltage scan spectrum is then[12]

$$T = \frac{x^2 m_2^2 eV\, \Delta V^2}{16 y m_1 m_3 \bar{V}^2} \qquad (10)$$

In arriving at equation (10) Beynon et al.[12] showed that the maximum and minimum possible velocities v_2 of the daughter ions m_2 travelling in the original direction of motion of the ions m_1 are

$$v_2(max) = v_1 + (2m_3T/m_1m_2)^{1/2} \quad \text{and} \quad v_2(min) = v_1 - (2m_3T/m_1m_2)^{1/2}$$

Thus the effect of a release of internal energy during a metastable transition is to cause the ion of mass m_2 to be given a velocity increment additional to that of the original ion of mass m_1 and velocity v_1. The kinetic energy of these m_2 ions is

$$\begin{aligned}\tfrac{1}{2}m_2v_2^2 &= \tfrac{1}{2}\, m_2\left[v_1 \pm (2m_3T/m_1m_2)^{1/2}\right]^2 \\ &= \tfrac{1}{2}m_2v_1^2\left[1 \pm (2m_3T/m_1m_2v_1^2)^{1/2}\right]^2 \\ &= \tfrac{1}{2}m_1v_1^2\,\frac{m_2}{m_1}\left[1 \pm (m_3T/m_2xeV)^{1/2}\right]^2 \\ &\qquad\qquad (\text{since } \tfrac{1}{2}m_1v_1^2 = xeV) \\ &= xeV\,\frac{m_2}{m_1}\left[1 + m_3T/m_2xeV \pm 2(m_3T/m_2xeV)^{1/2}\right] \qquad (11)\end{aligned}$$

The radius of curvature of this daughter ion in a magnetic sector is given by

$$r = m_2v_2/Hey \qquad (12)$$

Upon combination of equation (11) and (12) and rearranging, the extreme spread of the metastable peak in mass units is

$$d = (4xm_2^2/y^2m_1).(m_3T/m_2xeV)^{1/2} \text{ or } T = y^4m_1^2d^2eV/16xm_2^3m_3$$

The maximum fractional spread of energy of the daughter ions m_2 can be expressed as a fraction $\Delta V/V$ if the high voltage scan method is used. To a close approximation,

$$\Delta V/V_1 = 4(m_3T/m_2xeV)^{1/2} \qquad (13)$$

where V_1 is the accelerating voltage corresponding to the center of the peak and ΔV is the range of HV values the peak is observed.

From equation (13)

$$T = (xm_2eV_1/16m_3) \cdot (\Delta V/V_1)^2 \qquad (14)$$

Since $V_1 = (m_1y/m_2x)V$,

$$T = (x^2m_2^2eV/16ym_1m_3) \cdot (\Delta V/V)^2 \qquad (10)$$

ENERGY RELEASE AS AN ION STRUCTURE CHARACTERISTIC

The use of kinetic energy (T) released in metastable ion fragmentation as an ion structure parameter was initiated by McLafferty and co-workers[16]. These authors examined the decomposition of $C_2H_5O^+$ ions arising from different precursor molecular ions by secondary fragmentation. It was suggested that the identical T values observed in the metastable decomposition of $C_2H_5O^+$ ions generated from various precursors imply a common transition state for the fragmentation. This proposal is supported by the observation that the metastable peak shape and intensity was independent of the precursor ion used to generate $C_2H_5O^+$. Since the metastable peak usually arises from a particular decomposition reaction, the ions identical in energy that exhibit identical decomposition reactions have identical structure. However, as pointed out by the authors,

metastable transitions occur with a relatively narrow range of rate constants of 10^5 to 10^6 sec^{-1} (see p.22), so that the measurements of the metastable reactions represents only a small sample of the total internal energy distribution of the $C_2H_5O^+$ ion.

Application of this method was limited for several years by the fact that most reactions occur with small energy releases and T could not be reliably measured.

Energy releases of less than one milli-electron volt were first measured by Beynon et al.[17] in 1970 who used ion kinetic energy spectroscopy(IKES),which involves the variation of the electric sector voltage(cf.p.19).

In 1972 Beynon et al.[18] studied the effect of experimental conditions and methods of ion preparation upon the measured energy release. The authors concluded that the kinetic energy release accompanying unimolecular metastable ion fragmentation shows only a small dependence on such parameters as source temperature, ion-source residence time and acceleration voltage. Molecular ions formed by electron impact have been found to release slightly less kinetic energy on fragmentation then the corresponding ions formed via a fragmentation sequence. These variations in energy release with ion origin do not prevent a valid comparison of ion structures.

From the above study and references therein[18] it is apparent that the kinetic energy released by metastable ions is a characteristic of ion structure and

is approximately independent of internal energy. This is particularly so when the kinetic energy release is large. Even when it is small and due not to the reverse activation energy but to the partitioning of the non-fixed energy of the activated complex $E^{\ddagger}$, variations in $E^{\ddagger}$ have a relatively small effect upon T, since the mass spectrometer selects metastable ions having a relatively small and well defined range of internal energies. Thus, provided the reverse activation energy E_o^r is at least a few tenths of an electron volt, the manner in which it is partitioned can be determined.

The importance of energy partitioning in studying ion structure and reaction mechanism has been demonstrated in numerous studies, and it has been suggested[19] that a large fraction of the excess energy($E^{\ddagger} + E_o^r$) is partitioned into translational energy of the products when a cyclic activated complex of small ring size is involved.

Cooks et al.[20] measured the kinetic energy release accompanying H· loss from $C_7H_8^+$ ion, generated from different compounds. The results are so similar, as shown in Table III-1, that it is believed that the reactive ions have a common structure. Furthermore the authors studied the energy partitioning behaviour for this reaction, considering cycloheptatriene as the reactant and taking the appropriate heats of formations and appearance energies from the literature:

Kinetic energy release for $C_7H_8^{\cdot+} \longrightarrow C_7H_7^{+} + H\cdot$

Compound	T(eV)
Benzyl methyl ether	0.17[2]
Tropyl methyl ether	0.17[3]
p-Methylanisole	0.17[2]
m-Methylanisole	0.17[1]
o-Methylanisole	0.17[4]
n-Butylbenzene	0.17[1]
Cycloheptatriene	0.17[5]
Toluene	0.17[2]

Table III-1

$\Delta H_f(C_7H_7)^+$ = 9.06 eV(ionization energy of cycloheptatrienyl radical plus ΔH_f cycloheptatrienyl radical),

$AE(C_7H_7)^+_{\text{cycloheptatriene}}$ = 10.45 eV,

ΔH_f(cycloheptatriene) = 1.88 eV, and

$\Delta H_f(H\cdot)$ = 2.26 eV.

The thermochemical relationship for the reaction is

$$AE(C_7H_7)^+ + \Delta H_f(C_7H_8) = \Delta H_f(C_7H_7)^+ + \Delta H_f(H\cdot) + E_{excess},$$

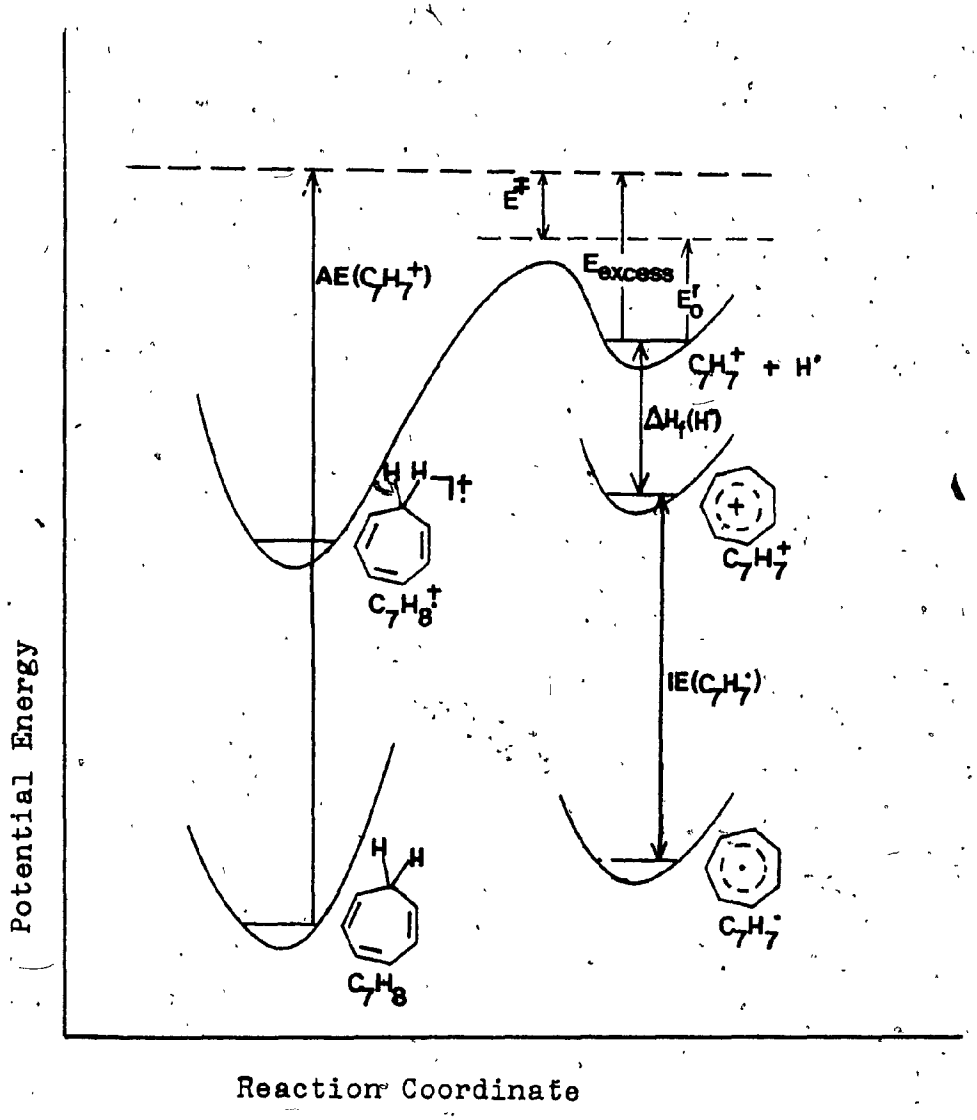

Fig. III-6

and therefore

E_{excess} = 10.45 + 1.88 - 9.06 - 2.26 = 1.01 eV (cf. Fig III-6).

For an E_{excess} value of this magnitude, the approximation $E_{excess} \approx E_o^r$ is valid[20]. It follows that in this simple cleavage reaction only 18% of the reverse activation energy is partitioned as translational kinetic energy.

ISOTOPE EFFECTS

Another criterion that can provide information on ionic reaction mechanism and ionic structures is the effect or isotopic substitution either on metastable peak abundances or upon kinetic energy release.

The isotope effect k_H/k_D is given by the relative abundances of the $(M-H)^+$ and $(M-D)^+$ product ions(Fig.III-7). k_H/k_D for different H° loss metastable ion reactions can vary, using the same instrument and the same experimental conditions, from 1.9 for benzene to >1000 for isobutane[20]. It has been suggested that these differences are directly related to the differences in the non-fixed energy E^* of the activated complexes $(M-D)^+$ and $(M-H)^+$ as illustrated.

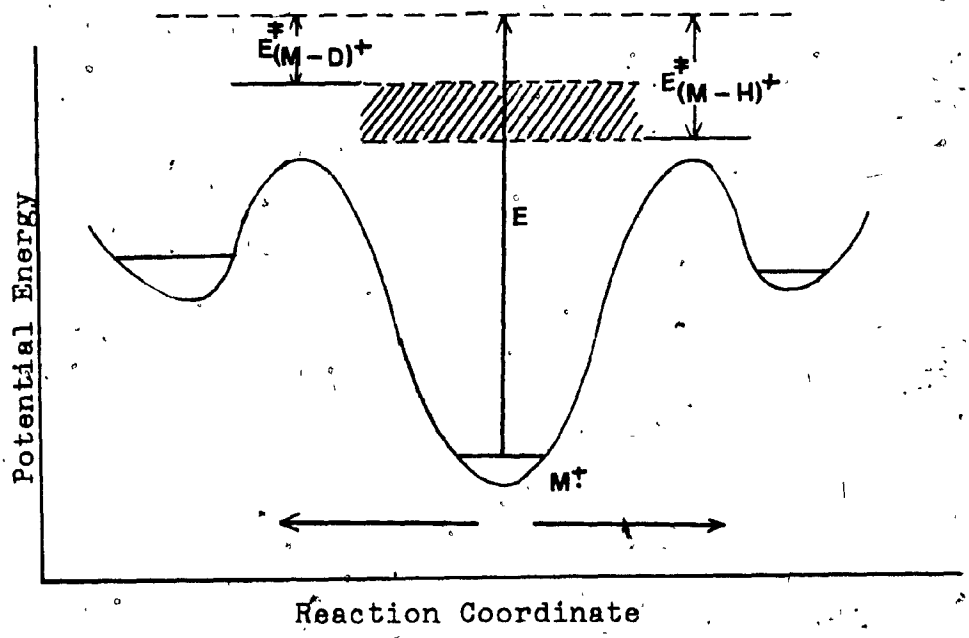

Fig.III-7

in Fig.III-7, where single molecular ion $M^{\cdot+}$ is considered to lose $D^{\cdot}$ or $H^{\cdot}$. Because of the differences in zero-point energies associated with C-H and C-D bonds the non-fixed energy $E^{\ddagger}$ of the activated complex for $H^{\cdot}$ loss is greater than for $D^{\cdot}$ loss. As the internal energy E increases, the ratio of $E^{\ddagger}_{(M-H)^{+}}$ to $E^{\ddagger}_{(M-D)^{+}}$ will decrease and k_H/k_D will approach unity. Thus, reactions possessing rate constants which increase rapidly with internal energy E, give a large isotope effect while in the processes where the rate increases slowly, the k_H/k_D approaches unity, as indicated in Fig.III-8a and b respectively. Furthermore it is apparent from Fig.III-8b that ions of internal energy such that $H^{\cdot}$ loss has a rate constant corresponding to metastable ion fragmentation, undergo $D^{\cdot}$ loss with a rate constant which is only a little smaller. On the other hand, for reaction illustrated in Fig.III-8a the rate constants for $H^{\cdot}$ and $D^{\cdot}$ loss differ by much greater factor.

The isotope effect upon kinetic energy release has been also observed and it has been suggested[21] that $H^{\cdot}$ loss should give $T_H/T_D \approx 1$. Table III-2 shows some experimental data. The results indicate that the above postulate is valid even when two different isotopically substituted compounds are used to follow $H^{\cdot}$ and $D^{\cdot}$ loss, e.g. toluene and d_8-toluene. However, not enough evidence has been provided to draw any general conclusions from these and other isolated results.

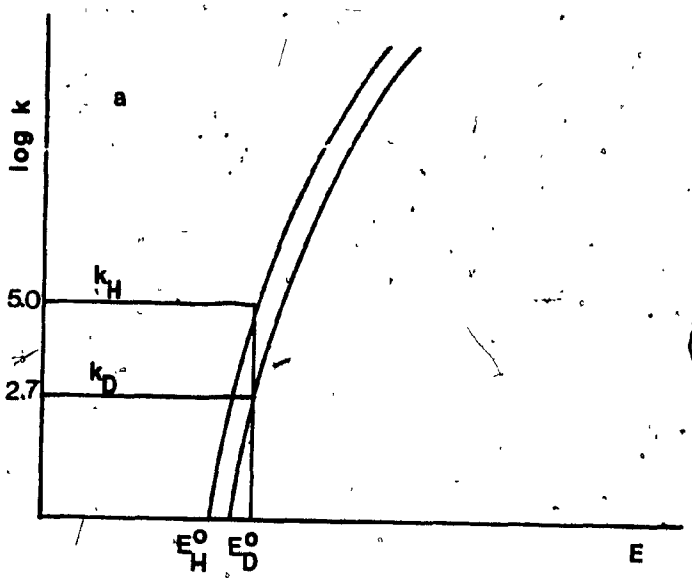

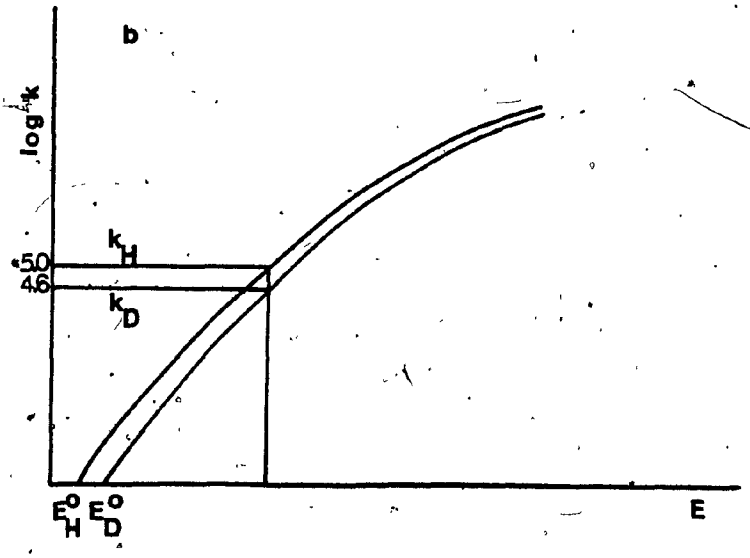

Fig. III-8

The results can be understood by reference back to Fig.III-7, where the same molecular ion can lose either H· or D· by simple C-H(D) bond cleavage. The potential energy surface is symmetrical about the molecular ion configuration and only differences in zero-point energies are of concern. The simplification is made that the internal energy distribution appropriate to fragmentations in the field-free region can be represented as a single discrete value. The two sets of products $(M-H)^+ + H\cdot$ and $(M-D)^+ + D\cdot$ differ only in zero-point energies of ions, the former being lower by approximately 1 kcal.mole^{-1}.

Kinetic energy released in H·(D·) elimination reactions

Compound	Reaction	T_H(meV)	T_D(meV)	T_H/T_D
Toluene	$M^+ - H\cdot$	160	-	> 0.93
d_8-Toluene	$M^+ - D\cdot$	-	175	
o,o'-d_2-Toluene	$M^+ - H\cdot(D\cdot)$	175	183	0.96
α-d_3-Toluene	$M^+ - H\cdot(D\cdot)$	171	176	0.97
ring-d_5-Toluene	$M^+ - H\cdot(D\cdot)$	171	180	0.95
Benzene	$M^+ - H\cdot$	60	-	> 0.94
d_6-Benzene	$M^+ - D\cdot$	-	64	
d_5-Benzene	$M^+ - H\cdot(D\cdot)$	60	60	1.00
CH_3OH	$M^+ - H\cdot$	5.7	-	> 0.93
CD_3OH	$M^+ - D\cdot$	-	6.1	
CH_3OCH_3	$M^+ - H\cdot$	3.6	-	> 0.9
CD_3OCD_3	$M^+ - D\cdot$	-	4.1	

Table III-2

The two activated complexes differ in that one(in which H· is lost) retains a C-D bond, the other retains a C-H bond. These particular bonds, whether C-D or C-H, may be a little stronger or a little weaker in the activated complex than in the products and, hence will tend either to make the difference in zero-point energies of the two activated complexes slightly greater than or slightly less than the difference in zero-point energies of two sets of products. Thus $E_o{}^r(M\text{-}H)^+ \cong E_o{}^r(M\text{-}D)$, i.e. $T_H/T_D \cong 1$[21].

The above discussion does not cover cases where T is largely due to the non-fixed energy $E^{\ddagger}$ of the activated complex. In such cases the ratio of T_H/T_D will depend on the internal energies of the metastable ions. If a single molecular ion is considered to lose H· or D·, then $E^{\ddagger}$ for loss of H· should be greater than for loss of D·(Fig.III-7) and $T_H > T_D$. The magnitude of the isotope effect will again be dependent upon the rate of increase of k with E. However, the excess energies for the two reactions will differ marginally if sampling over the appropriate distribution were different for the two cases.

IONIZATION AND APPEARANCE ENERGIES

Appearance and ionization energies in electron impact mass spectrometry are related to the energies of the electron beams which are required to produce the ions in the mass spectrometer. A plot of ion current against electron energy is known as the ionization efficiency

curve(cf. Fig. III-9). The threshold electron voltage is termed the appearance energy of the particular ion. The energy at which molecular ions first appear is called the ionization energy. The initial curved portion is due mainly to the energy spread of the bombarding electrons. Because of this energy spread in the electron beam at the threshold it is not possible to determine directly the absolute value of the electron beam energy at which ions are first produced. Consequently ionization and appearance energies are determined by comparing the ionization efficiency curve of the unknown sample with that of a standard substance, usually an inert gas, whose ionization potential is accurately known. The greatest source of error in measuring ionization and appearance energies is in the determination of the origin of the ionization efficiency curves since the curves approach the abscissa asymptotically. A common method to overcome the difficulty is to plot ion abundance on a logarithmic scale against electron volts both for the internal

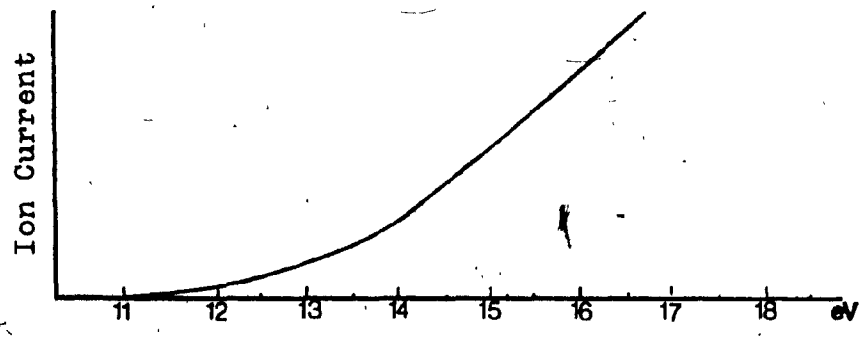

Fig. III-9

standard and for the sample. If the two curves are essentially parallel, the difference in appearance energies can be determined as the current falls towards zero.

HEAT OF FORMATION OF GASEOUS IONS[39]

Ionization and appearance energies can be used to determine the heats of formation of gaseous ions and thus give information about the ions characteristic. For example, an ion $C_2H_5O^+$ can be generated from methyl ethers and secondary alcohols, but it is not known whether these ions have the same structure. The appearance energy for $C_2H_5O^+$ generated from dimethyl ether is 10.70eV (247 kcal/mole). The literature values for $\Delta H_f(CH_3OCH_3)$ = -44 kcal/mole and $\Delta H_f(H^\cdot)$ = 52 kcal/mole. Thus

$$\Delta H \text{ reaction} = \Delta H_f(C_2H_5O^+) + \Delta H_f(H^\cdot) - \Delta H_f(CH_3OCH_3)$$
$$= 247 \text{ kcal/mole}$$
$$\Delta H_f(C_2H_5O^+) = 247 - 52 - 44 = 151 \text{ kcal/mole}$$

The figure is different from a value of 141 kcal/mole for the ion generated from a series of secondary alcohols. It is believed that the ion generated from dimethyl ether does not possess appreciable excess energy at threshold since the kinetic energy release accompanying the fragmentation of the metastable ion is only 0.1 kcal/mole. Hence the ions are indeed isomeric and the structures $CH_3-\overset{+}{O}=CH_2$ and $CH_3-CH=\overset{+}{O}-H$ are suggested. The isomeric $C_2H_5O^+$ ions were reviewed in later years by Lossing[62a].

IV - EXPERIMENTAL SECTION

1/ COMPOUNDS

a/ Origin

The unlabelled compounds were prepared by published procedures which, in some cases, were slightly modified. Unless indicated otherwise, the starting materials were purchased. The known compounds were identified by melting points, IR and NMR spectra. Some compounds, especially those not found in the literature, were submitted for microanalysis to Galbraith Labs. Inc. Knoxville, Tennesee.

Synthesis of the labelled compouds usually consisted of several steps from readily available labelled starting materials. The individual steps basically involved literature methods. Each overall synthesis was repeated several times with the unlabelled starting material in order to obtain a reasonable yield. However, once a sufficient amount of the required compound was obtained, the yield was not optimized further, and the synthesis was repeated using labelled starting material. All purchased labelled compounds were obtained from Merck Sharp and Dohme, Canada Ltd. The sites of deuterium labelling were checked by NMR and the deuterium content by mass spectrometry.

NMR spectra were obtained on Varian A-60A

spectrometer, infrared spectra were measured on Perkin Elmer IR 457 spectrometer, and melting points were taken with a capillary Gallenkamp melting point apparatus.

b/Preparations

The following compounds were prepared according to the procedures described in the author's previous work[11]:

2(1H)-pyrimidinone, 1-isopropyl-2-pyrimidinone, 1-benzyl--2-pyrimidinone, 2(1H)-pyrimidinthione, 1-methyl-2--pyrimidinthione, 1-d_1-2-pyrimidinone, 1-methyl-2-pyrimidinone, 1-(methyl-d_3)-2-pyrimidinone, 1-ethyl--2-pyrimidinone, 1-(ethyl-d_5)-2-pyrimidinone, 1-Phenyl--2-pyrimidinone, 1-ethyl-2-pyrimidinthione, 1-phenyl--2-pyrimidinthione

5-Deuterio-2-pyrimidinone[22]

Tetramethoxypropane(TMP)(0.01m) and conc. DCl(1ml) were mixed with D_2O(4.0ml) and stirred at room temperature for 5 min.. Urea(0.01m) was then added and the yellow solution was refluxed for 1 hour. The resultant mixture was neutralized with saturated $NaHCO_3$ to pH 7 and then vacuum evaporated. The powdered brown residue was submitted to soxhlet extraction with ethylacetate for two successive days using 2x 250ml of ethylacetate. After vacuum evaporation, the solid was recrystallized from benzene. The NMR spectrum in DMSO-d_6 did not show any evidence for the presence of H in the 5 position of the pyrimidine ring. Wt. = 0.35g, Yield = 38%, m.pt. 158° (lit. m.pt. for the

unlabelled compound[11]:160°;179-181°; N.B., this compound exists in two polymorphous forms[2b]).

5-Deuterio-1-methyl-2-pyrimidinone[22]

Tetramethoxypropane(0.01) and conc. DCl(1ml) were stirred at room temperature in D_2O(4ml) for 5 min.. Methylurea(0.01m) was then added and the solution was refluxed for 30 minutes. The resultant mixture was neutralized with saturated aqueous $NaHCO_3$ to pH 7 and extracted 5x with 20 ml of chloroform. The $CHCl_3$ extracts were passed through activated alumina column, evaporated and the residue was recrystallized from acetone-ligroin. The NMR spectrum did not show any evidence for the presence of H in the 5 position of the pyrimidine ring. Yield = 35%, m.pt. 130°(lit.[41]:131-132°).

Aniline-2,4,6-d_3

The reference (23) was followed for the synthesis. The mass spectrum of the pure product showed M^+ at m/z 96.

Phenyl-2,4,6-d_3-thiourea- cf. reference (24)

Ammonium thiocyanate(0.02m) and dry, freshly distilled acetone(10ml) were placed in a 100ml three necked flask. Through a dropping funnel, with stirring, benzoyl chloride(0.02m) was dropwise added and the mixture was refluxed for 5min.. The mixture was then stirred under reflux without applying any heat for another 15 minutes. Slowly a solution of aniline-2,4,6-d_3(0.02m) in 5ml of dry acetone was added and then the procedure

for synthesis of the unlabelled compound, described in the reference (24) was followed. D-incorporation ~70%, based upon the comparison of the mass spectra of the unlabelled and labelled phenylthiourea. Yield = 45%, m.pt. 152° (lit.[24]:154°).

1-(Phenyl-2,4,6-d_3)-2-pyrimidinthione

The procedure described in the reference (11) was followed for the synthesis, where phenyl-d_3-2,4,6-thiourea was substituted for the unlabelled starting material. D incorporation based upon the above synthesized phenyl-d_3-thiourea is ~70%. Yield = 38%, m.pt. 155° (lit.[11]:155°).

5-Deuterio-1-methyl-2-pyrimidinthione[22]

Tetramethoxypropane(0.005m) and conc. DCl(0.5ml) in D_2O(2ml) were stirred at room temperature for 5 minutes. Methylthiourea(0.005m) was then added and the mixture was refluxed for 2 hours. The cooled solution was neutralized with 20% aq. NaOH and the resulting yellow precipitate was filtered, washed with water and recrystallized with aqueous ethanol. NMR spectrum did not show any evidence for 5H. Yield = 30%, m.pt. 188°(lit.[46]:189-191.5°).

5-Deuterio-2-pyrimidinthione[22]

Tetramethoxypropane(0.01m) and conc. DCl(1ml) in 4ml D_2O were stirred for 5 minutes at room temperature Then thiourea(0.01m) was added and the mixture refluxed for 1 hour. Cooled, neutralized with 20% NaOH and recrystallized with aq. ethanol. No sign of 5H in

NMR spectrum. Yield = 75%, m.pt. 228°(lit.[47]:230°).

1-d_1-2-Pyrimidinthione - cf. reference (11)

2-Pyrimidinthione(0.1g) was dissolved in 4ml of D_2O by applying heat. The solution was then vacuum evaporated to yield the yellow crystals. The NMR spectrum in DMSO-d_6 did not show any trace of the broad peak present in the spectrum of the unlabelled 2-pyrimidinthione, due to the N-H(δ12.25)

Benzyl-α,α-d_2-alcohol - cf. reference (25)

LAD(1.9g) was placed in a 100ml 3-necked flask equipped with a dropping funnel and a reflux condenser. Anhydrous ether(15ml) was added and then a solution of benzoic acid(0.01m) in 20ml of ether was slowly added from the dropping funnel. Then the procedure described in the reference (25)was followed. Mass spectrum showed the molecular ion at m/z 110. Yield = 55%.

Benzyl-α,α-d_2-chloride - cf. reference (26)

The above synthesized benzyl-α,α-d_2-alcohol(0.025m) in 5ml of dry chloroform was placed in a round bottom flask equipped with a condenser and a dropping funnel. A solution of thionyl chloride(0.025m) in 4ml of dry chloroform was added dropwise while the reaction mixture was stirred and heated to keep the solution refluxing gently. When the addition was complete, stirring was continued at room temperature for 4 hours. Chloroform was distilled off and the residue was distilled under vacuum to obtain the clear product. Yield = 53%.

1-Benzyl-$\alpha\alpha d_2$-2-pyrimidinone - cf. reference (27)

The literature method[27] was followed using benzyl-$\alpha\alpha d_2$-chloride as the alkylating agent. The NMR spectrum did not show any trace of CH_2 protons. Yield=53%, m.pt. 137°(lit.[27]:137-138°), M^+ at m/z 188.

Methyl-d_3 isothiocyanate

The reference (28) was followed for the synthesis using purchased methyl-d_3-amine hydrochloride(min. 98%D) as the starting material.

Methyl-d_3-thiourea - cf. reference (11)

All of the methyl-d_3 isothiocyanate prepared above was dried over anh. sodium sulfate and then refluxed with conc. NH_4OH(4ml) in a water bath for 30 minutes. The final solution was then gently evaporated on a water bath almost to dryness. Upon adding acetone to the cool mixture white crystals appeared.Filtered, recrystallized 2x with a small amount of hot water and dried at room temperature. Yield = 35%(from methyl-d_3-amine HCl), m.pt. 118°(lit.[77]:118-9°).

1-Methyl-d_3-2-pyrimidinthione - cf. reference (46)

Cyclization of methyl-d_3-thiourea and TMP was carried out in the same fashion as described in the above reference for the synthesis of the 1-methyl-2-pyrimidinthione.NMR spectrum did not show any evidence for CH_3 protons. Yield = 40%, m.pt. 190°(lit.[46]:191-2°), M^+ at m/z 129, D incorporation ~98%(based upon methyl-d_3-amine HCl).

Phenyl-2,4,6-d_3-urea - cf. reference (29)

Aniline-2,4,6-d_3[23] (0.015m), nitrourea[30] (1.8g) and H_2O (60ml) were placed in a 50ml Erl. flask. Upon heating and stirring the mixture for one hour white needles appeared. The resultant was cooled, filtered and dried at 100° . D incorporation ~70%, based upon the comparison of the mass spectra of the unlabelled and labelled phenyl urea. M^+ at m/z 139, yield = 62%, m.pt. 146° (lit.[27]:147).

1-(Phenyl-2,4,6-d_3)-2-pyrimidinone - cf. reference (76)

The above synthesized phenyl-2,4,6-d_3-urea (0.006m), TMP (0.006m) and ethanol (6ml) were set aside at room temperaure for three days. The solution was vacuum evaporated to dryness, and the residue was triturated with 500ml of H_2O. The mixture was then filtered and the filtrate neutralized to pH 8 with dil. aq. NaOH. The solution was submitted to chloroform extraction; altogether 500ml of $CHCl_3$ was used. The chloroform extracts were passed through short column of activated alumina and vacuum evaporated. The residue was recrystallized with acetone-ligroin. D incorporation 70%, based upon phenyl-2,4,6-d_3-urea. M^+ at m/z 175, yield = 20%, m.pt. 154° (lit.[76]:155°).

Acetoxime d_6 - cf. reference (31)

The procedure described in the above reference was followed using $NH_2OH.HCl$ (5g in 10ml of D_2O), NaOD (7.5g, solution 40% w/w in D_2O) and $(CD_3)_2CO$ (5g).

M.pt. 60°(lit.[31]:60°).

Isopropyl-1,1,1,3,3,3-d_6-urea - cf. reference (32)

A solution of the above synthesized acetoxime-d_6 (2.5g) in 30ml of anhydrous ether was added dropwise from a closed system funnel to a mixture of $LiAlH_4$(3.5g) in 30ml of dry ether, which was placed in a three neck flask equipped with a condenser and a drying tube. The three neck flask was immersed in an ice-bath throughout the addition of the acetoxime solution and the mixture was stirred magnetically; then refluxed for 5 hours. The mixture was then cooled in dry ice-acetone bath. A condenser with dry ice-acetone was attached to the flask and H_2O(20ml) was dropwise added from a closed system separatory funnel. The mixture was then heated and thus ether and the produced isopropyl-d_6-amine were distilled over to a recieving flask immersed in a dry ice-acetone bath. Nitrourea[30](3g) dissolved in 180ml of H_2O was refluxed with the ether-isopropyl-d_6-amine mixture for 1.5 hours. The ethereal layer was evaporated by leaving the mixture exposed to air in the fumehood. Water was then evaporated on rotary evaporator and the residue treated with acetone and ether to obtain off white crystalline powder. D incorporation was 99.5%, based upon the comparison of the mass spectra of the unlabelled and labelled isopropyl urea. Yield = 62%,m.pt. 143°(lit.[77] =143).

1-(Isopropyl-1,1,1,3,3,3-d_6)-2-pyrimidinone- cf.(41)

Tetramethoxy propane(0.02m) and the above

synthesized isopropyl-d_6-urea(0.02m) were stirred with conc. HCl(4ml) and 20ml of ethanol for 3 days at room temperature. The mixture was then vacuum evaporated and the oily residue was dissolved in 20ml of H_2O. The solution was neutralized to pH 7 with saturated aqueous Na_2CO_3 solution. The product was then extracted 3x with 20ml portions of chloroform and the pooled chloroform extracts were vacuum evaporated. The residue was recrystallized first from acetone-ligroin, then from boiling cyclohexane. D incorporation ~99.5%, based upon the isopropyl-d_6 urea. Yield = 20%, m.pt. 86°(lit.[41]:90°), M^+ at m/z 144.

1-(isopropyl-2-d_1)-2-pyrimidinone

The same procedure was followed as for the above 1-(isopropyl -N-d_6)-2-pyrimidinone. The starting material, isopropyl-N-1-d_1-urea, was prepared by the reduction of acetoxime with LAD to obtain the isopropyl-d_1-amine which was then submitted to the reaction with nitrourea as described for the synthesis of the isopropyl-d_6-urea. D incorporation based upon the isopropyl-N-d_1-urea ~99.5%. Yield = 15%, m.pt. 85° (lit.[41]:90°), M^+ at m/z 139.

Ethyl-d_5-amine-hydrochloride[33]

Acetonitrile-d_3 in 80ml of anhydrous ether was dropwise added to the mixture of LAD in 80ml of anhydrous ether in a 3-neck flask equipped with a condenser and cooled in an ice-bath. After the mixture was refluxed

for 3 hours, it was cooled in a dry ice-acetone bath and the water condenser was changed for a dry ice-acetone one. The three neck flask was connected with rubber and glass tubing to an Erlenmeyer flask containing anhydrous ether and cooled in dry ice-acetone bath. Then water (10.8ml) was slowly added to the original mixture from a pressure equalizing funnel. The ethylamine produced partly bubbled into the ether and partly stayed dissolved in the original mixture. In order to obtain the latter, the original mixture was heated and the residual ethylamine plus ether was distilled over into the second flask containing the first portion of the product. Hydrogen chloride was bubbled through the product solution and the white precipitate which developed was suction filtered and washed 3x with 20ml portions of anhydrous ether. NMR spectrum in D_2O did not show any sign of ethyl hydrogens. Yield = 54%.

Ethyl-1-d_2-amine hydrochloride

Acetonitrile was reduced with LAD according to the procedure described for the above synthesis of ethyl-d_5 amine hydrochloride. NMR spectrum in D_2O did not show any trace of the methylene hydrogens.

Ethyl-2-d_3- amine hydrochloride

Acetonitrile-d_3 was reduced with LAH according to the procedure described for the above synthesis of ethyl-d_5 amine hydrochloride. NMR spectrum in D_2O showed just methylene hydrogens.

1-Ethyl-d_5 thiourea, 1-ethyl-1-d_2 thiourea, 1-ethyl-2-d_3 thiourea

The literature method[11,28] for the synthesis of methyl thiourea was followed to produce the three differently labelled thioureas from the above appropriately labelled ethylamine hydrochlorides.

1-(Ethyl-d_5)-2-pyrimidinthione- cf. reference (11)

The literature method for the synthesis of 1-ethyl-2-pyrimidinthione was followed, starting with the above synthesized N-ethyl-d_5-thiourea. NMR spectrum in acetone-d_6 did not show any trace of ethyl hydrogens. Yield = 50%, m.pt. 102°(lit.[11]:102°).

1-(Ethyl-1-d_2)-2-pyrimidinthione - cf. reference (11)

The literature method for the synthesis of 1-ethyl-2-pyrimidinthione was followed, starting with the above synthesized N-ethyl-1-d_2-thiourea. NMR spectrum in acetone-d_6 did not show any trace of the methylene hydrogens. Yield = 40%, m.pt. 102°(lit[11]:102°).

1-(Ethyl-2-d_3)-2-pyrimidinthione - cf. reference (11)

The literature method for the synthesis of 1-ethyl-2-pyrimidinthione was followed, starting with the above synthesized N-ethyl-2-d_3-thiourea. NMR spectrum in acetone-d_6 did not show any trace of the methyl hydrogens. Yield = 35%, m.pt. 102°(lit.[11]:102°).

2(1H)-Pyrimidinselenone - cf. reference (41)

The purchased selenourea was submitted to the cyclization with TMP according to the literature method

for the synthesis of 2(1H)-pyrimidinthione. Yield = 38%, m.pt. 175°, $M^{\cdot+}$ at m/z 160(corresponds to Se^{80}).

NMR spectrum(DMSO,TMS): δ7.3(T,1),δ8.6(D,2), J=6Hz.

Analysis:

$C_4H_4N_2Se$ calc. C 30.20; H 2.53; N 17.61; Se 49.64 %

found C 29.99; H 2.58; n 17.57; Se 49.62 %.

2/ INSTRUMENTAL METHODS

a/The mass spectrometer

The conventional spectra were obtained on a HITACHI RMU-7 mass spectrometer, a double focusing mass spectrometer with Nier-Johnson geometry[12,34a] (Fig. III-1). In this configuration the electric sector precedes the magnetic sector, the former giving energy, or velocity focusing, while the latter separates the monoenergetic beam of ions with respect to their mass-to-charge ratio. By increasing the magnetic field the positively charged ions are brought to focus on a collector plate in increasing m/z. When the ions strike the collector plate, secondary electrons are emitted from the metal and are multiplied by 16 dynodes[34b]. The yield ratio γ for this emission is expressed as the number of emitted secondary electrons divided by the number of positively charged ions. The amplified current is transferred into a pen recorder or a visirecorder. At an accelerating voltage of 3.6 kV and a multiplier voltage of 3.5 kV, current gain of the electron multiplier is 5×10^7.

Depending on the accelerating voltage V_a the RMU-7 covers the following mass/charge ranges by scanning the magnetic field:

m/z_{max}	Va	m/z_{max}	Va
300	3600	900	1200
450	2400	1200	900
600	1800	1800	600

b/The energy analyzer

The relationship between the accelerating voltage V_a and electric sector voltage V_e is determined by the maximum and minimum deviation, r_2 and r_1, from the central arc of the electrostatic field having radius r_e (Fig. IV-1). Focusing of the ions with the appropriate kinetic energy is achieved by placing two cylindrical segments in a cylindrical electrostatic field, which

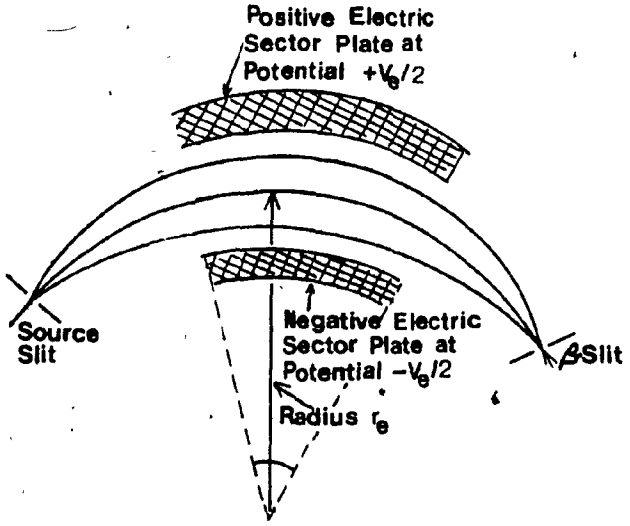

Fig. IV-1

function as two electrodes. If a voltage V_e is impressed between these electrodes, an electrostatic field E given by the following equation is created in the radial direction of the cylinders[34a].

$$E = (2/(r_1+r_2))(V_e/\ln(r_2/r_1)) \qquad (16)$$

If a beam of ions with a range of kinetic energies enters this field, there will be some ions having kinetic energy $mv^2/2$ such that the electrostatic force E_{ex} imposed upon the ions is exactly balanced by the centrifugal force mv^2/r_e.

Thus

$$mv^2/r_e = xeE \qquad (17)$$

where

$$r_e = \frac{1}{2}(r_1+r_2) \qquad (18)$$

= radius of the circular trajectory of the main beam of ions, and it is a line of equipotential(Fig.IV-1),

E = field strength,

x = number of charges, carried by the ions.

From equation (1), section III

$$mv^2 = 2xeV_a. \qquad (19)$$

By eliminating velocity v from equations (17) and (19)

$$r_e = 2V_a/E. \qquad (20)$$

The mass m and the number of charges x carried by the ions do not appear in equation (20), thus ions of all masses carrying any number of charges will follow the same radius through the electric sector, provided that they have been accelerated through a voltage V_a.

Substituing E and r_e from equations (16) and (18) respectively

$$V_e = 2V_a \ln(r_2/r_1) \qquad (21)$$

For the Hitachi RMU-7

$r_e = 25.0$cm, $r_2 = 25.6$cm, $r_1 = 24.4$cm,

$$V_e/V_a = 2 \ln(25.6/24.4) = 0.09602$$

or

$$V_a = V_e 10.414$$

c/The magnetic analyzer

The monoenergetic beam of ions that emerge from the energy analyzer is sorted by scanning the magnetic field. The m/z value of the collected ion is proportional to the square of the magnetic field strength B and inversely proportional to the accelerating voltage V_a. This relationship is derived as follows:

The radius r of the circular trajectory described by a particle of charge e and mass m in a magnetic field depends on the accelerating voltage V_a and the strength of the magnetic field B. In the magnetic field, the particle with the velocity v will experience a centripetal force Bev, which is counterbalanced by a centrifugal force mv^2/r.

$$Bev = mv^2/r, \quad \therefore \quad r = mv/eB, \qquad (22)$$

but

$$eV_a = \tfrac{1}{2}mv^2, \qquad \text{cf.(1)}$$

thus elimination of v from the above equations results in

$$m/e = B^2r^2/2V_a = m/z \text{(for singly charged ions)}. \qquad (23)$$

d/Sample handling

All measurements were made using 70 volt electrons, unless indicated otherwise. The solid

samples were introduced directly into ion source of the mass spectrometer. The liquid samples were placed in a small vial, attached to the glass tubing assembly by a ground joint. The vial containing the sample was cooled with liquid nitrogen, while the sample was degassed. When the system reached room temperature, the vaporized sample was introduced into the source through the Granville Philips valve[35]. The pressure in the analyzer tube was nominally 10^{-7}mm.The pressure in the ionization chamber was probably an order of magnitude greater than this[12]. The source temperature was adjusted according to the physical properties of the sample.

e/Defocusing techniques

To detect decompositions occuring in the first field free region, two methods were used.

The electric sector voltage variation method developed by Kiser was used as follows[36]:

Focus adjustments were made in order to find the sector voltage V_e for the main beam of ions using the electric sector voltage supply and keeping the accelerating voltage at constant value. Then a survey was made in the region close to m^* by successive magnetic scans of the spectrum, in which the electric voltage was each time decreased by 0.2 V increments, starting ~1V above the theoretical voltage V_e', at which the expected metastable transition was to be observed. If the expected transition was observed, each scan

produced a diffuse peak. Heights of the successive peaks first increased till the maximum was reached and then went down again. From these data a graph can be constructed of the metastable peak intensities as a function of sector voltage(Fig. IV-2). The V_e' value that gave the maximum intensity peak corresponded to the center of the metastable peak and should be the same as the V_e' theoretical. Finally, the mass position of the metastable peak was evaluated comparing the center with peak positions of the normal mass spectrum, using a marker.

e.g. The molecular ion of 1-ethyl-2-pyrimidinone at m/z 124 loses methyl radical to form an ion at m/z 109

$$\underset{m_1}{124} \xrightarrow{-15} \underset{m_2}{109}$$

The metastable peak for loss of 15 mass units from the molecular ion appeared in the conventional spectrum at $m^* = 95.8$. The electric sector voltage for the main beam of ions was

$$V_e = 242.7V$$

The theoretical sector voltage for observation of the metastable process in the first field free region was

$$V_{e\ \text{theoretical}}' = V_e m_2/m_1 = 242.7 \times 109/124 = 213.3V$$

The electric sector voltage, corresponding to the maximum intensity peak was

$V'_{e\ measured} = 213.9V$

At this V_e, the mass calibration confirmed the value of $m^* = 95.8$.

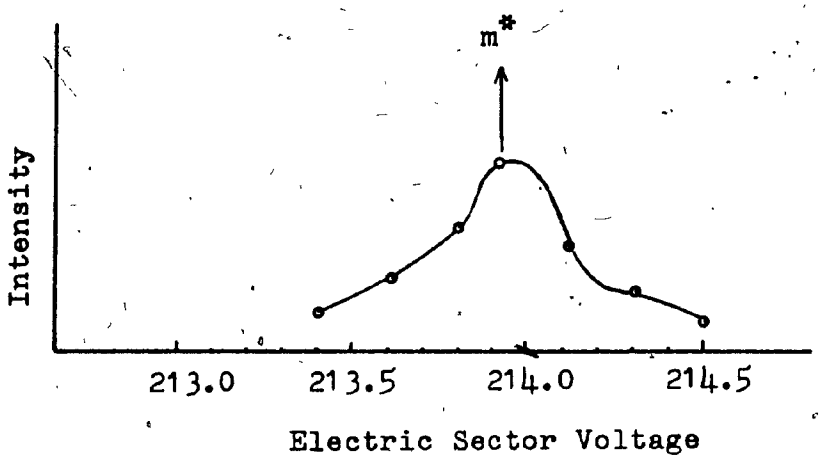

Fig. IV-2. Defocused daughter ions arising in the FFFR for the process

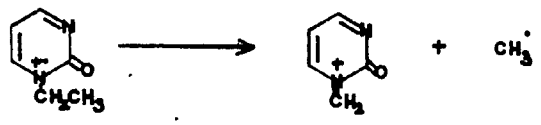

m/z 124 m/z 109

Jennings [37] developed another method for observing the metastable transition in the FFFR, which is based on scanning the accelerating voltage(p.19). To make use of this method a separate scanable power supply(SPS) was built following McGillivray et al.[38].

The SPS consists of a scanner, which generates a ramp voltage, and of an off-set amplifier with a digital voltmeter. The amplified output ramp voltage is connected between the common end of the floating acceleration potential and ground. This connection is necessary to avoid difficulties caused by the direct connection of the ramp voltage to the control circuitry of the acceleration power supply. Due to a very long RC time constant present in the network, such a direct connection rules out a rapid sweeping of the acceleration potential.

At the beginning of the measurement the SPS voltage was adjusted to ~30V. Thus, with the SPS in the operating mode, the accelerating voltage was enhanced by this initial SPS voltage value. Ions that emerged from the source were brought to the focus by regulating the electric sector voltage as usual. Then the daughter ion of interest was found, scanning the magnetic field as for any conventional spectrum. The SPS voltage was then slowly increased until the desired metastable peak appeared. The voltage, corresponding to the center of the metastable peak was recorded. On the basis of the relationship described before(p. 25), the following calculations were performed.

e.g. Consider the metastable peak for the process

$$\underset{92}{C_7H_8^{+\bullet}} \longrightarrow \underset{91}{C_7H_7^{+}} + H^{\bullet}$$

$$m_1 \qquad\qquad m_2$$

that occurs in the mass spectrum of toluene. The electric sector voltage with the initial SPS voltage of 30.6V was

$$V_e = 249.9V$$

The SPS voltage at the center of the metastable peak was

$$V_{SPS} = 54.0V$$

The real SPS voltage at the center of the metastable peak was obtained after subtracting from the above value the initial SPS voltage that was already included in the total accelerating voltage, when the focus adjustments were performed.

$$V_{SPS} = 54.0 - 30.6 = 23.4V$$

The accelerating voltage for the daughter ion arising in the source was

$$V_a = V_e \times 10.414 = 249.9 \times 10.414 = 2602.4V$$

The measured accelerating voltage for the daughter ion arising in the FFFR was

$$V'_{a\ measured} = 2602.4 + 23.4 = 2626V$$

The theoretical accelerating voltage for the daughter ion arising in the FFFR was

$$V'_{a\ calculated} = 2602.4 \times 92/91 = 2631.0V$$

$$(V_{calc.} - V_{measured} = 5V = 0.2\%)$$

The high voltage scan method was mainly used for the evaluation of the kinetic energy T, released as a result of a metastable decomposition(cf. p.24). First, measurements were tried, using the metastable transition for loss of hydrogen radical from the molecular ion of toluene. The kinetic energy release accompanying this metastable transition is well defined in the literature[20].

Considering the same value of V_e with the SPS in the operating mode as above, the accelerating voltage for the main beam of ions was 2602.4V. The metastable peak width at half maximum was 9.1V. This had to be corrected for the main beam width, which was 3.3V. The corrected square of the metastable peak width ΔV^2 was $(\Delta V^2_{metastable} - \Delta V^2_{main\ beam})^{12a} = 71.9 V^2$

Substituing in the equation (10)

$$T_{0.5} = (91^2 \times eV/16 \times 92 \times 1) \times 71.9/2602.4^2 =$$

$$= (91^2 \times 2602.4/16 \times 92 \times 1) \times 71.9/2602.4^2 =$$

$$= 0.16\ eV\ (lit.^{20}: 0.17eV).$$

f/Appearance energy measurements

Xenon, which was used as the calibrant gas was connected to the glass tubing used for a liquid sample introduction(cf.p.55), and the desired amount was introduced into the source through the Granville Phillips valve[35]. A digital voltmeter (DVM) was introduced into the emission regulator circuit so that the chamber voltage could be continuously measured. For safety reasons the DVM was placed in a plastic box and operated with a glass or plastic rod. Since the samples were all solids of various volatility, the sample heater had to be applied accordingly. Glass tubes commonly used for introduction of solid compounds into the source are made to carry only a small amount of sample which is usually vaporized relatively fast. These were not adequate, since appearance energy measurements require more time than a record of an ordinary mass spectra or a detection of a metastable peak. Therefore, auxiliary sample glass tubes were made, which were sealed on one side and when filled with the sample, were almost sealed on the other end, to prevent a quick evaporation. The measurement of the ion beam intensity started at 20 eV. The electron energy was then gradually decreased untill the measured peak disappeared. The peak intensities were recorded each 1.0 or 0.5 eV.

For interpretation of the results the semilog

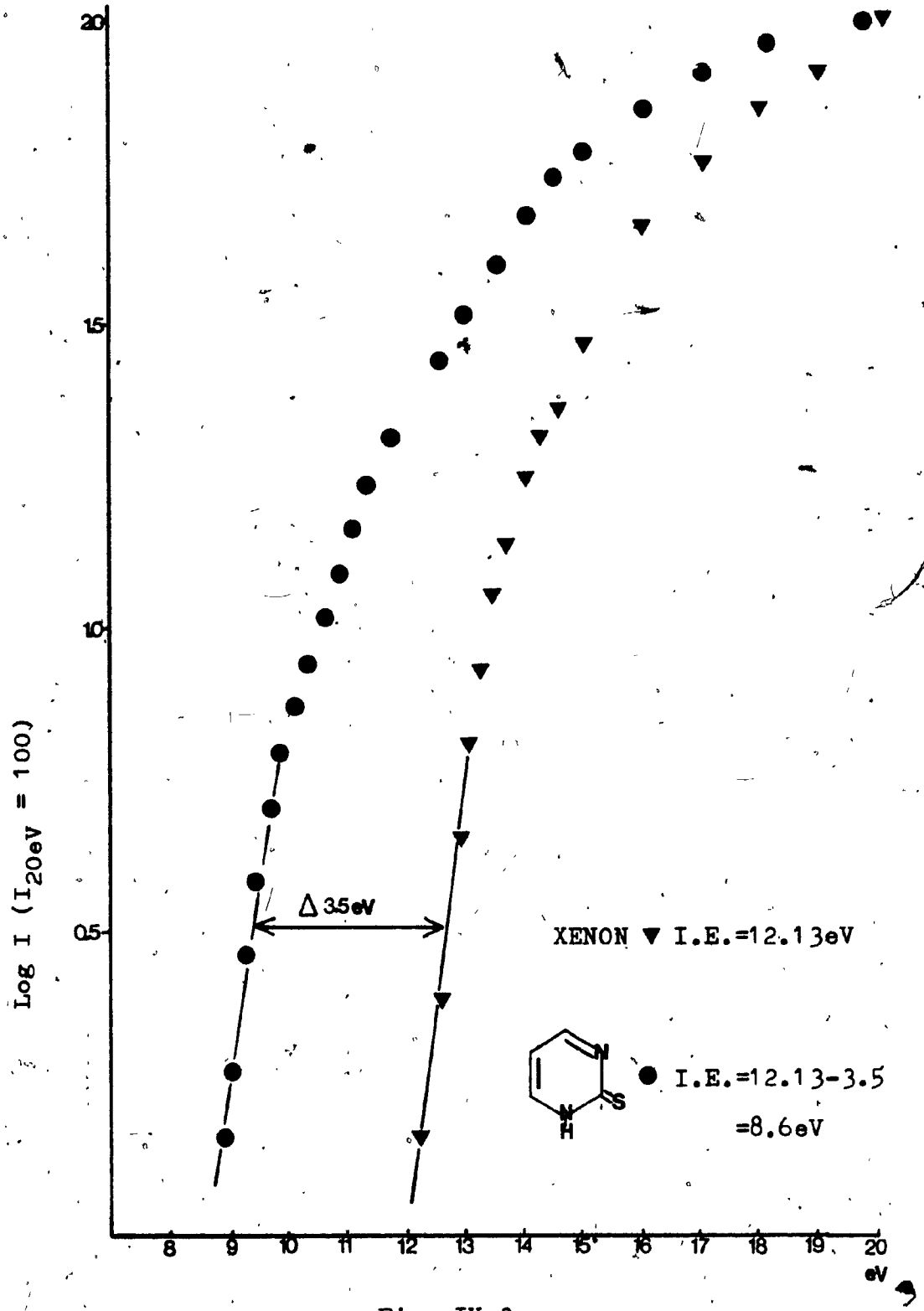
20
15
10
0.5
Log I (I_{20eV} = 100)
Δ 3.5eV
XENON ▼ I.E.=12.13eV
● I.E.=12.13-3.5
=8.6eV
N
S
N
H
8
9
10
11
12
13
14
15
16
17
18
19
20
eV

Fig. IV-3

plot method was used[40]. Each sample was measured twice and the measurement of the ionization energy of the standard gas followed every sample measurement. Fig. IV-3 shows the semilog plot using xenon, I.E. 12.13 eV, as standard. The peak heights at 20 eV for the sample and the standard were normalized to 100 and the lower peak intensities were recalculated accordingly. Logarithms of the normalized values were plotted against the electron volt energies. Examination of the two curves shows that they are nearly parallel in the lower portion of the graph. the difference of 3.5 eV was subtracted from 12.13 eV to obtain 8.6 eV for the ionization energy of 2-pyrimidinthione.

V - RESULTS AND DISCUSSION

1/ SYNTHESIS

The unlabelled compounds (V-a) were synthesized using 1,1,3,3-tetramethoxypropane(TMP) as a precursor for malondialdehyde, which reacts with the appropriate urea in the presence of acid to give first the salt of the pyrimidine (V-b). Subsequent neutralization and work up yields the free base[41].

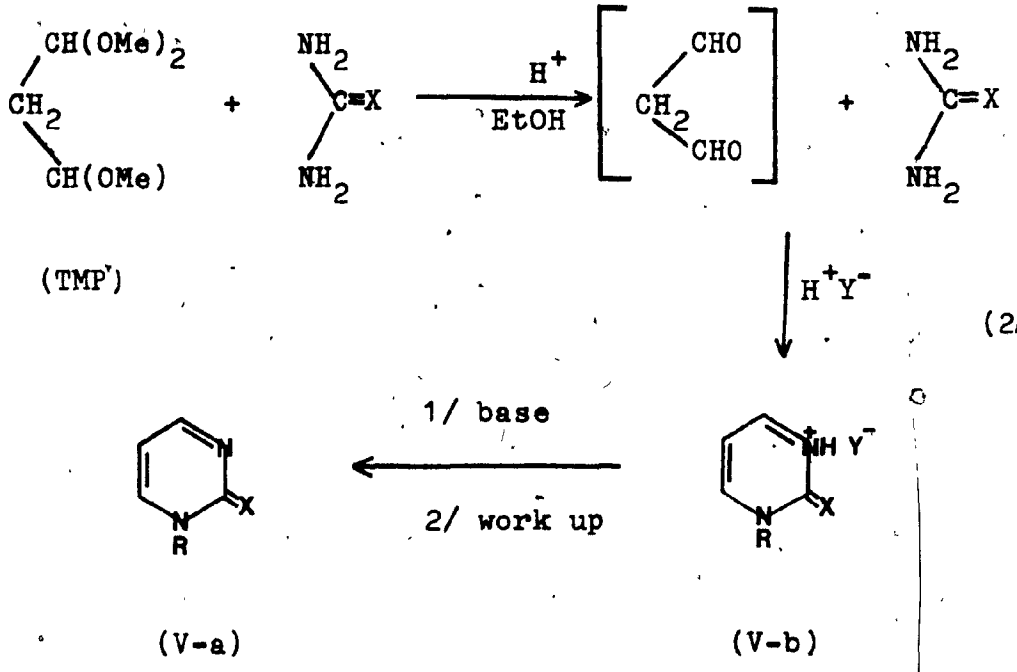

(24)

(V-a) (V-b)

X = O,S or Se

R = H,Me,Et,i-Pr,Ph,$PhCH_2$

The second method for the synthesis of N-substituted pyrimidinones is a direct N-alkylation applied to the silver or sodium salt of 2-pyrimidinone[27].

M = Na or Ag

R = alkyl

Z = Cl,Br,I

Used for R = CD_3, CD_2CD_3 and CD_2Ph

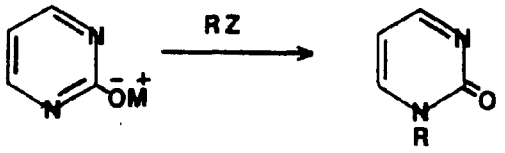

(25)

The deuterated methyl and ethyl iodide were purchased from Merck, Sharp and Dohme. The deuterated benzyl chloride was synthesized by the reduction of benzoic acid with lithium aluminium deuteride(LAD) to obtain the labelled benzyl alcohol[25] which was then chlorinated with thionyl chloride[26].

$$PhCOOH \xrightarrow{LAD} PhCD_2OH \xrightarrow{SOCl_2} PhCD_2Cl$$

The attempt to synthesize the 1-isopropyl-2-pyrimidinone by direct alkylation failed:

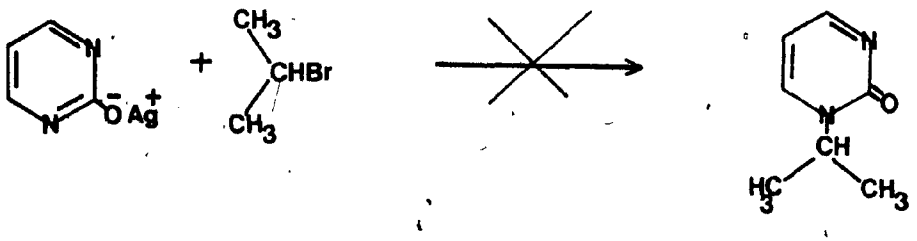

Instead of nucleophilic substitution at the secondary carbon of 2-bromopropane, elimination of HBr took place and unsubstituted 2-pyrimidinone was recovered.

The appropriate commercially available deuterated isopropyl bromides could therefore not be used for the preparation of (V-4b) and (V-4c).

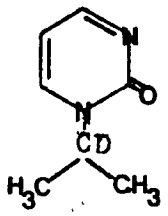

(V-4b)

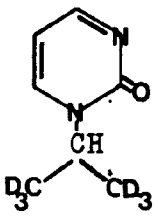

(V-4c)

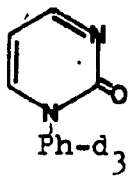

(V-6b)

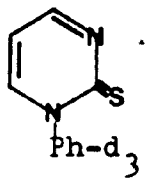

(V-10b)

Alkylation of 2-pyrimidinthione results in the formation of 2-alkylmercaptopyrimidine[43].

e.g.

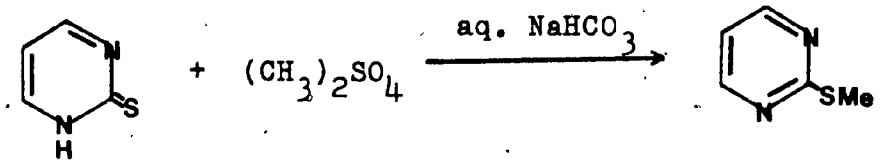

(V-c)

N-alkylation according to the reaction (25) of 2-pyrimidinthione with the appropriate commercially available deuterated alkyl halides could not be used for synthesis of the pyrimidinthiones (V-8b), (V-9b), (V-9c) and (V-9d). However, 2-methyl-thio-pyrimidine (V-c) was synthesized[43] and treated further with methyl iodide[44].

e.g.

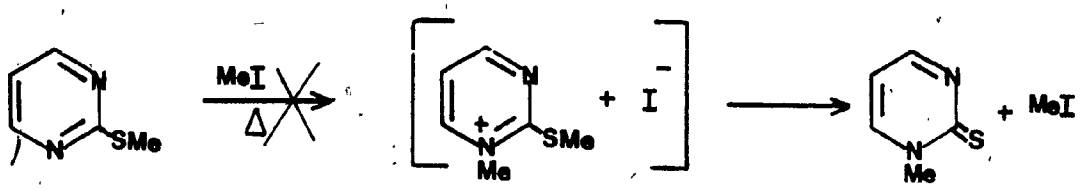

(V-c)

The above reaction is described in the literature[44] for the oxo homologue, however, did not work with 2-methyl-thio-pyrimidine.

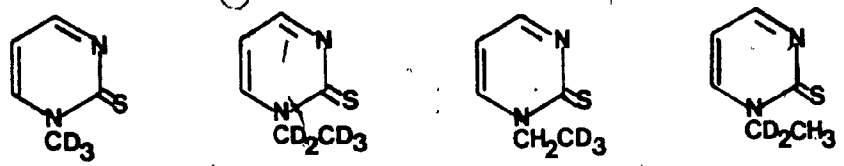

(V-8c) (V-9b) (V-9c) (V-9d)

Two other methods were tried in order to find out whether the labelled pyrimidinthiones could be obtained using the appropriately deuterated alkyl halides, but without success.

e.g.

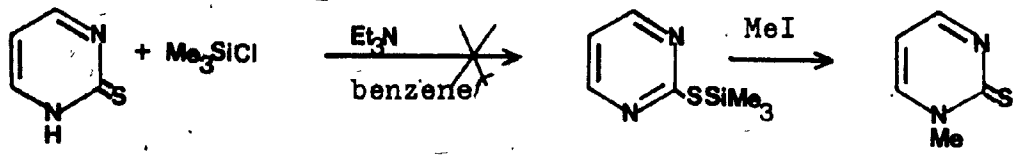

(cf. ref. 45)

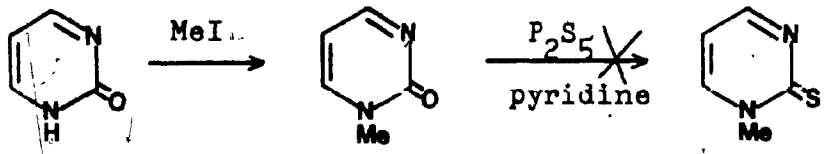

(cf. eqn. 24) (cf. ref. 46)

The only feasible reaction for synthesis of the pyrimidinthiones (V-8c), (V-9b), (V-9c), (V-9d), (V-10b) and the pyrimidinones (V-4b), (V-4c) and (V-6b) was the cyclization of TMP and the appropriately labelled thiourea or urea as described in the equation (24).

The following schemes illustrate the preparation of the labelled ureas or thioureas, which were then submitted to cyclization.

$$(CH_3)_2C{=}NOH \xrightarrow{LAD} (CH_3)_2CDNH_2 \xrightarrow{NH_2CONHNO_2} (CH_3)_2CDNHCONH_2 \quad \text{(cf. refs. 31,32)}$$

$$(CD_3)_2CO \xrightarrow{NH_2OH.HCl} (CD_3)_2C{=}NOH \xrightarrow{LAH} (CD_3)_2CHNH_2 \xrightarrow{NH_2CONHNO_2} (CD_3)_2CHNHCONH_2 \quad \text{(cf. refs. 31,32)}$$

$$d_3\text{-PhNH}_2 \xrightarrow{NH_2CONHNO_2} d_3\text{-PhNHCONH}_2 \text{ (cf.ref. 23)}$$

The above deuterated aniline was obtained from the unlabelled homologue by electrophilic substitution of hydrogen by deuterium[23].

$$CD_3NH_2HCl \xrightarrow{CS_2,NaOH} CD_3NHCS_2Na \xrightarrow{ClCO_2Et} CD_3NCS \longrightarrow$$

$$\xrightarrow{NH_3} CD_3NHCSNH_2 \quad \text{(cf. refs. 28,11)}$$

$$CD_3CN \xrightarrow{LAD} \xrightarrow{HCl} CD_3CD_2NH_2.HCl \xrightarrow{CS_2,NaOH} \xrightarrow{ClCO_2Et}$$

$$\longrightarrow CD_3CD_2NCS \xrightarrow{NH_3} OD_3CD_2NHCSNH_2 \quad \text{(cf. refs. 28,11)}$$

$$CD_3CN \xrightarrow{LAH} \xrightarrow{HCl} CD_3CH_2NH_2.HCl \xrightarrow{CS_2,NaOH} \xrightarrow{ClCO_2Et}$$

$$\longrightarrow CD_3CH_2NCS \xrightarrow{NH_3} CD_3CH_2NHCSNH_2 \quad \text{(cf. refs. 28,11)}$$

$$CH_3CN \xrightarrow{LAD} \xrightarrow{HCl} CH_3CD_2NH_2.HCl \xrightarrow{CS_2,NaOH}$$

$$\xrightarrow{ClCO_2Et} CH_3CD_2NCS \xrightarrow{NH_3} CH_3CD_2NHCSNH_2 \quad \text{(cf.refs.28,11)}$$

$$NH_4SCN + PhCOCl \longrightarrow PhCONCS + NH_4Cl$$

$$PhCONCS + d_3\text{-}PhNH_2 \longrightarrow PhCONHCSNHPh\text{-}d_3 \longrightarrow$$

$$\longrightarrow H_2NCSNHPh\text{-}d_3 \quad \text{(cf.ref.24)}$$

For the synthesis of (V-1d), (V-2c), (V-7b) and (V-8b), where the 5-position of the pyrimidine ring is labelled, the cyclization reaction was carried out in D_2O, catalyzed by DCl[22] (cf. reaction 26). For

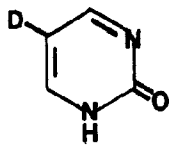

(V-1d)

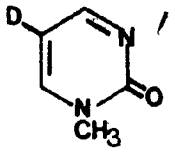

(V-2c)

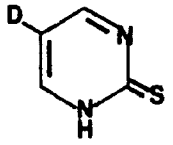

(V-7b)

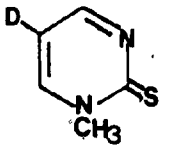

(V-8b)

(X=O, R=H or Me) deuterium incorporation to the 5-position can be achieved by direct exchange in dilute deuterated aqueous acid at 100° for 2 days[48]. Beside the length of time required, this method has the disadvantage that

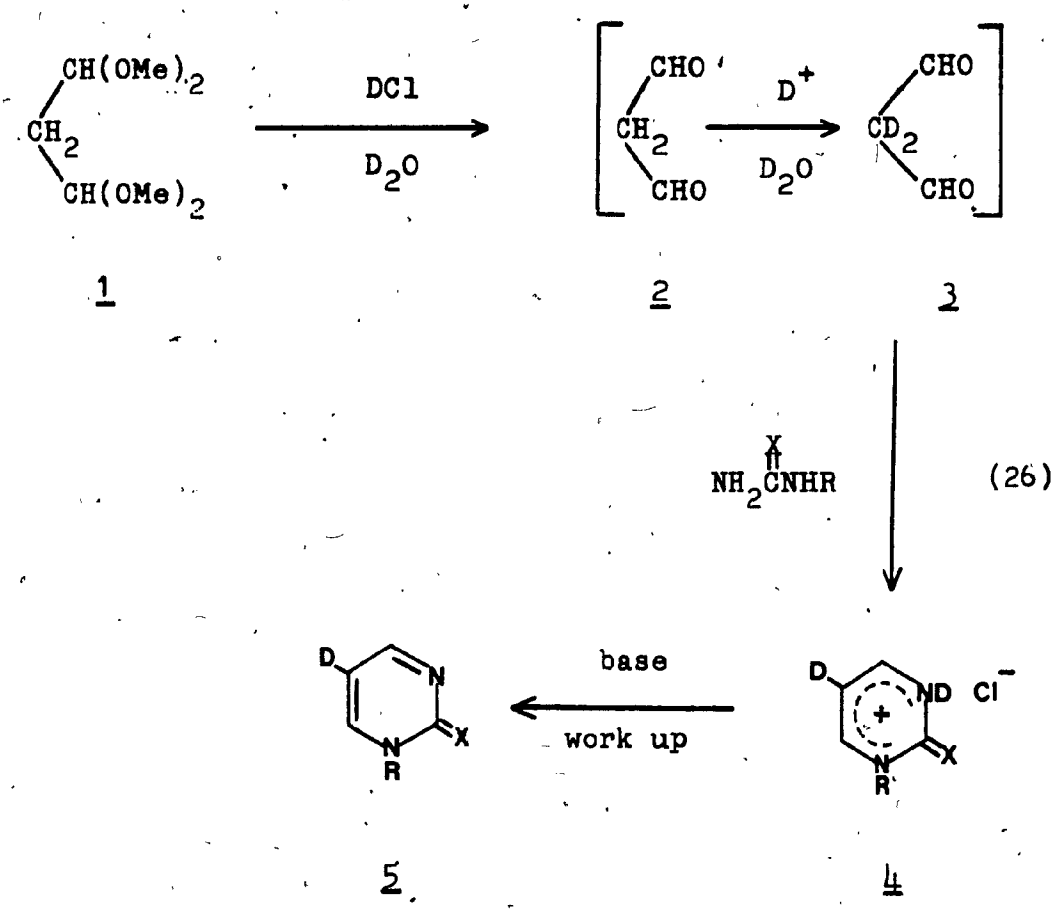

concomitant decomposition diminishes product recovery. Moreover, prolonged application of hot acid to the sulfur analogues 5(X=S) could cause hydrolytic replacement of the sulfur by oxygen[44]. Accordingly we considered synthesis of 5 from a commom labelled precursor.

The normal route to unlabelled 5 involved reactions of malondialdehyde bis(dimethylacetal) 1 (or similar acetal) with a urea or thiourea in alcoholic acid (cf.reaction 24). Application of this method would require 1 labelled with two deuteriums at the central methylene. Routes to this labelled 1 (or its tetraethyl homologue) would require several steps[49] from available

[42,47]

deuterated materials. In addition we foresaw the problem that during the course of the reaction with the urea there might be loss of deuterium by exchange between reaction intermediates derived from 1 and the medium. On the other hand by working with a deuterated medium and unlabelled 1 we might be able to achieve deuterium incorporation into the product 5.

Formally the reaction of 1 with urea is a condensation between malondialdehyde 2 and the urea. Although 2 is probably not involved in the reaction carried out in an alcoholic medium, it almost certainly would be if the reaction were carried out in water. Moreover, 2 in deuterated aqueous acid should undergo facile exchange to give the labelled 3, and then condensation of 3 with the urea should yield the desired labelled 5. These expectations were realized and afforded facile syntheses of desired compounds 5.

2/ FRAGMENTATION

The following section describes the major fragmentation pathways of the synthesized pyrimidines. The various structures that are assigned to some fragments are in this part of the thesis only hypothetical. Relative intensities of the fragments are in most cases indicated in brackets behind the described ions and are also tabulated together with $\%\Sigma_{30}$ in Appendix I. The high resolution mass measurements were carried out at the University of Ottawa, using a Kratos-AEI MS-902S mass spectrometer. The discussed fragmentation pathways were confirmed by appropriate metastable peaks and if necessary the metastable defocusing technique was used.

The numbering of pyrimidine ring is as follows:

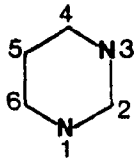

2-Pyrimidinone (V-1a) (Fig. V-1)

Due to the potentially tautomeric structure of this molecule, various studies has been performed to determine the position of equilibrium for the protomeric system (V-1a) and (V-1b).

(V-1a) 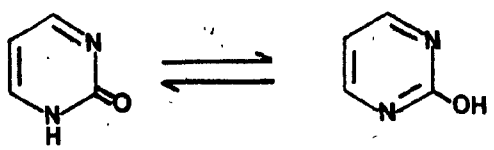 (V-1b)

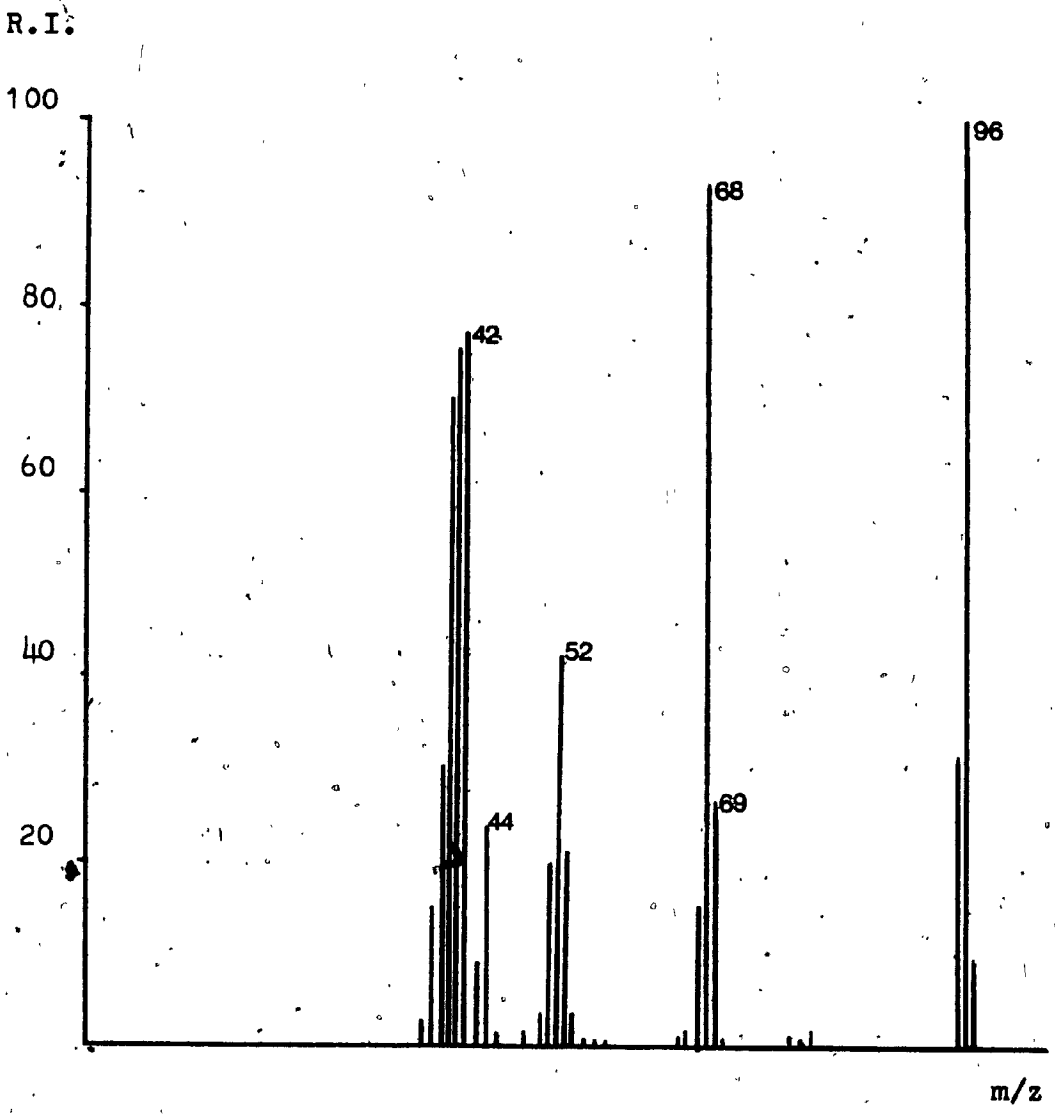

Fig. V-1 Mass spectrum of 2-pyrimidinone

Ultraviolet spectroscopy reveals that 2-pyrimidinone (V-1a) is the major tautomer in aqueous or ethanolic solution(>94%)[50], while 2-hydroxypyrimidine(V-1b) predominates in the vapour phase(>91%)[50]. In the solid state the material most probably contains molecules in the keto form[51]. The structure of the molecular ion may be derived therefore either from the keto form or from the enol form[11].

The mass spectrum of this compound shows the molecular ion as the base peak at m/z 96(100.0%). A significant fragmentation pathway is loss of hydrogen from the molecular ion to form the (M-1) peak of relative intensity 31.8%. However, this process is probably very fast, since no sign of any metastable decomposition was observed. The M-1 peak(not M-2) is significant also in the mass spectra of the two labelled species (V-1c) and (V-1d).

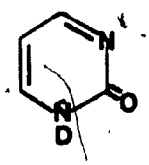

(V-1c)

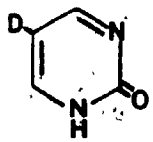

(V-1d)

This indicates that the primary loss of hydrogen from the molecular ion involves rupture of the H-C bond in the 4 or 6 position of the pyrimidine ring.

After $M^{+\cdot}$ and $(M-1)^{+}$ ions, the next significant peaks occur at m/z 69(27.3%), 68(93.2%) and 67(18.2%). For the two above labelled substrates, the three fragment

ions are replaced by peaks at m/z 70, 69 and 68 in a similar proportional abundance. Thus, these ions appear to still contain the tautomeric H or D, and the H or D from the 5 position of the ring.

For the unlabelled substrate high-resolution mass spectroscopy showed that the m/z 69 peak contains only one ion of composition C_3H_3NO (calc. 69.0215, observed 69.0212). This corresponds to loss of HCN from the molecular ion and may involve the formation of the oxazole cation (V-1e).

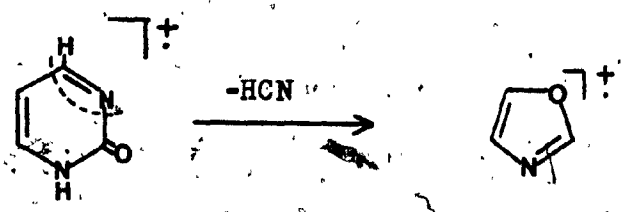

$M^{+\cdot}$ m/z 96 m/z 69.0212

(V-1e)

The intense m/z 68(93.2%) is due to two ions, $C_3H_4N_2^{+\cdot}$ (calc.68.0374, obs.68.0373) and $C_3H_2NO^+$ (calc. 68.0136, obs.68.0138) in the ratio 6:1. The following scheme describes the origin of the m/z peak.

$C_4H_4N_2O^{+\cdot}$ $\xrightarrow{-CO}$ $C_3H_4N_2^{+\cdot}$

$M^{+\cdot}$ m/z 96 $m^* = 48.17$ (weak) m/z 68.0373(79.9%)

$\downarrow -H^\cdot$

$C_4H_3N_2O^+$ $\xrightarrow{-HCN}$ $C_3H_2NO^+$

m/z 95 $m^* = 48.67$ (strong) m/z 68.0138(13.3%)

The two resolved metastable peaks indicate that loss of CO from $M^{+\cdot}$ is a relatively fast process, involving simple bond cleavage, while the loss of HCN from M-1 ion is accompanied by a rearrangement. The former may involve formation of the pyrazole cation (V-1f).

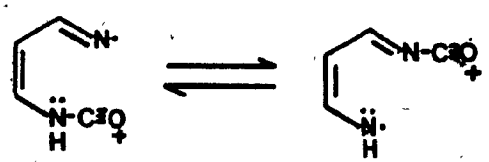

$M^{+\cdot}$ m/z 96

-CO

m/z 68.0373

(V-1f)

The minor ion $C_3H_2NO^+$ resulting from the M-1 ion by loss of HCN or HNC, may have various structures, and it is hard to determine which part of the M-1 ion is cleaved.

The smaller m/z 67 peak appeared to be also due to [illegible] ions, $C_3H_3N_2^+$(calc.67.0296, obs.67.0298) and $C_3HNO^{+\cdot}$ [illegible].0058,obs.67.0057) in the ratio 4:1. The strong metastable decomposition in the first field free region indicates that the $C_3H_3N_2^+$ ion arises from the fragment (V-1f) by loss of hydrogen. The origin of $C_3HNO^{+\cdot}$ is not

easy to rationalize. However, since it is an odd-electron ion, it most likely arises from either the molecular ion or the m/z 69 ion:

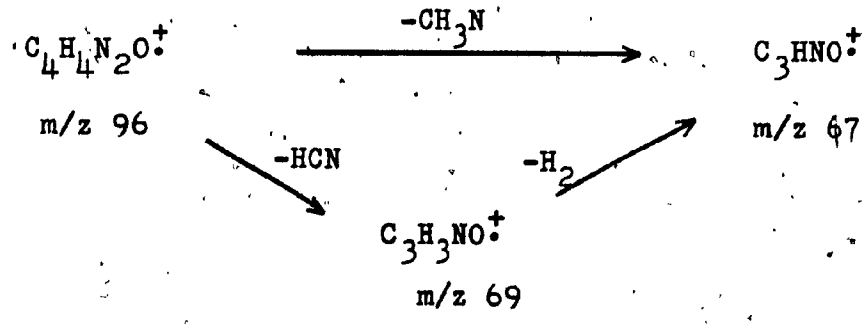

The major fragmentation pathways, discussed above are outlined in Scheme V-1.

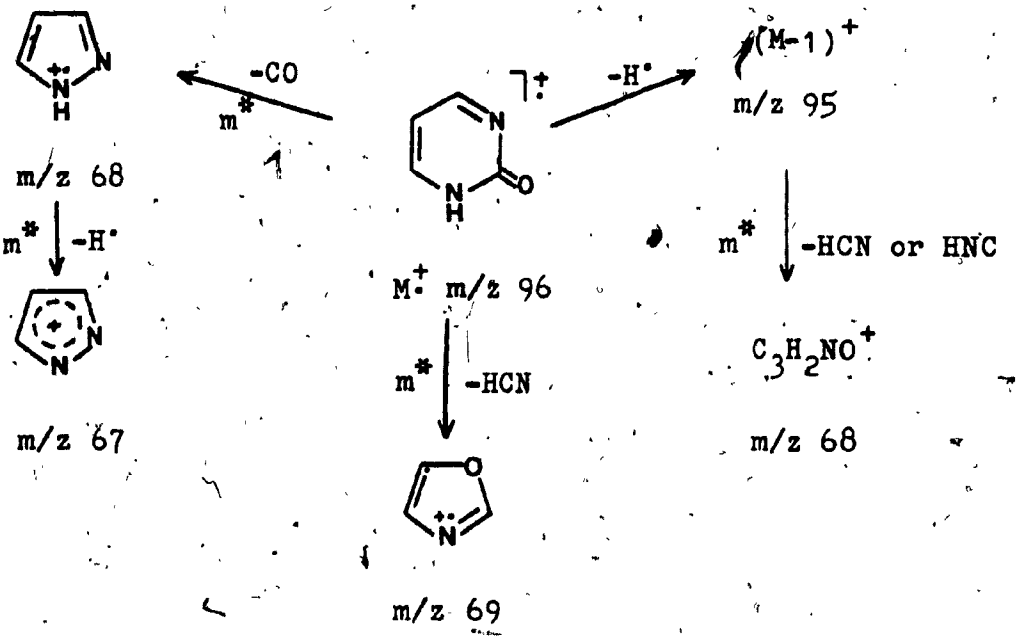

Scheme V-1. Fragmentation pattern for 2-pyrimidinone

1-Methyl-2-pyrimidinone (V-2a) (Fig. V-2)

The molecular ion at m/z 110(100.0%) loses hydrogen to form a highly abundant ion at m/z 109(79.3%). However, no sign of any such fragmentation has been detected in the first or second field free region. The labelled compounds 1-(d_3-methyl)-2-pyrimidinone(V-2b) and 1-methyl-2-pyrimidinone-5-d_1(V-2c) form relatively abundant M-1 ion(86.6% and 84.9% respectively), which shows that the H-C bond rupture mainly affects the 4 or 6 position of the pyrimidine ring and not the methyl group.

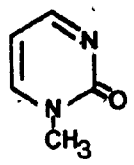

(V-2a)

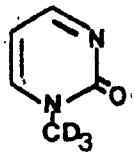

(V-2b)

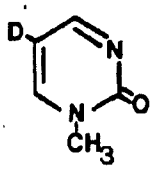

(V-2c)

The next significant peak is at m/z 82(58.7%), and contains two fragments analogous to the fragmentation pattern of the unsubstituted 2-pyrimidinone(V-1a). The first fragment, which arises from the molecular ion by expulsion of CO to form an ion $C_4H_6N_2^{+\cdot}$, could be the N-methyl-pyrazole ion(V-2d).

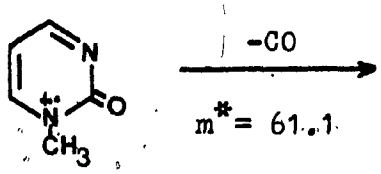

m/z 110

$M^{+\cdot}$

m/z 82

(V-2d)

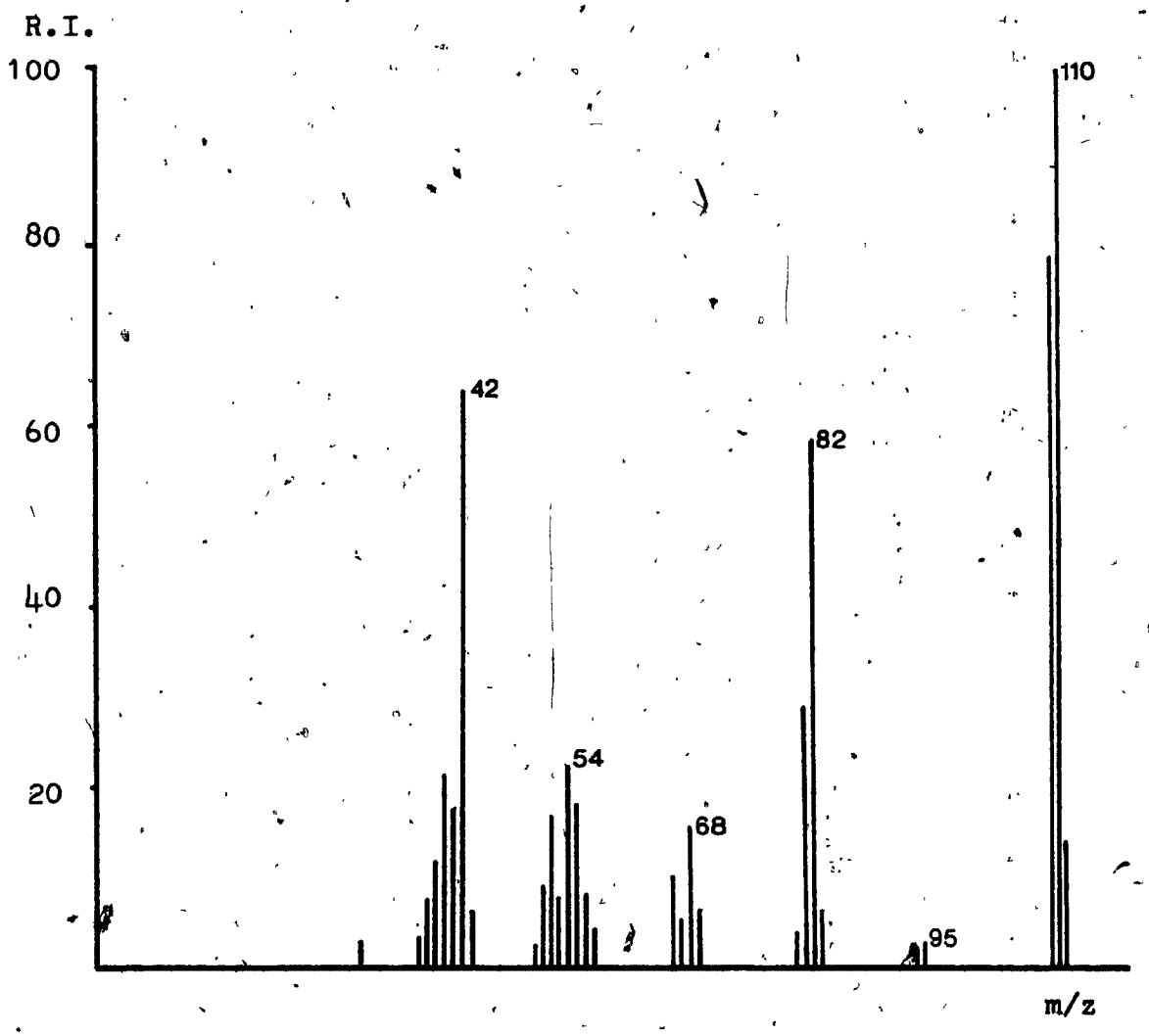

Fig. V-2 Mass spectrum of 1-methyl-2-pyrimidinone

The corresponding peaks for the two labelled compounds (V-2b) and (V-2c) appear at m/z 85 and 83 respectively, indicating retention of deuterium.

The second fragment derives from the M-1 ion by loss of HCN to yield the $C_4H_4NO^+$ ion. The corresponding peaks in the mass spectra of the two labelled substrates appear again at m/e 85 and 83.

$$\underset{m/z\ 109}{(M-1)^+} \xrightarrow[m^*= 61.7]{-HCN} \underset{m/z\ 82}{C_4H_4NO^+}$$

Metastable decompositions for both processes were detected in the FFFR.

Another important fragment is at m/z 81(29.4%), which in the spectra of (V-2b) and (V-2c) appear at m/z 84 and 82, respectively. According to the observed fragmentation in the FFFR, the ion has two origins, loss of carbon monoxide from the M-1 ion,

$$\underset{m/z\ 109}{(M-1)^+} \xrightarrow[m^*= 60.2]{-CO} \underset{m/z\ 81}{C_4H_5N_2^+}$$

and loss of hydrogen from the ion (V-2d) at m/z 82.

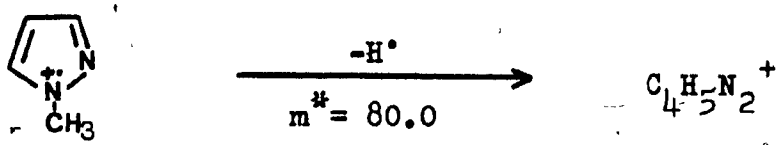

(V-2d)

Of interest is the relatively abundant ion at m/z 83(19.7%) in the spectrum of (V-2b). It was suggested previously[11] that this ion might arise by the same process as indicated above for the unlabelled species (V-2d), but by loss of deuterium instead of hydrogen. That means the methyl hydrogen isotopes would have to be affected. A similar process has been observed for 1-methyl-pyrazole, where hydrogen is expelled to a large extent(93%) from the methyl group[52]. No metastable transition corresponding to the origin of m/z 83 was observed for the labelled

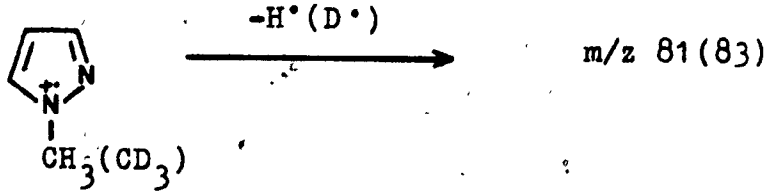

species (V-2b), while the transition (85 $\xrightarrow{-H^{\cdot}}$ 84) was detected in the FFFR. This indicates that the ring hydrogen of the hypothetical 1-methyl-pyrazole ring is involved in the loss, but does not exclude the possibility

that also deuterium is expelled from m/z 85.

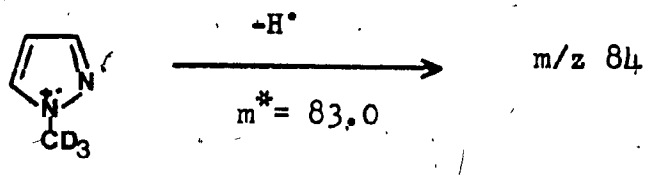

m/z 85

The molecular ion further expels NCO to form the ion at m/z 68. This process was also observed in the FFFR and yields fragments at m/z 71 and m/z 69 in the fragmentation patterns of (V-2b) and (V-2c), respectively.

Finally, there is a highly abundant fragment at m/z 42, which propably is protonated methylisonitrile. There are numerous possibilities that can give rise to this ion occurring in the low m/z region. One of the pathways, that also was confirmed in the FFFR, is loss of 26 mass units, very likely C_2H_2, from m/z 68.

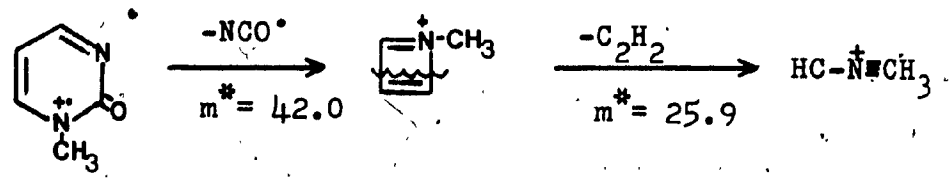

M^+ m/z 110 m/z 68 m/z 42

In the spectrum of (V-2b) this ion appears at m/z 45 (77.5%), which indicates that no significant scrambling of the methyl and ring hydrogens occurs. In the fragmentation pattern of the other labelled compound (V-2c) the

ion appears at m/z 42 and involves loss of C_2HD from m/z 69.

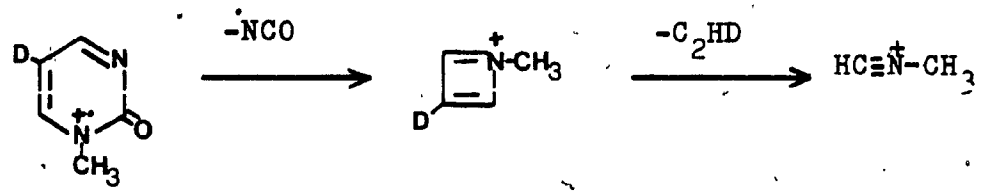

$M^{+\cdot}$ m/z 111 (V-2c) m/z 69 m/z 42

The major fragmentation pathways are outlined in Scheme V-2.

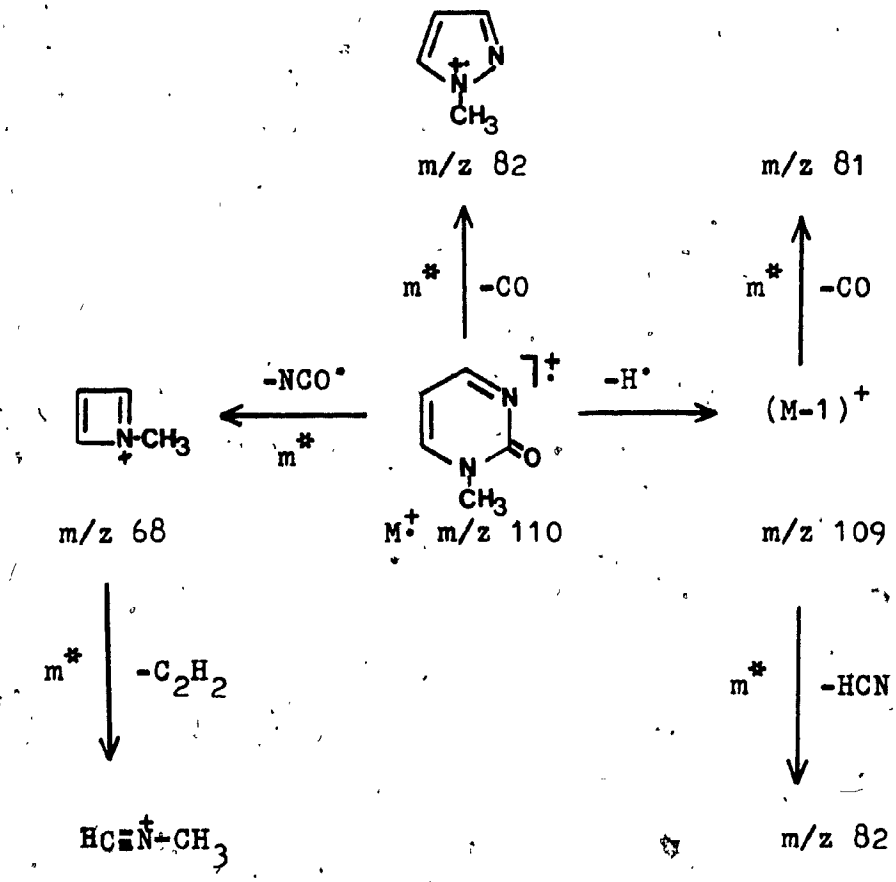

Scheme V-2. Fragmentation pattern for 1-methyl-2-pyrimidinone

1-Ethyl-2-pyrimidinone (V-3a) (Fig. V-3)

The dominant fragmentation pathway for this compound is loss of C_2H_4(28 m.u.) from the molecular ion to form the peak at m/z 96(60.3%). It is believed that this process proceeds by McLafferty rearrangement and very likely gives rise to the unsubstituted 2-pyrimidinone (V-1a). However, the m/z 96 ion also originates from the molecular ion by the expulsion of carbon monoxide (28 m.u.). This was confirmed by the fragmentation pattern of the labelled 1-(ethyl-d_5)-2-pyrimidinone (V-3b). There, the ion due to the loss of CO appears at m/z 101 in relatively low abundance(4.0%), while the expulsion of C_2D_4(32 m.u.), gives an intense peak at m/z 97(60.0%). The latter process was also observed in the FFFR.

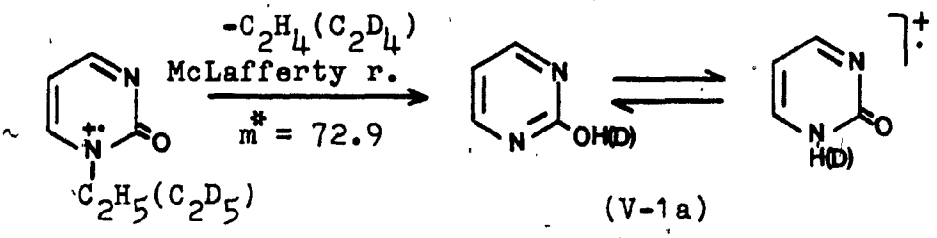

M^+ m/z 124(129) (V-1a) m/z 96(97)

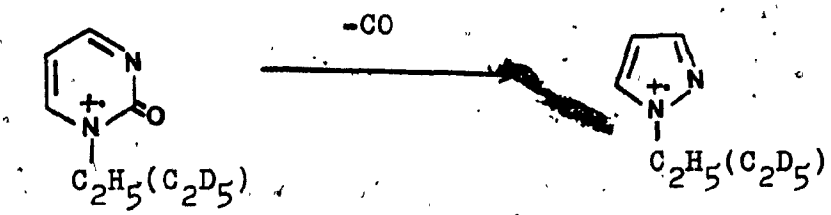

M^+ m/z 124(129) m/z 96(101)

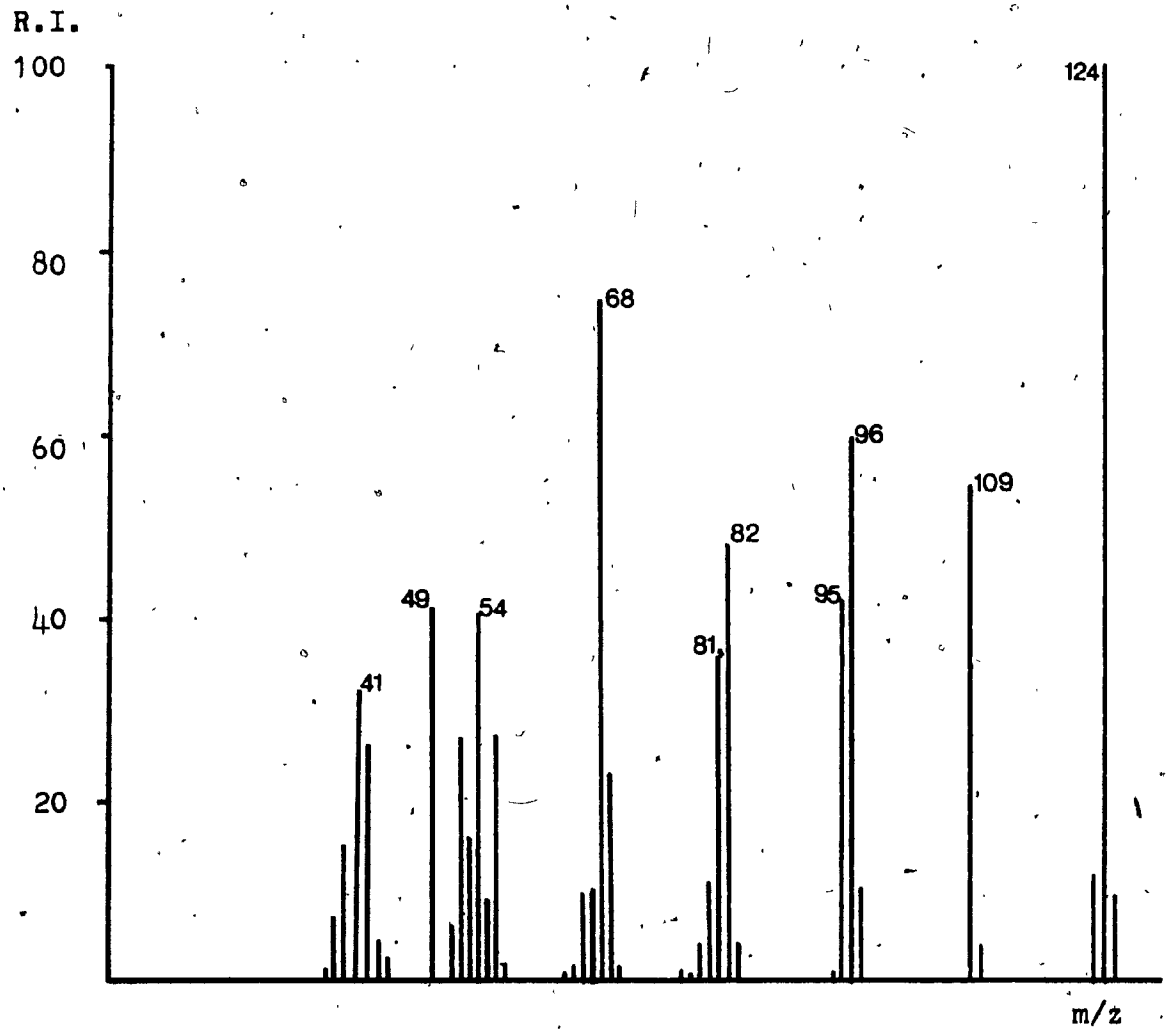

Fig. V-3 Mass spectrum of 1-ethyl-2-pyrimidinone

According to the observed metastable transitions in both field free regions, the fragment at m/z 96 decomposes further by loss of CO to form an intense ion at m/z 68(75.2%), which appears in the spectrum of (V-3b) at m/z 69(86.7%).

The expulsion of methyl radical from the molecular ion forms an abundant ion at m/z 109(55.0%), which in turn fragments by losing CO or HCN to yield the fragments at m/z 81(36.5%) and 82(48.4%), respectively. For the labelled species (V-3b) the three ions appear at m/z 111(80.0%), 83(53.3%) and 84(40.0%).

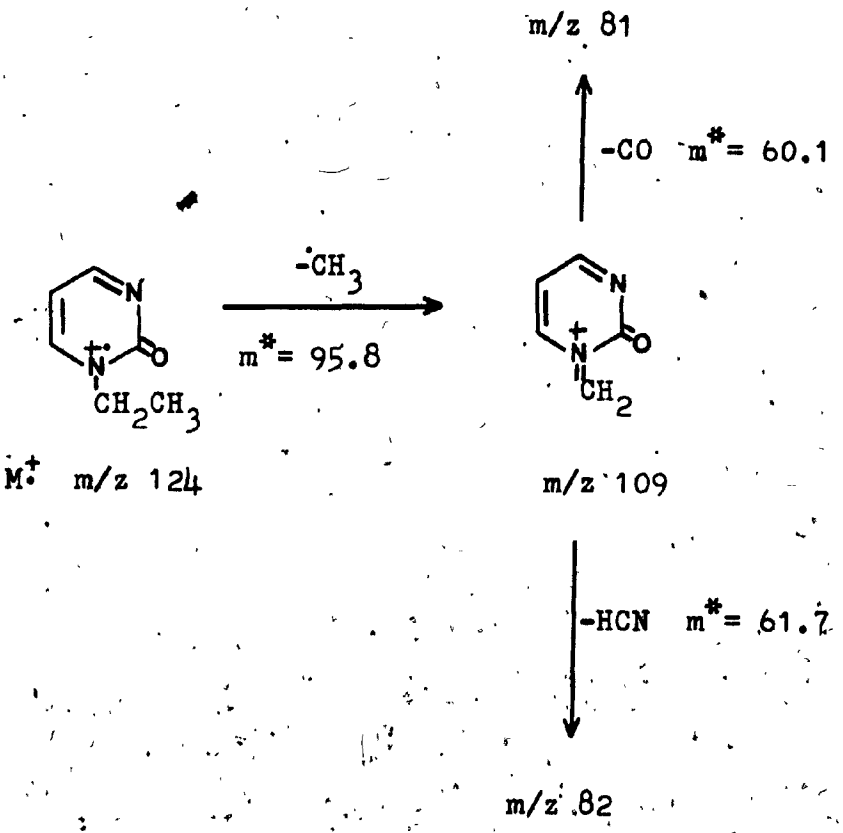

From the peak intensities, the loss of hydrogen from the molecular ion does not seem to be of great importance. However, the minor M-1 ion at m/z 123(12.0%) fragments further in the source and in the FFFR losing C_2H_4.

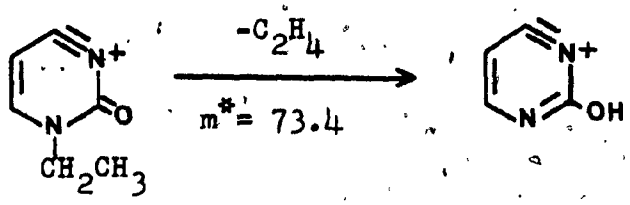

M-1 m/z 123 m/z 95

The analogous process for the labelled species (V-3b) indicates that it is the ring hydrogen that is lost

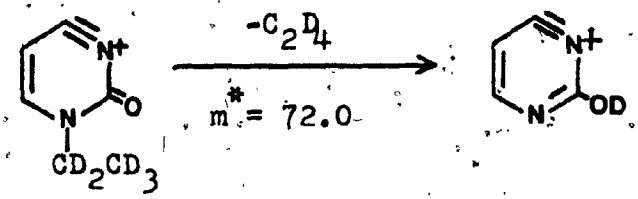

M-1 m/z 128 m/z 96

to form the above M-1 ion.

The main fragmentation pathways are outlined in Scheme V-3.

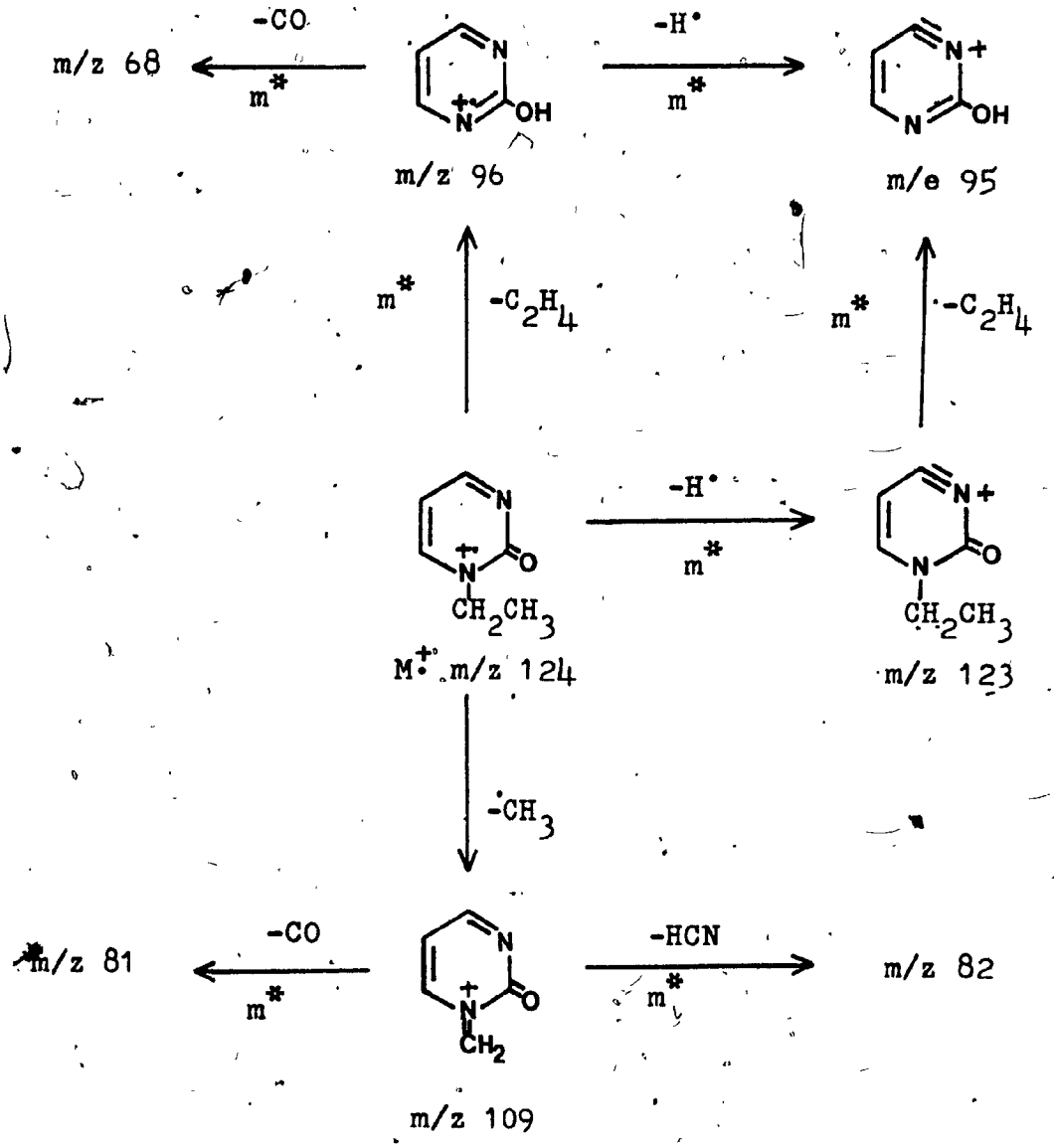

Scheme V-3. Fragmentation pattern for 1-ethyl-2-pyrimidinone

1-Isopropyl-2-pyrimidinone (V-4a) (Fig. V-4)

The base peak in the spectrum of (V-4a) is at

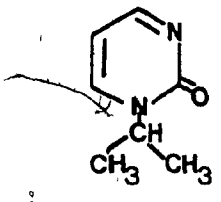

(V-4a)

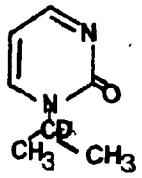

(V-4b)

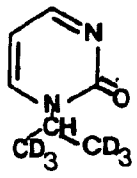

(V-4c)

m/z 97, which most probably originates from the molecular ion by a double hydrogen rearrangement. This process occurs frequently with compounds where an iso-propyl group is present[53]. The driving force for this reaction is very likely formation of the allyl radical and the stable cation (V-4d).

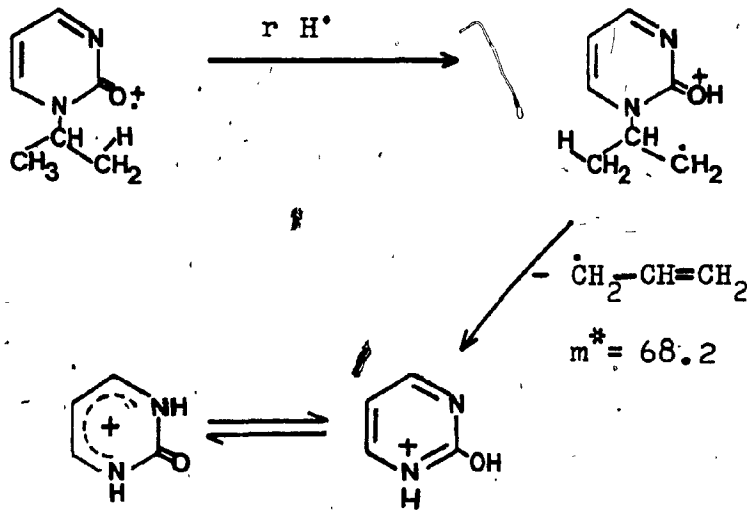

m/z 97 (V-4d)

This process agrees with the fragmentation patterns of the labelled species (V-4b) and (V-4c) where the corresponding

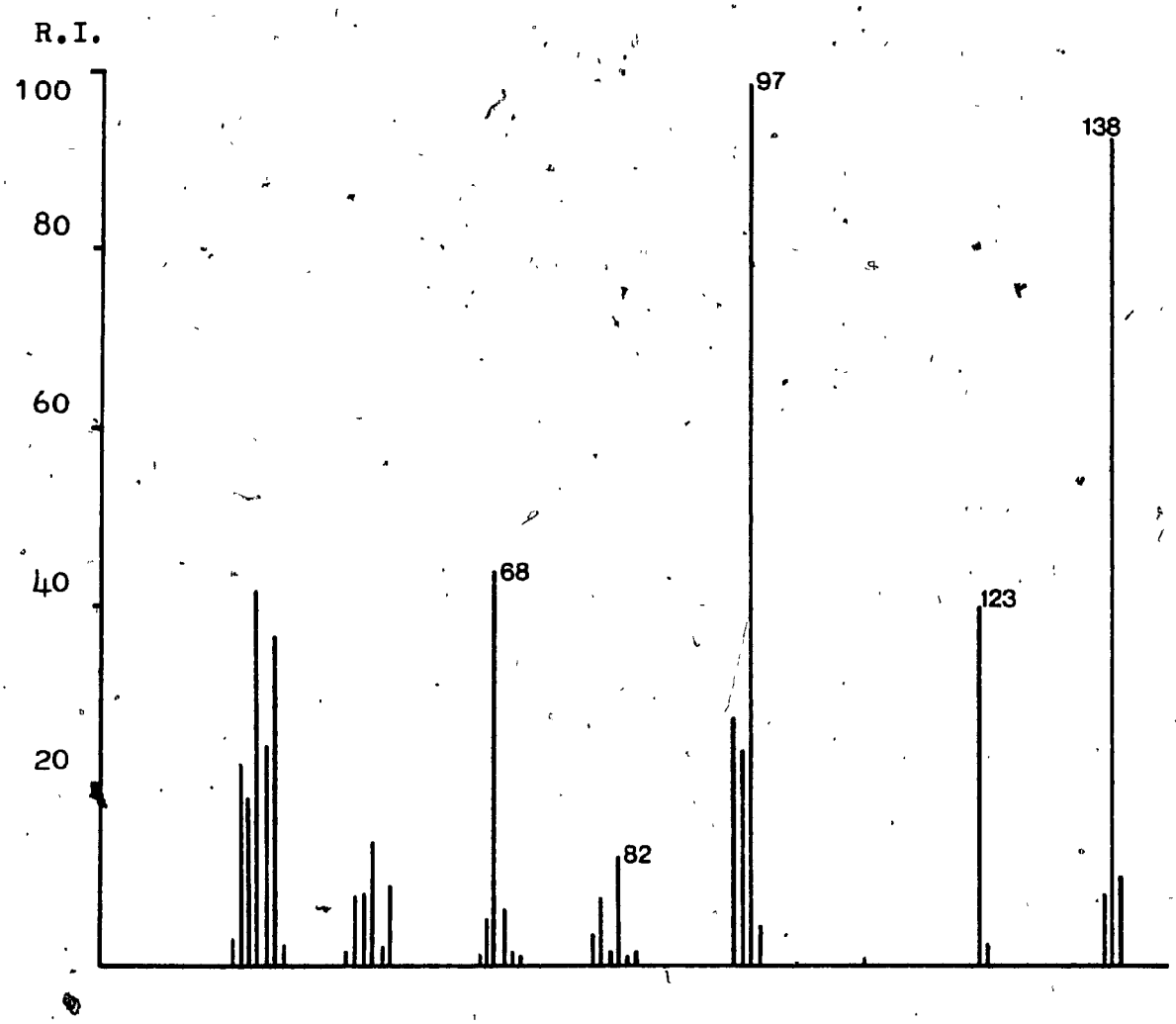

Fig. V-4 Mass spectrum of 1-isopropyl-2-pyrimidinone

ions appear at m/z 97(100.0%) and 99(84.1%), respectively. Obviously, the methyl hydrogens are involved in the transfer to the ring, as shown above.

Loss of a methyl radical from the molecular ion gives a fragment at m/z 123(41.3%) which decomposes further by loss of carbon monoxide or CH_3CN. Metastable decomposition was observed in both field free regions for the three processes and the corresponding fragments in the spectra of the labelled compounds (V-4b) and (V-4c) have intensities comparable with these observed for the unlabelled compound.

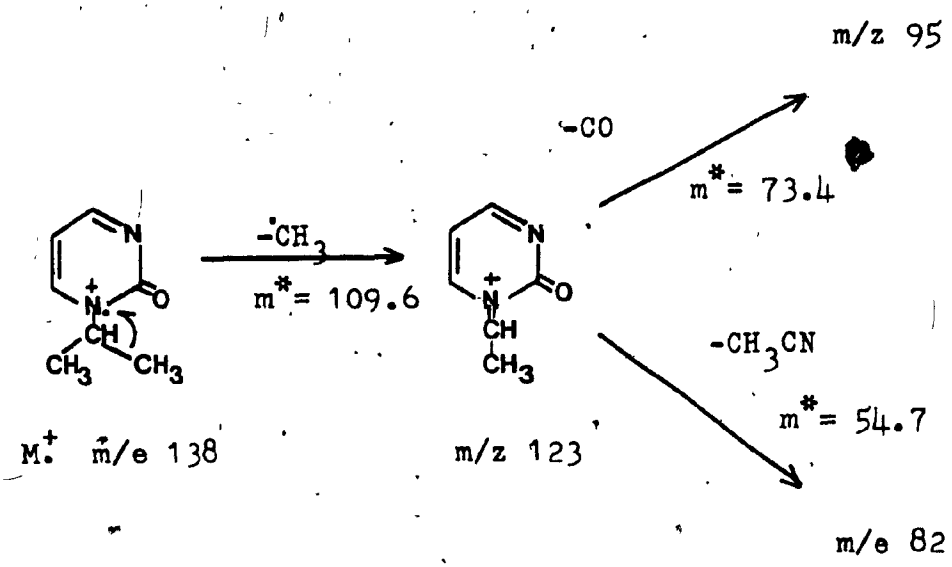

Another significant process, confirmed by the transition in the FFFR, is loss of C_3H_6 from the molecular ion to yield m/z 96(24.6%). By analogy with 1-ethyl-2-pyrimidinone, the decomposition probably proceeds by a

McLafferty rearrangement. The resulting fragment further expels CO to give an ion at m/z 68(44.3%). In the spectra of the labelled species the corresponding two ions appear at m/z 96(40.0%) and 68(72.6%) for (V-4b) and at m/z 97 (29.5%) and 69(33.5%) for (V-4c).

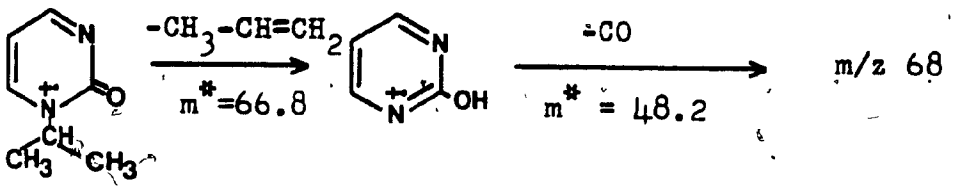

M^+ m/z 138 m/z 96

The expulsion of hydrogen is not very significant in the normal spectrum. However, a relatively intense metastable transition is observed in the FFFR for this process. Moreover, metastable transitions for loss of hydrogen and deuterium were observed in the FFFR for the labelled compounds (V-4b) and (V-4c). It is believed therefore, that the molecular ion expels hydrogen partly from the ring and partly from the isopropyl group.

The major fragmentation pathways are outlined in Scheme V-4.

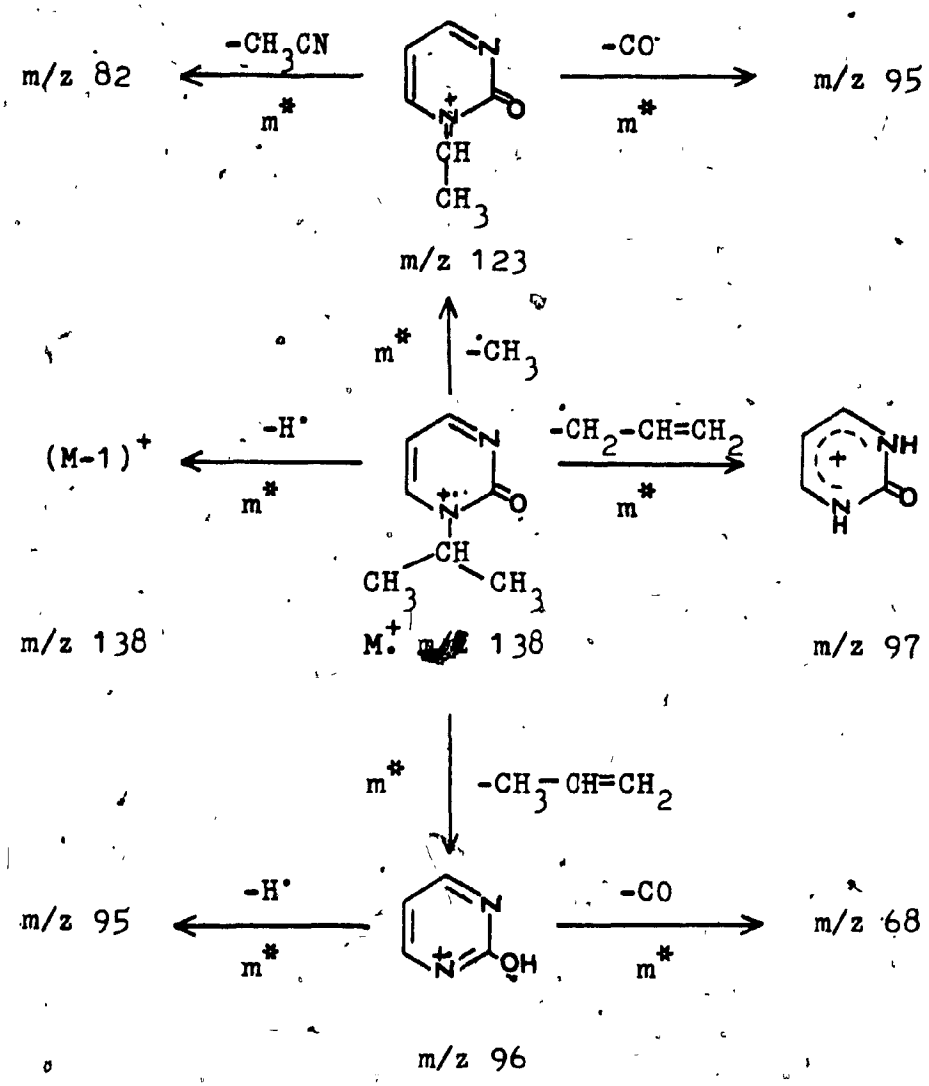

Scheme V-4. Fragmentation pattern for 1-isopropyl-2-pyrimidinone

1-Benzyl-2-pyrimidinone (V-5a) (Fig. V-5)

The most significant fragment in the spectrum of (V-5a) is at m/z 91(87.9%), which almost certainly is

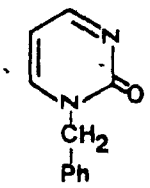

(V-5a)

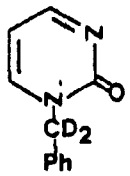

(V-5b)

the tropylium ion. This was confirmed by the metastable transitions for its formation(m/z 186 → 91) and for its successive fragmentation(→ 65 → 39)[54]. It may be formed directly from the parent ion by N-C bond cleavage to form a stable 2-oxypyrimidine radical and benzyl cation which then rearranges to the tropylium ion.

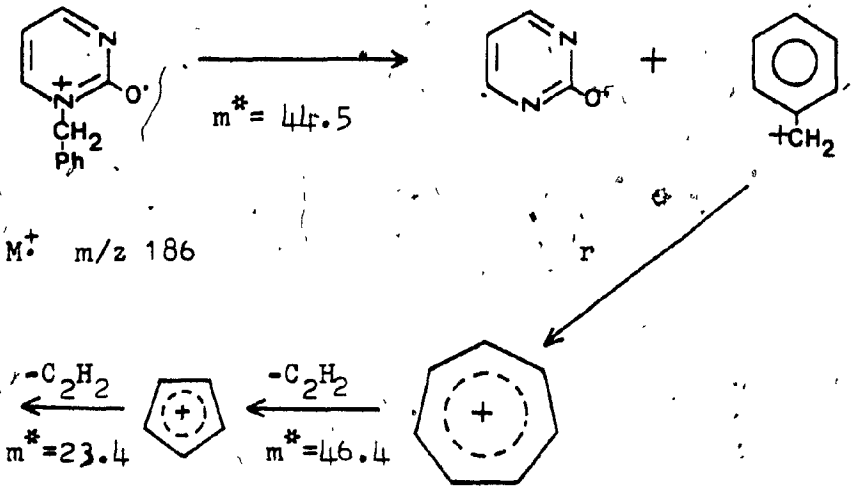

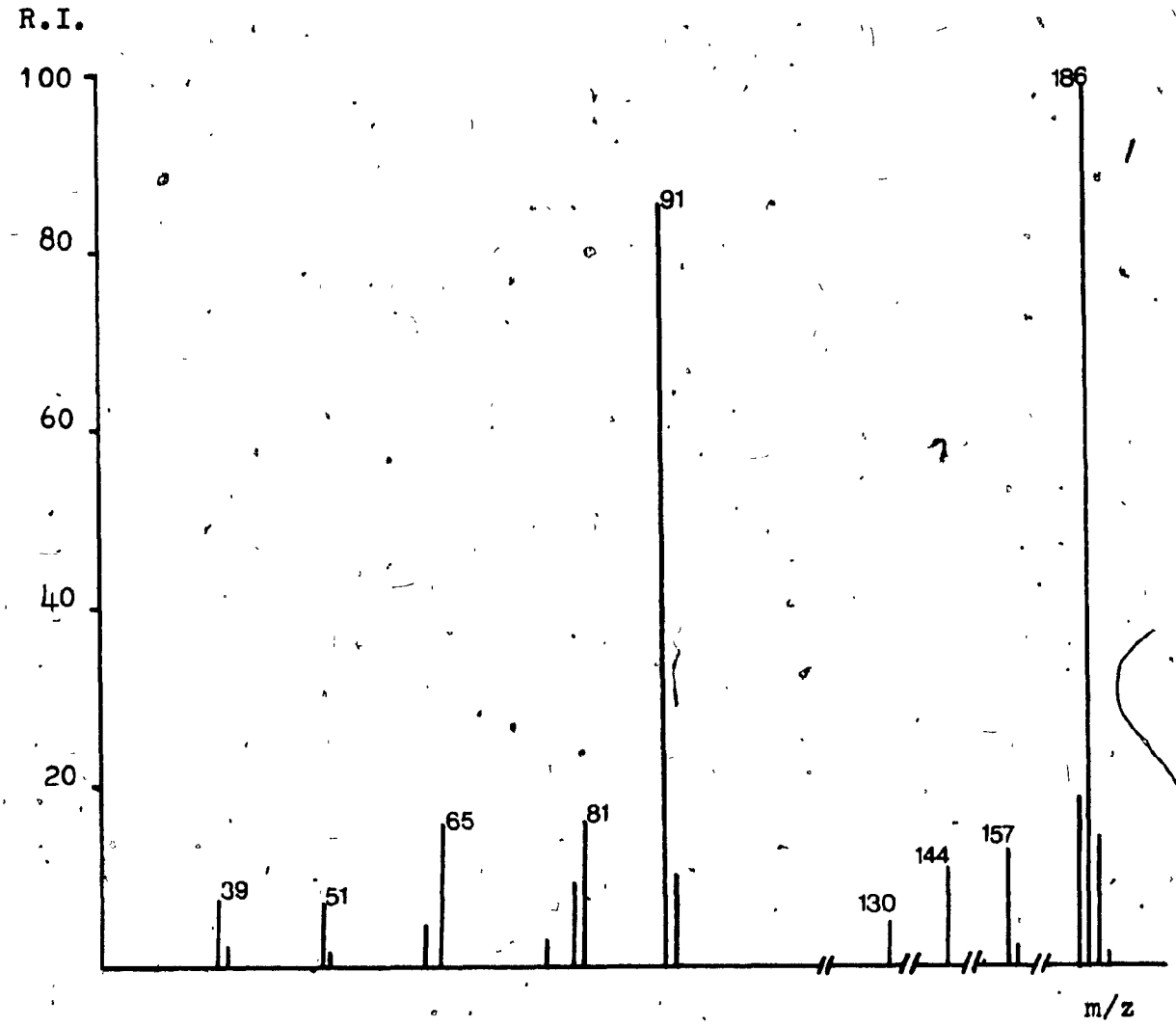

Fig. V-5 Mass spectrum of 1-benzyl-2-pyrimidinone

Judging from the observed transition in the FFFR, the tropylium ion originates also from the $C_7H_8^{\cdot+}$ at m/z 92(10.3%) by loss of hydrogen. The latter ion is probably formed directly from the molecular ion by a hydrogen transfer, a process analogous to the fragmentation of some alkyl benzenes[53].

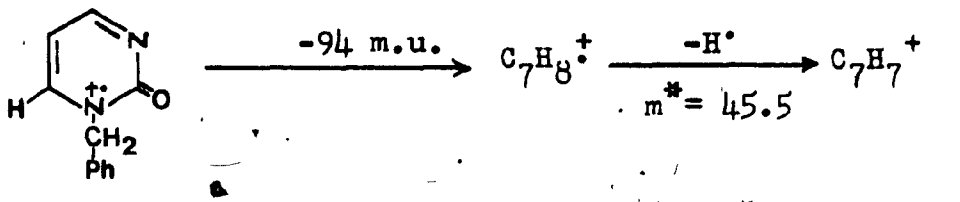

Cooks et al.[20] studied the kinetic energy release accompanying H· loss from $C_7H_8^{\cdot+}$ ions generated as secondary fragments or by direct ionization of toluene and cycloheptatriene(cf.p.29). Based upon these studies it has been suggested that the reactive $C_7H_8^{\cdot+}$ ions react through the same intermediate, probably of the cycloheptatriene structure. In the spectrum of the labelled species (V-5b) the hypothetical tropylium and cycloheptatriene ions possess two deuteriums and appear accordingly at m/z 93(100%) and 94(13.5%) respectively.

The formation of the M-1 ion was also observed in the FFFR. Examination of the labelled species (V-5b) revealed that beside the pyrimidine and/or the phenyl ring hydrogens, also the benzylic hydrogens are involved in the process. However,no metastable peak was observed for the latter.

There are three minor fragments in the high mass region, at m/z 144(12.5%), 130(6.5%) and 157(14.0%). In accord with the spectrum of (V-5b), these ions are due to the expulsion of NCO• from the molecular ion, and HCNCO and CO from the M-1 ion.

The analyzed processes are summarized in Scheme V-5.

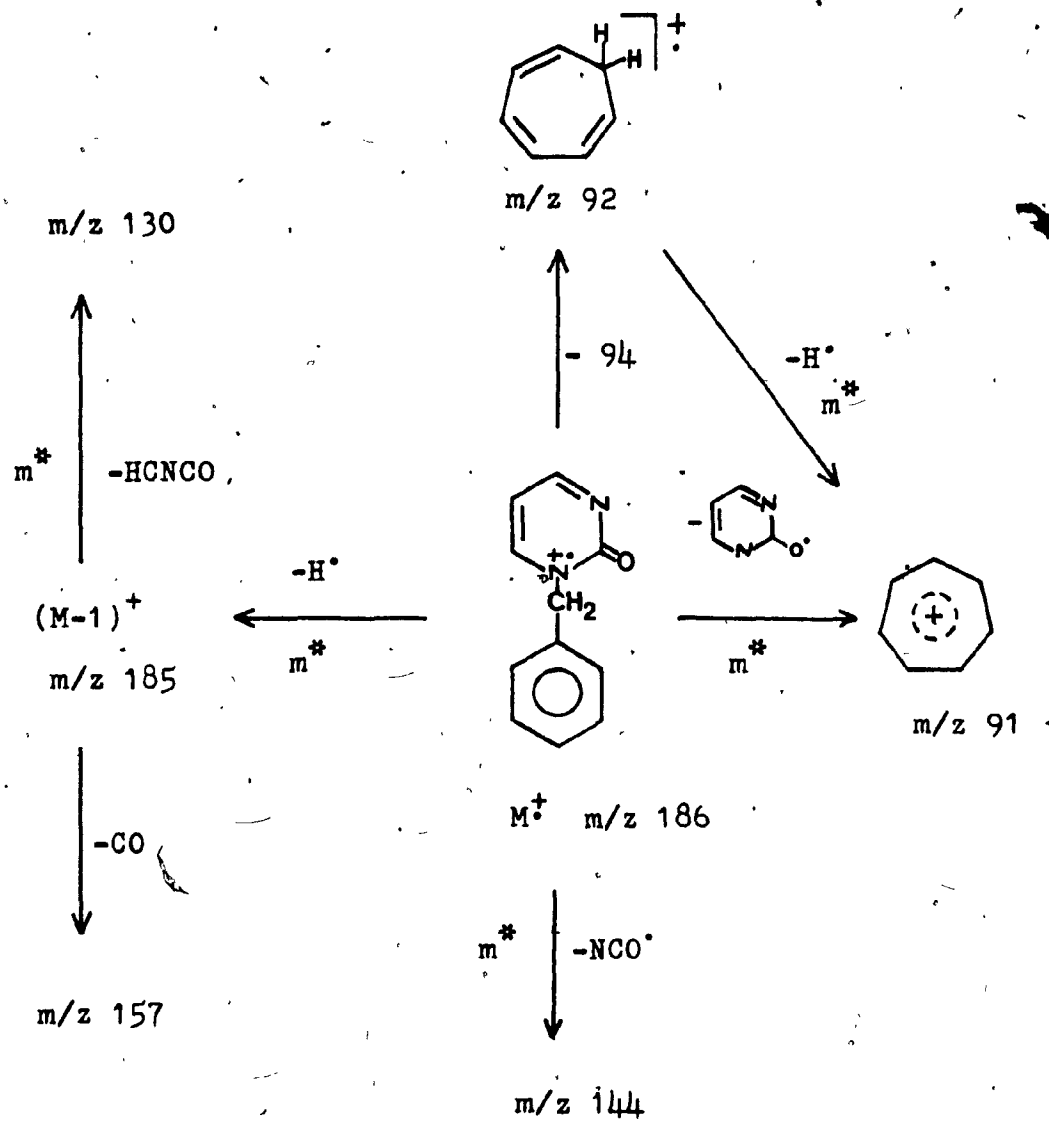

Scheme V-5. Fragmentation pattern for 1-benzyl-2-pyrimidinone

1-Phenyl-2-pyrimidinone (V-6a) (Fig. V-6)

The molecular ion of (V-6a) loses hydrogen to an appreciable extent to form the M-1 ion at m/z 171 (41.7%).

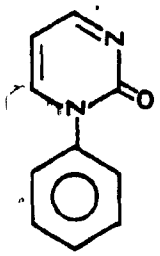

(V-6a)

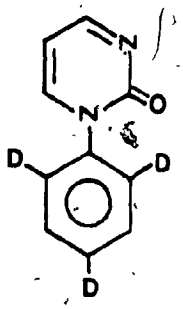

(V-6b)

It was suggested previously[11] that the hydrogen loss involves an ortho position of the benzene ring and that the resulting ion assumes an oxazolium structure. A similar process has been suggested for the fragmentation pattern of 1-phenyl-2-pyridone[55].

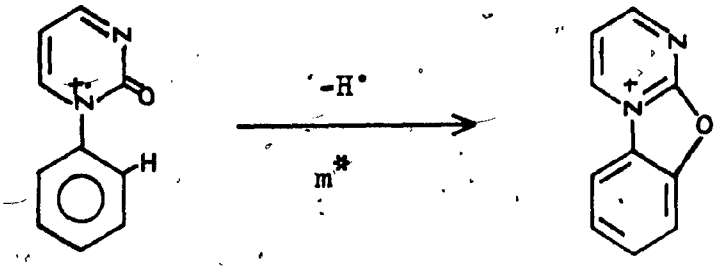

$M^{+\cdot}$ m/z 172 m/z 171

However, the fragmentation pattern of the labelled compound (V-6b) proved otherwise and helped to discern the processes involved in the formation of the M-1 ion.

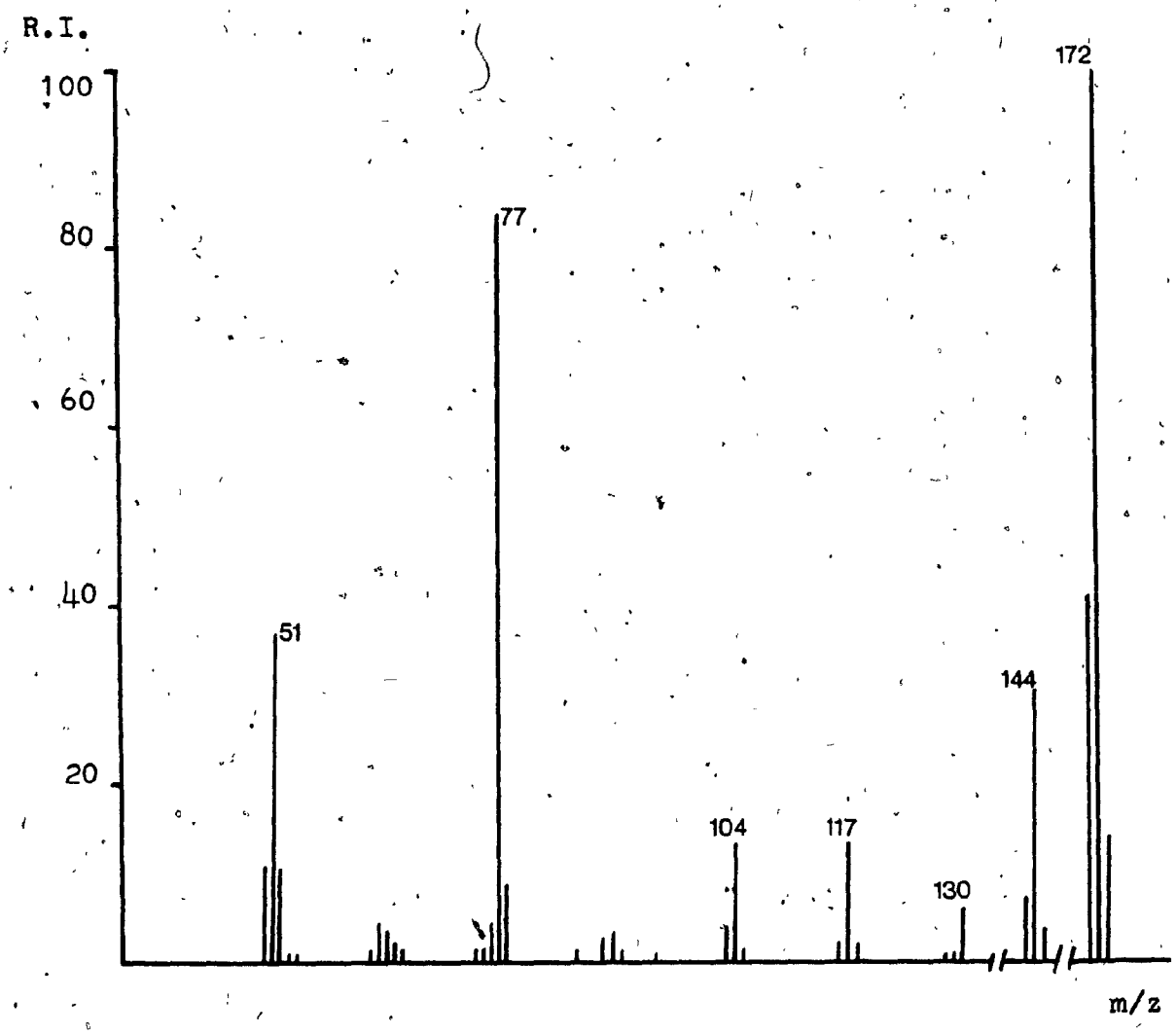

Fig. V-6 Mass spectrum of 1-phenyl-2-pyrimidinone

The conventional spectrum of (V-6b) shows an intense M-1 ion(58.3%), and less intense M-2 ion(19.5%). It should be noted, that due to the relatively poor deuterium incorporation (~70%), the M-1 fragment also contains to some extent the molecular ion of the partially labelled species. This problem did not preclude distinguishing between loss of hydrogen and deuterium when the metastable processes were examined. The following decompositions in the FFFR were observed, measured under the same experimental conditions.

(i) Strong metastable peaks of comparable intensities for loss of H$^{\bullet}$ from the molecular ions of (V-6a) and (V-6b).

(ii) A very weak metastable peak for loss of D$^{\bullet}$ from the molecular ion of (V-6b), and a very weak metastable peak for the process (M-1)-1, also therein.

(iii) No metastable transition for processes M-2 or (M-1)-1 in the spectrum of the unlabelled (V-6a).

Even if a deuterium isotope effect is considered, the above observations indicate that loss of hydrogen for the ortho(and/or para) position(s) of the phenyl ring is of minor importance. Thus it is not the hypothetical oxazolium fragment which is mainly responsible for the intense M-1 ion. This behaviour is in contrast to that of the sulfur analogue(cf.p.121).

The remaining fragments to be discussed all appear in the spectrum of the labelled species at 3 mass units higher. This means that they all still contain the benzene ring in some form and originate by various fragmentations of the pyrimidine ring.

The second most abundant peak after the base peak is at m/z 77(83.3%) and is most probably the phenyl cation $C_6H_5^+$. It could originate from more than one ionic species. One of the confirmed pathways is loss of the stable 2-oxypyrimidine radical from the molecular ion.

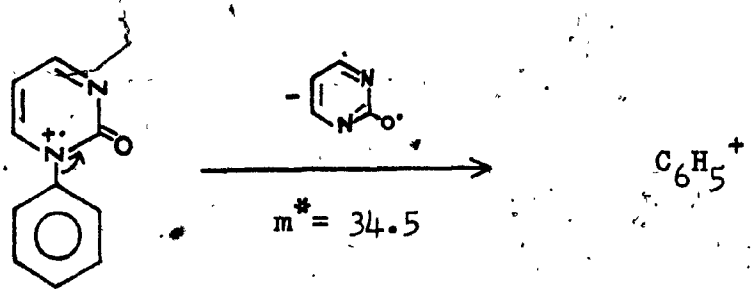

m/z 172 m/z 77

The molecular ion also expels CO to form a fragment of medium intensity at m/z 144(31.7%). However, there is another pathway that leads to this ion, namely, the loss of HCN from the M-1 ion. The fragment at m/z 144 further expels another molecule of HCN.

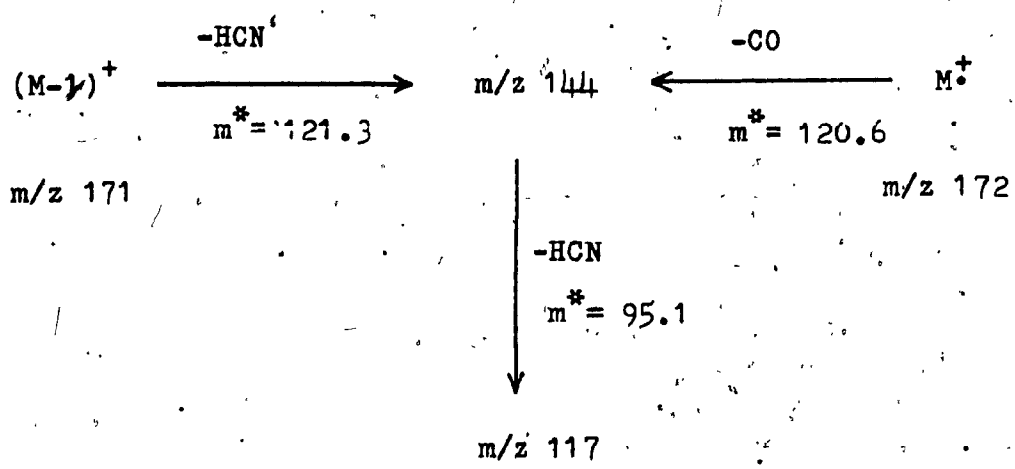

The fragment at m/z 130 arises from the molecular ion by loss $NCO^{\bullet}$. A possible structure for the ion at m/z 104 could be $PhN^{+}{=}CH$, which can originate from almost any of the above fragments.

Finally, the ion at m/z 51(38.3%), most probably $C_4H_3^+$, is associated with the loss of acetylene from the phenyl cation[56].

The major fragmentation pathways are outlined in Scheme V-6.

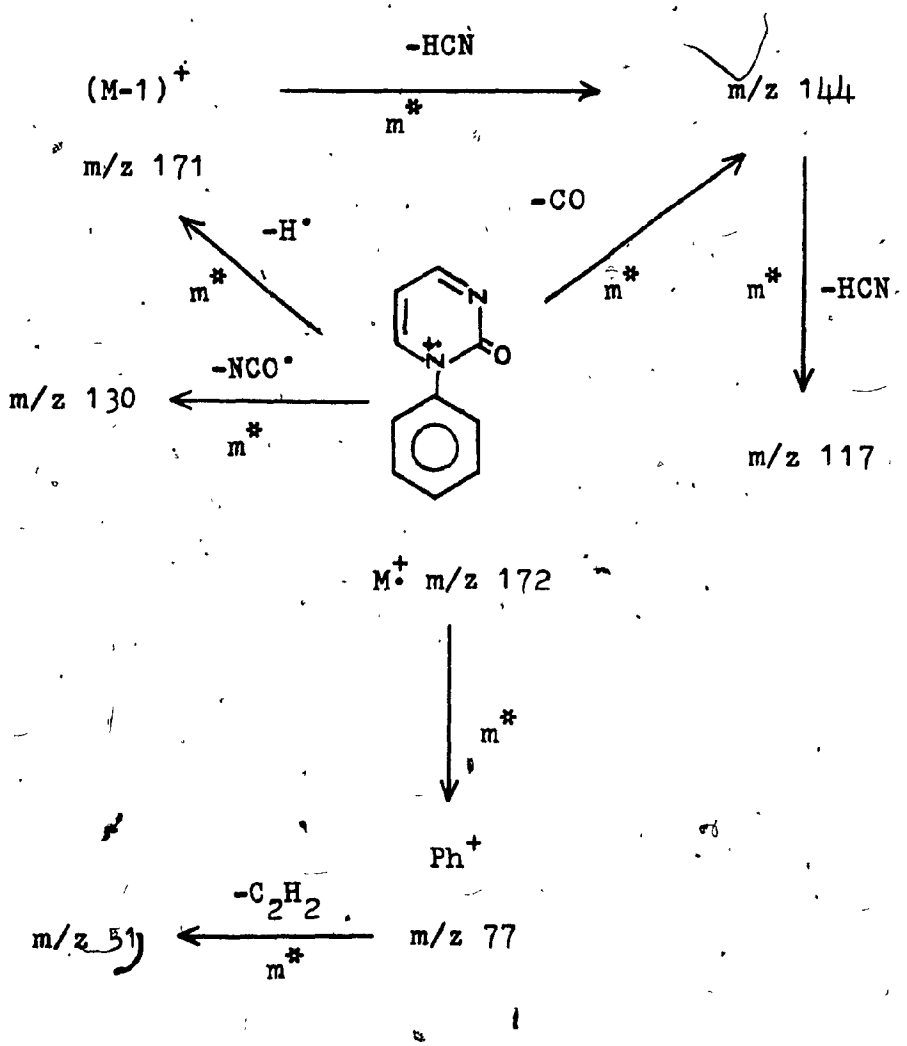

Scheme V-6. Fragmentation pattern for 1-phenyl-2-pyrimidinone

2-Pyrimidinthione (V-7a) (Fig. V-7)

The molecular ion of (V-7a) loses hydrogen to form a peak of medium intensity at m/z 111(13.5%).

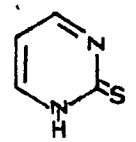

(V-7a)

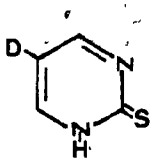

(V-7b)

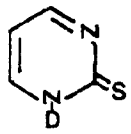

(V-7c)

As apparent from the spectra of the labelled compounds (V-7b) and (V-7c) it is the hydrogen from the 4 or 6 position of the ring that contributes mainly to the M-1 ion. In contrast to 2-pyrimidinone, a strong metastable peak was observed in the FFFR for this process. Moreover a weak metastable transition was detected also for loss of D· from the molecular ion of (V-7c)

By analogy with its oxo-homologue, the molecular ion probably loses CS and HCN to form fragments at m/z 68 (33.3%) and 85(17.2%). The ion at m/z 85 decomposes further by loss of HCN and H·.

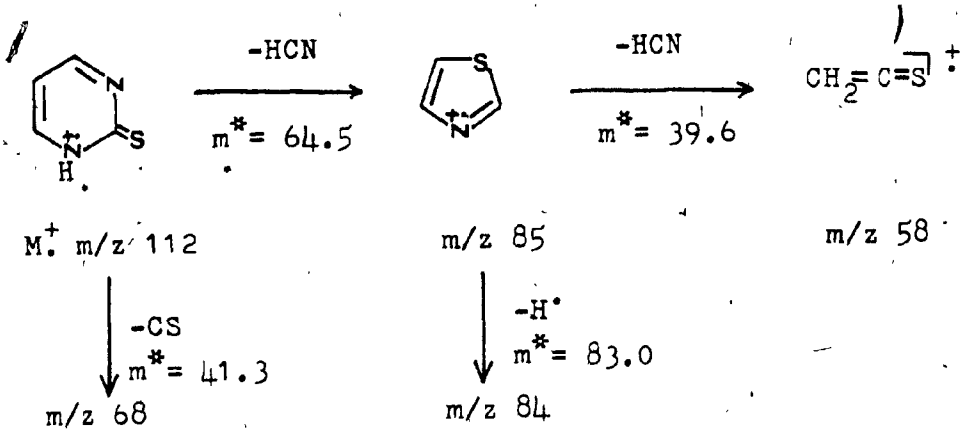

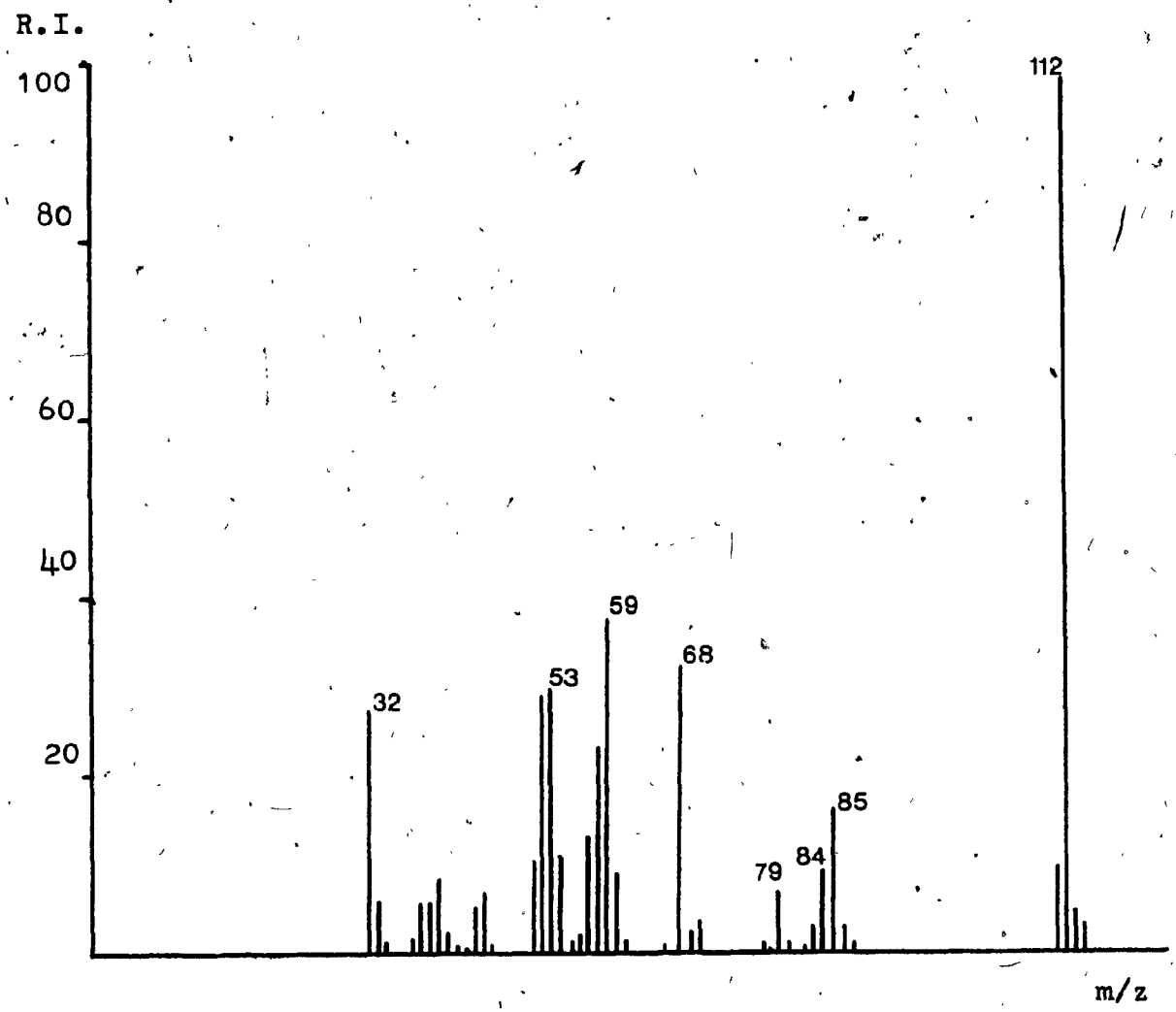

Fig. V-7 Mass spectrum of 2-pyrimidinthione

A second origin of the ion at m/z 84 is loss of HCN from the M-1 ion.

The small peak at m/z 79(7.8%) is due to loss of SH· from the molecular ion.

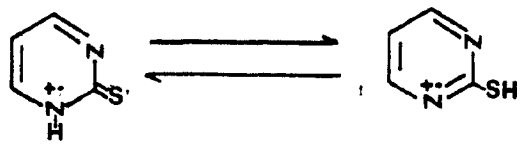

M^+ m/z 112

$-SH\cdot$ $m^* = 55.7$

$C_4H_3N_2$

m/z 79

In addition to the metastable peaks observed for the above processes, the corresponding products of decomposition appear as expected in the spectrum of the labelled compound (V-7b) at one m/z higher and have comparable intensities.

The most abundant fragment after the base peak is at m/z 59(38.9%). It is most probably the isothiocyanate ion, $HNCS^+$, but its origin is obscure.

The major fragmentation pathways are outlined in Scheme V-7.

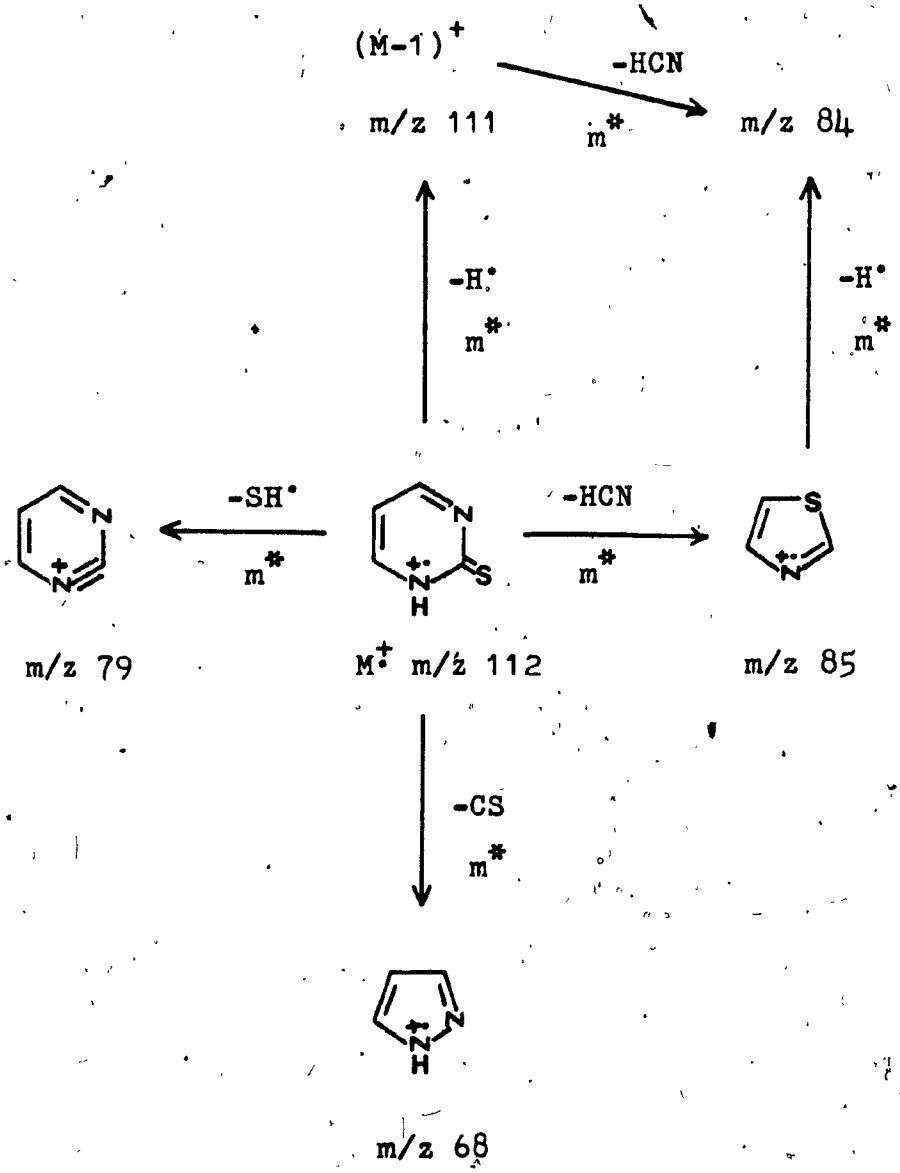

Scheme V-7. Fragmentation pattern for 2-pyrimidinthione

1-Methyl-2-pyrimidinthione (V-8a) (Fig. V-8)

Loss of NCS· from the molecular ion of (V-8a) to form the relatively abundant peak at m/z 68(22.2%) appears to be the major fragmentation route. In accord with

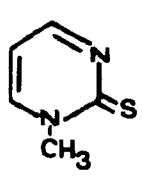

(V-8a)

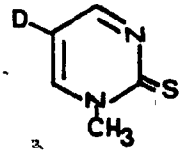

(V-8b)

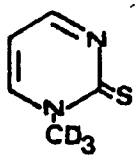

(V-8c)

this route the labelled compounds (V-8b) and (V-8c) show corresponding peaks at m/z 69 and 71 respectively.

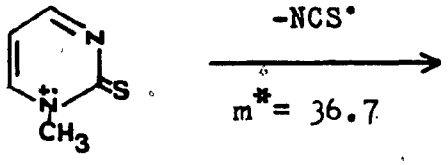

$M^{+\cdot}$ m/z 126

Loss of SH· from the molecular ion forms a relatively minor fragment at m/z 93(2.5%), however, a strong metastable peak in the FFFR was observed for this process. The resulting fragment expels HCN to yield the ion at m/z 66(16.1%).

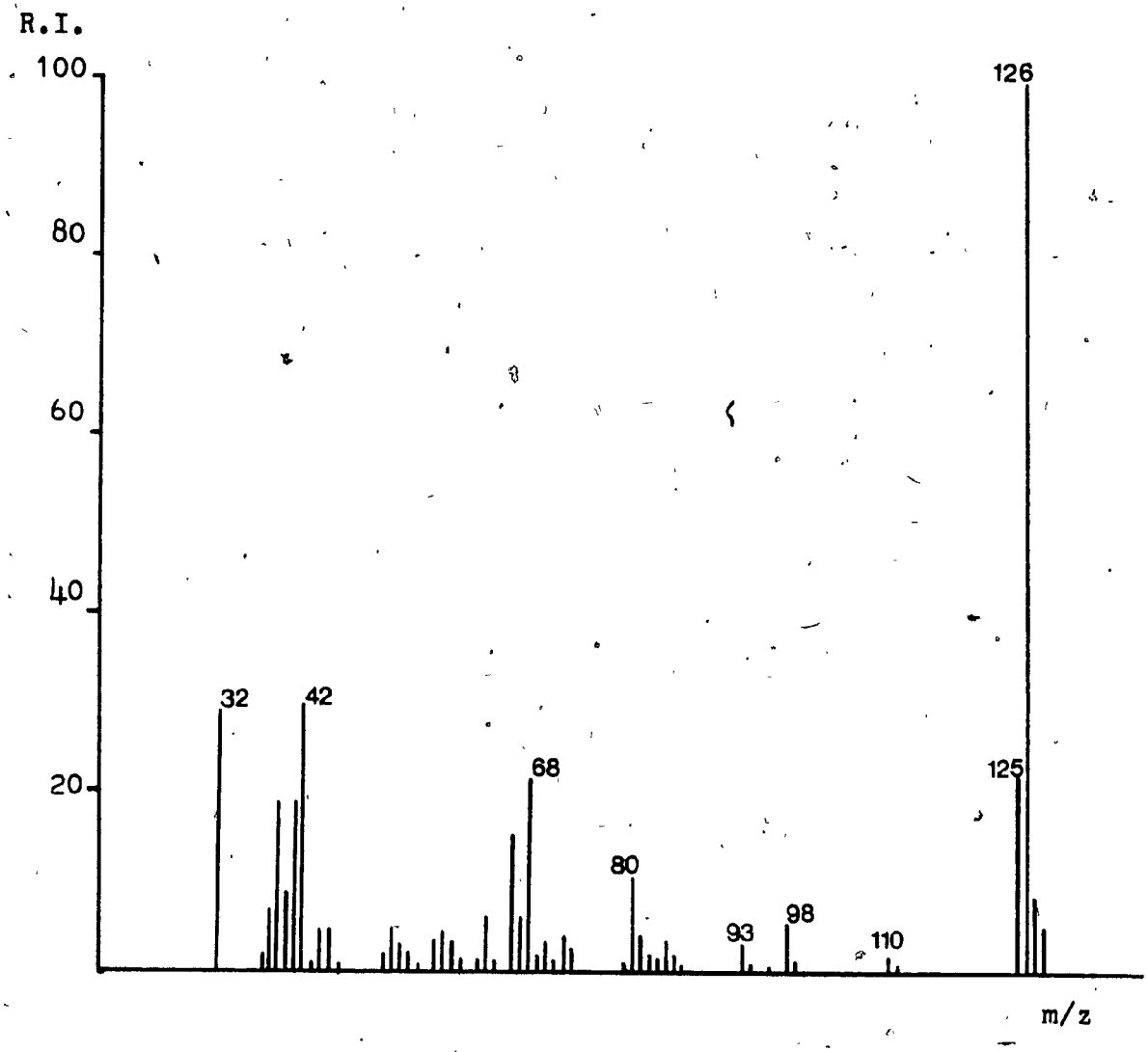

Fig. V-8 Mass spectrum of 1-methyl-2-pyrimidinthione

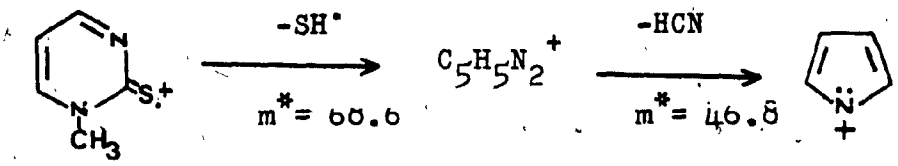

$M^{+\cdot}$ m/z 126 m/z 93 m/z 66

The ion at m/z 80(10.8%), which appears in the spectra of both labelled compounds at m/z 81, is due to the expulsion of CH_2S from the molecular ion. It could be that the nucleophilic sulfur attacks the methyl carbon, followed by hydrogen transfer to the ring. The driving force for this reaction would be formation of the stable pyrimidinium ion.

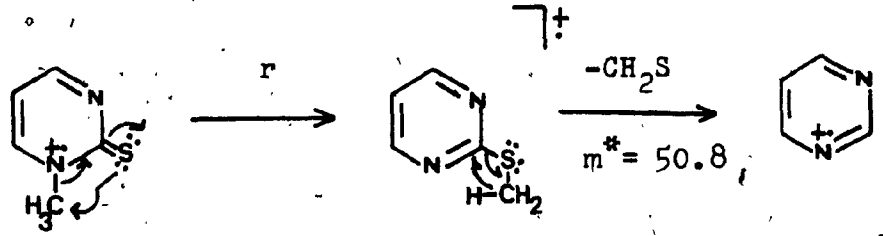

m/z 80

$M^{+\cdot}$ m/z 126

Loss of CS from the molecular ion is insignificant. However, it is expelled to some extent together with HCN from the M-1 ion.

Similar to the unsubstituted 2-pyrimidinthione, the molecular ion loses hydrogen from two sites, i.e. partly from the ring and partly from the substituent on nitrogen. The two processes are discerned in the mass spectrum of the labelled species (V-8c), where a strong metastable peak in the FFFR was observed for loss of deuterium from the molecular ion.

It was suggested previously that formation of the ring with sulphur is the driving force for the latter process[11].

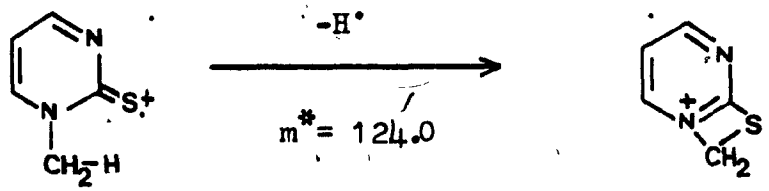

$M^{+\cdot}$ m/z 126 m/z 125

The main fragmentation pathways are outlined in Scheme V-8.

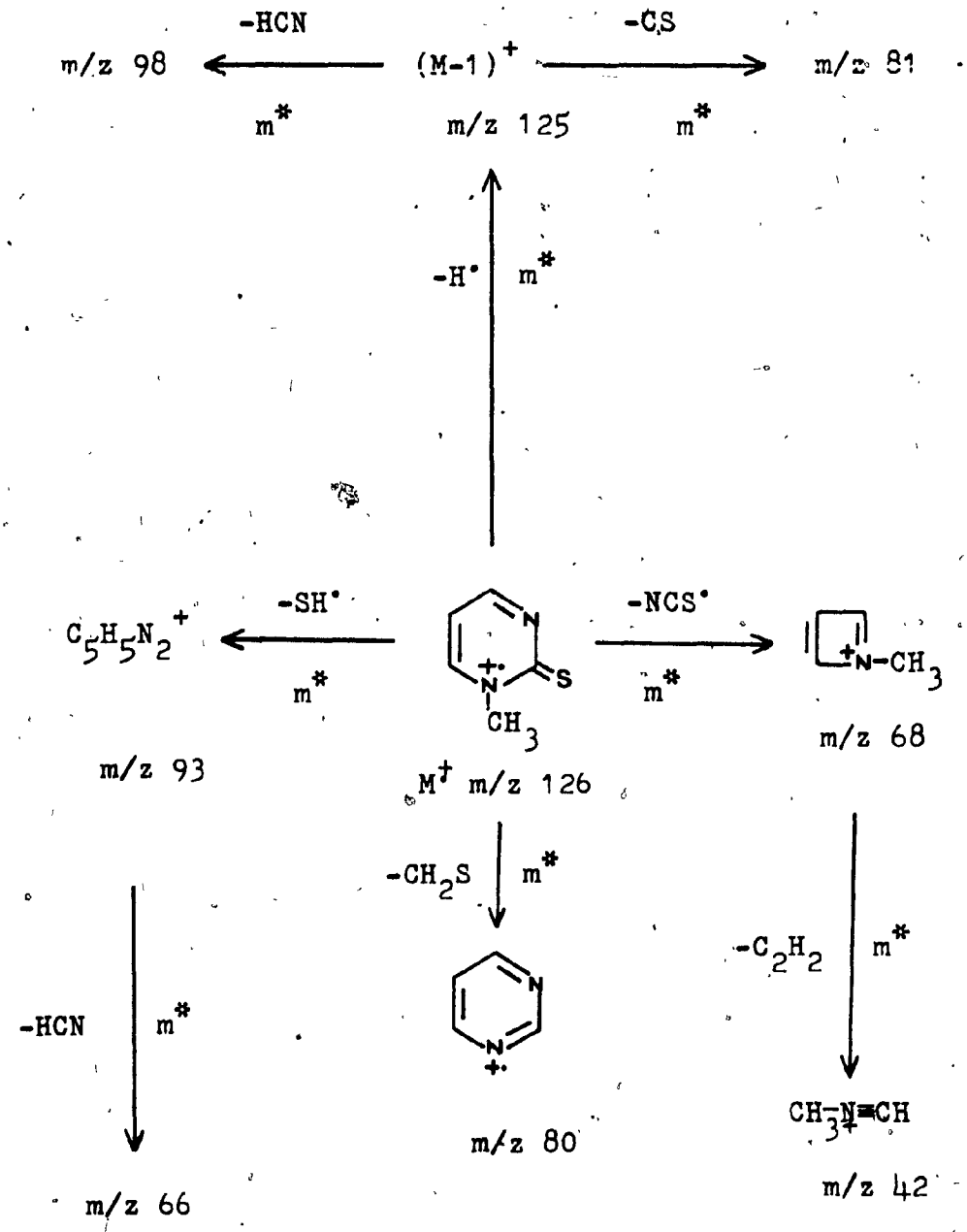

Scheme V-8. Fragmentation pattern for 1-methyl-2-pyrimidinthione

1-Ethyl-2-pyrimidinthione (V-9a) (Fig. V-9)

The molecular ion undergoes McLafferty rearrangement, as does its oxygen analogue, and loses ethylene to give an intense peak at m/z 112(77.8%).

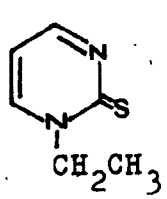

(V-9a)

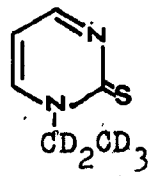

(V-9b)

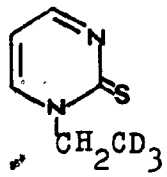

(V-9c)

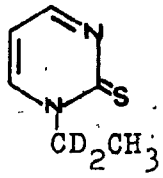

(V-9d)

In the spectrum of the labelled compound (V-9b) the corresponding ion forms the second most intense peak after the base peak and appears at m/z 113(44.7%). The resulting fragment, which probably adopts the 2-pyrimidinthione structure, fragments further, as indicated below.

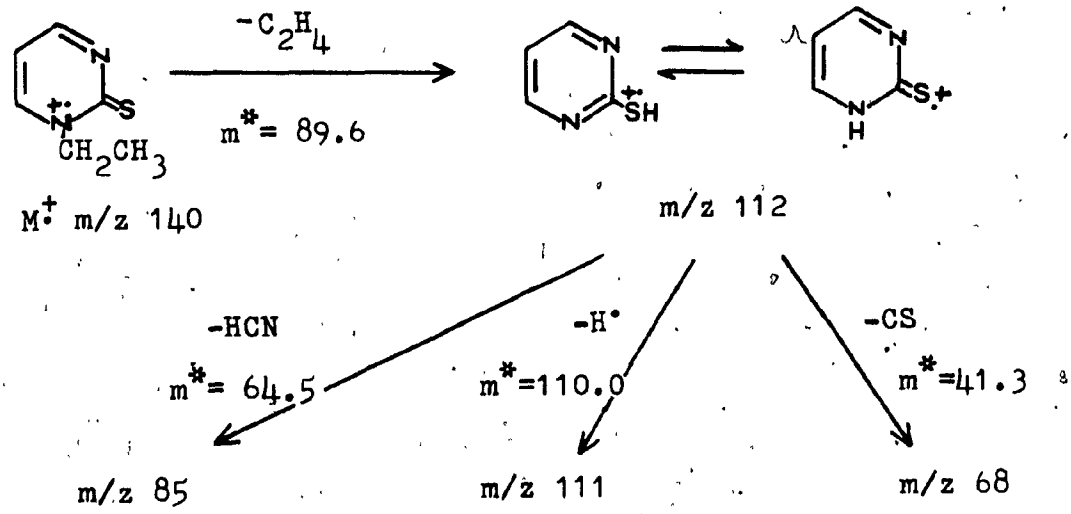

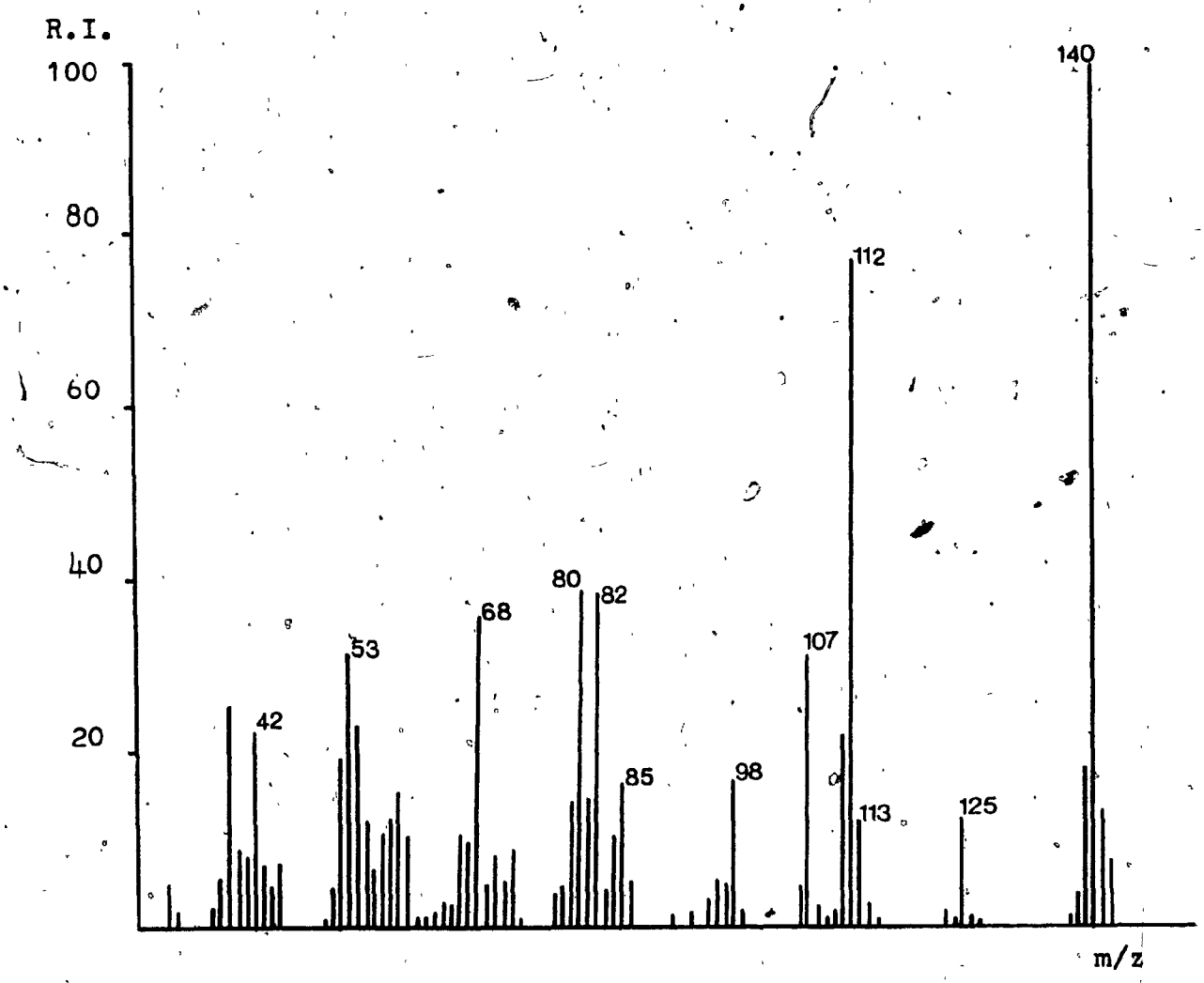

Fig. V-9 Mass spectrum of 1-ethyl-2-pyrimidinthione

The corresponding decomposition products appear in the spectrum of the labelled compound (V-9b) at m/z 87(due to loss of HCN), 112 and 111(due to loss of H° and D°, cf. (V-7b))and 69(loss of CS).

Expulsion of CH_3° from the molecular ion gives the fragment at m/z 125(13.3%), which further decomposes by loss of HCN to form an ion at m/z 98(18.3%).

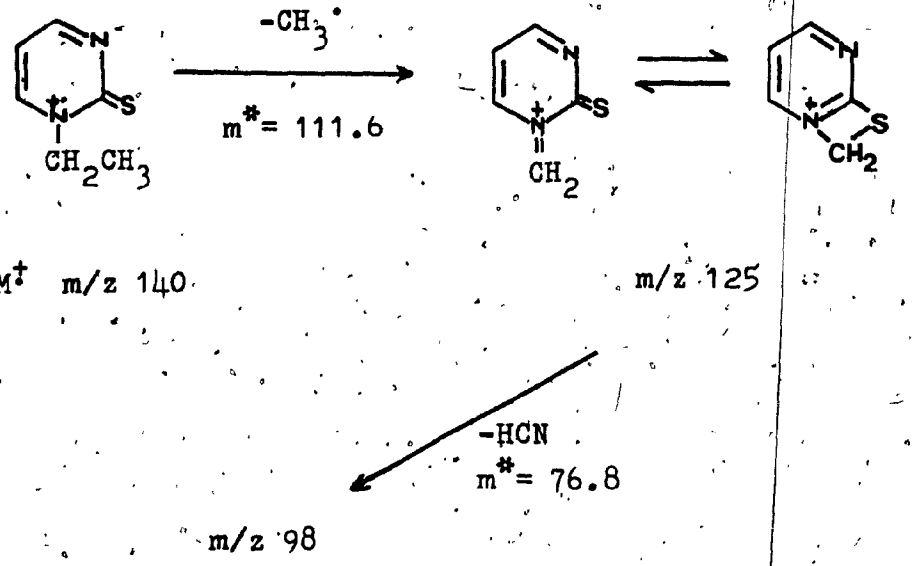

In view of the observed metastable decompositions, the molecular ion also loses SH°,60m.u.(probably ethylene sulfide), 80 m.u.(probably pyrimidine) and NCS°.

Some features of the fragmentation of 1-ethyl-2-pyrimidinthione are discussed in more detail in the next section. There is evidence that the molecular ion expels hydrogen from three sites, i.e. from the ring, from the methylene group and from the methyl group. Moreover, the M-1 ion, formed by loss of the ring hydrogen, further expels a C_2H_4 molecule. This process probably involves a proton transfer to sulphur, a sort of McLafferty rearrangement.

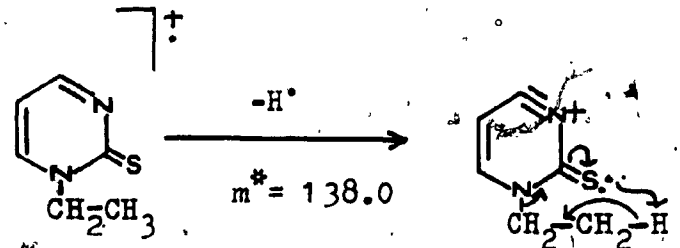

$M^{+\cdot}$ m/z 140 m/z 139

$-C_2H_4$

m* = 88.6

$C_4H_3N_2S^+$ m/z 111

The above discussed fragments all appear in the mass spectra of the labelled compounds (V-9c) and (V-9d) in comparable intensities.

The main fragmentation pathways are outlined

in Scheme V-9.

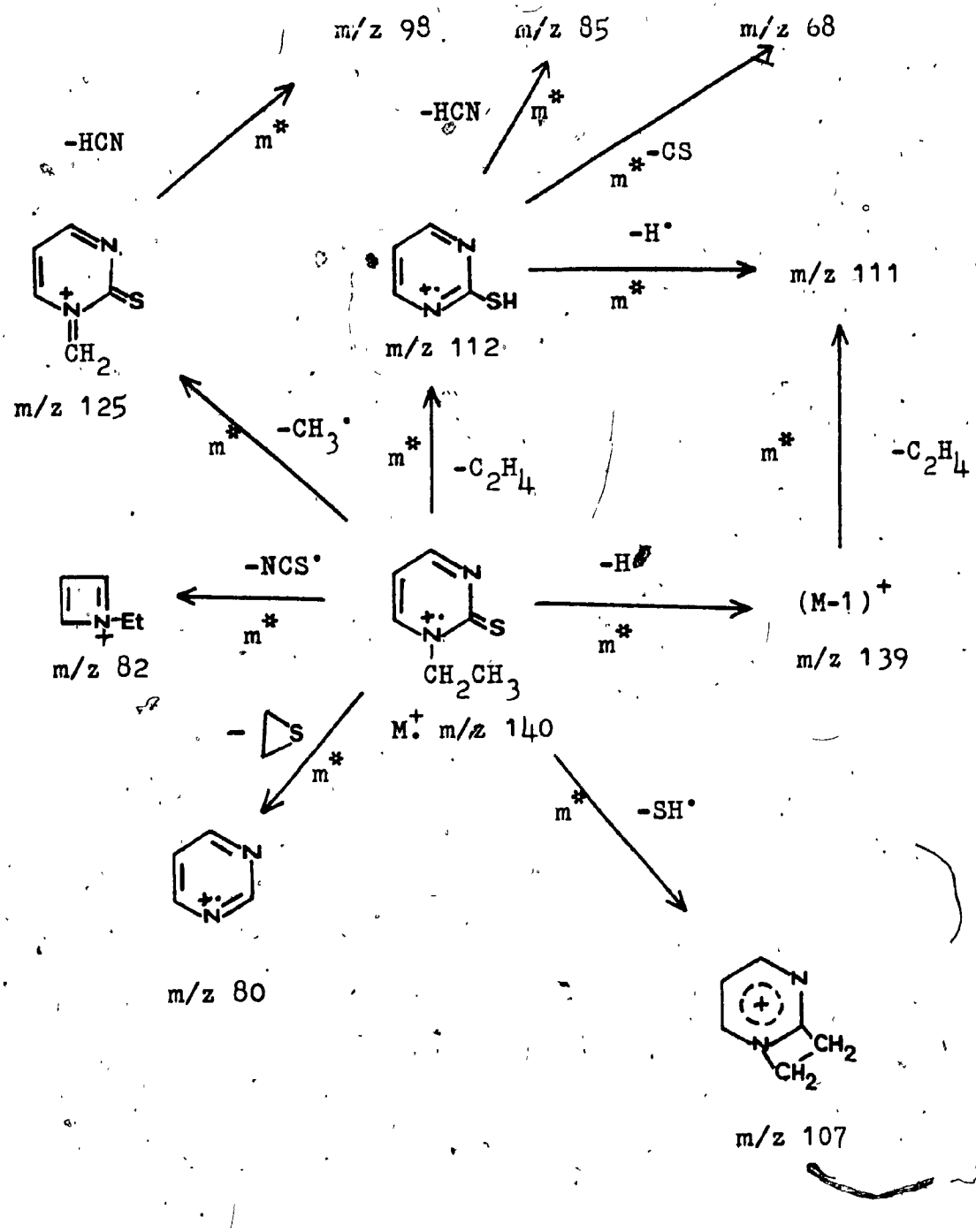

Scheme V-9. Fragmentation pattern for 1-ethyl-2-pyrimidinthione

1-Phenyl-2-pyrimidinthione (V-10a) Fig. (V-10)

The spectrum of this compound is very simple and the dominant peak is at M-1. Moreover, this peak carries 25% of the total ionization current. It was suggested

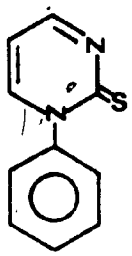

(V-10a)

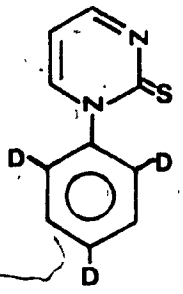

(V-10b)

earlier[11] that as in the case of 1-phenyl-2-pyrimidinone the lost hydrogen probably comes from the benzene ring by a process which is an intramolecular radical substitution reaction.

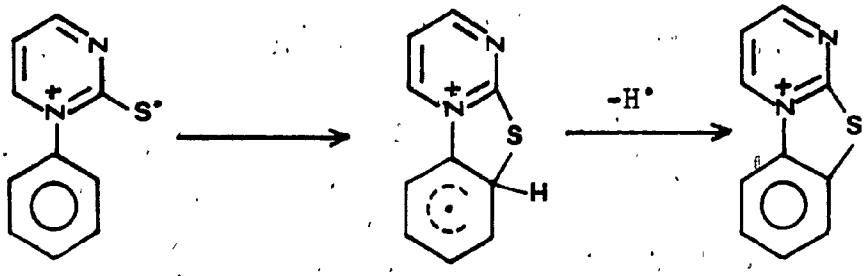

$M^{+\bullet}$ m/z 188

m/z 187

The fragmentation patterns of (V-10a) and the labelled (V-10b) differ significantly from the two corresponding oxo homologues (V-6a) and (V-6b), though the deuterium incorporation is the same(~70%).

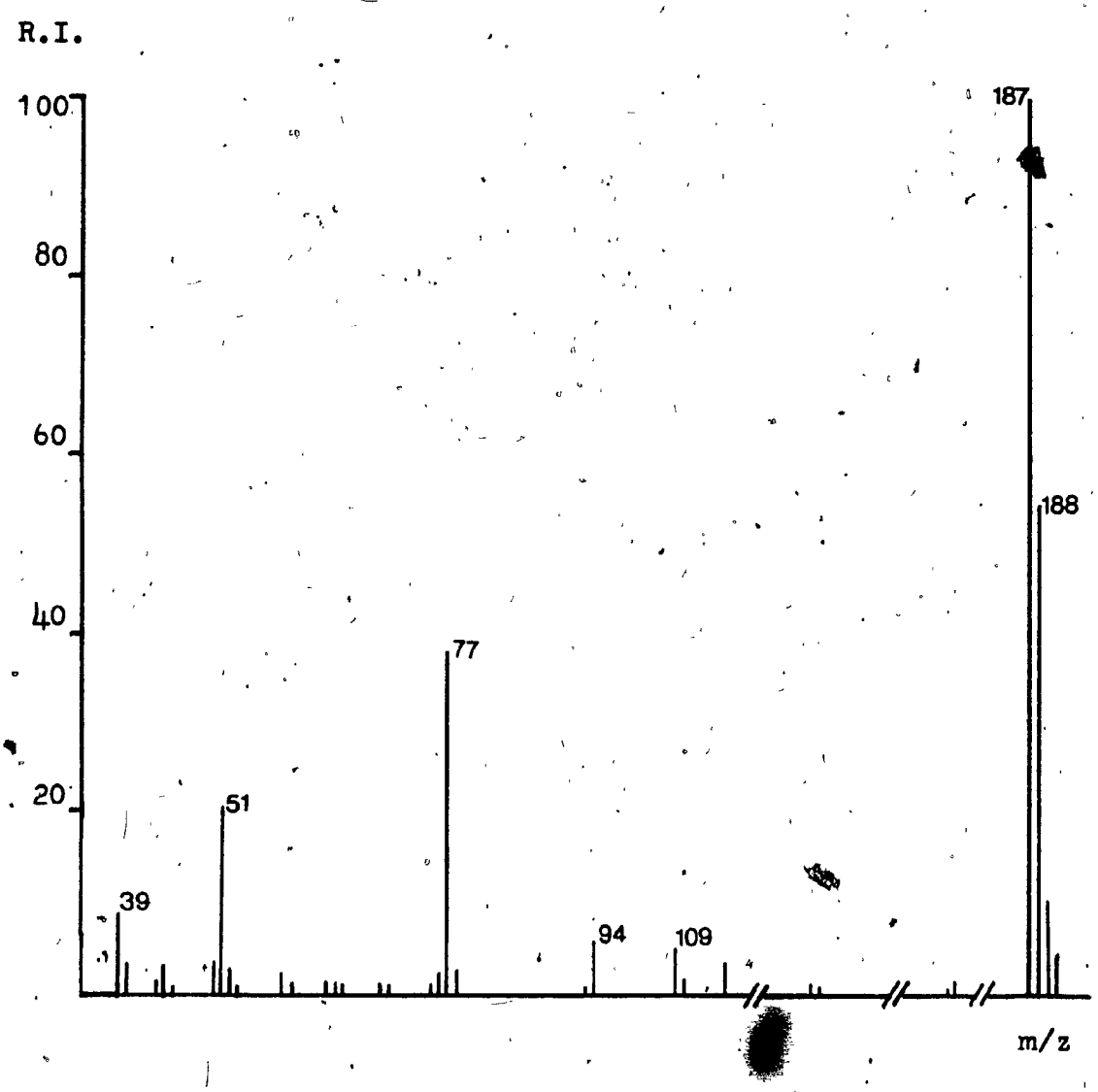

Fig. V-10 Mass spectrum of 1-phenyl-2-pyrimidinthione

The conventional spectrum of (V-10b) shows an intense M-2 ion(100.0%), and less intense M-1 ion(39.8%). The following decompositions in the FFFR were observed, all measured under the same experimental conditions.

(i) A very strong metastable peak for loss of H° from the molecular ion (V-10a) and a weak metastable peak for loss of H° from the molecular ion of (V-10b).

(ii) A strong metastable peak for loss of D° from the molecular ion of (V-10b) and very weak metastable peak for the process (M-1)-1, also therein.

(iii) No metastable transition for processes M-2 or (M-1)-1 in the spectrum of the unlabelled (V-10a).

As the evidence shows, two sites are involved again in the hydrogen loss. However, the benzene ring is mainly responsible for the formation of the highly abundant M-1 ion. The resulting fragment at m/z 187 almost certainly adopts the above stable thiazolium structure, a salt of which was easily synthesized by the reaction shown below[11].

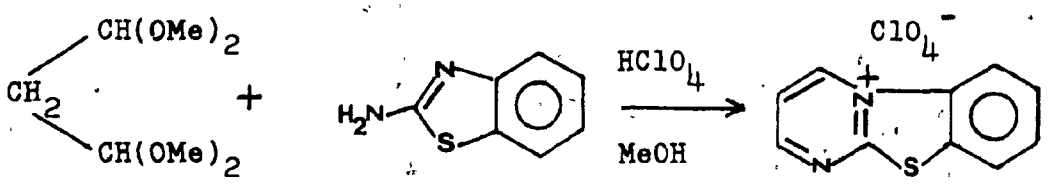

Attempts to obtain mass spectra from this salt were not successful.

The process m/z 188→187 is apparently much more important than the analogous loss of H· from 1-phenyl-2-pyrimidinone. This observation is in accord with the known greater stability of thiazolium versus oxazolium systems[57].

Besides the molecular ion the only other intense peaks in the mass spectrum are at m/z 77, 51 and 39. The m/z 77 ion is presumably the phenyl cation resulting from simple cleavage of the molecular ion. In the spectrum of (V-10b) this ion has three deuterium atoms and appears at m/z 80.

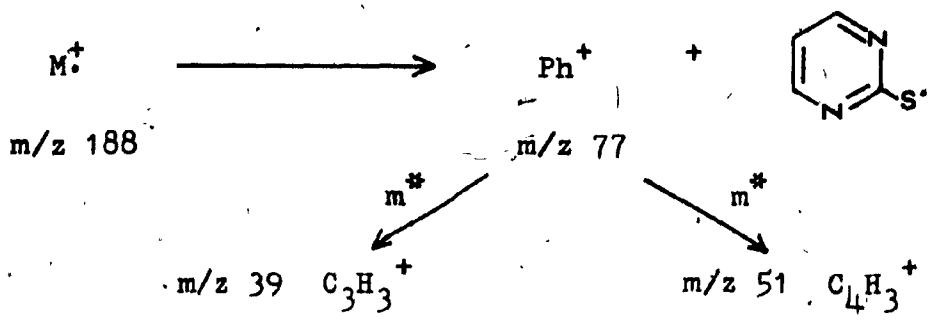

A m/z 51 ion is a common fragment of aromatic compounds[54] resulting from the loss of acetylene from the $C_6H_5^+$ ion. The corresponding ion in the spectrum (V-10b) appears at m/z 53 and 52, which could indicate scrambling of the benzene hydrogens. The same situation holds for the ion at m/z 39, which in the spectrum of the labelled compound appears at m/z 39 and 40.

2-Pyrimidinselenone (V-11a) (Fig. V-11)

Selenium exists in six natural isotopic forms,

Se^{82} 9.19%

Se^{80} 49.82%

Se^{78} 23.52%

Se^{77} 7.58%

Se^{76} 9.02%

Se^{74} 0.87%

(V-11a)

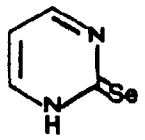

The mass spectrum accordingly shows six molecular ions at m/z 162, 160, 158, 156, 157 and 154. The base peak is at m/z 160 corresponding to the molecular ion of the most abundant isotope, Se^{80}. The peak at m/z 159 is due to the expulsion of H$^{\bullet}$ from the molecular ion at m/z 160. A strong metastable peak was observed in the FFFR for this process.

The major fragmentation pathway is loss of selenium and SeH$^{\bullet}$ from the molecular ions to form the highly abundant peaks at m/z 80 and 79 respectively. This process is different from the fragmentation patterns of the thio and oxo homologues, where loss of sulphur occurs only to a very limited extend and loss of oxygen is not observed at all.

The cluster of peaks at m/z 133 and below is due to the loss of HCN from $M^{+\bullet}$ and M-1 ions and the fragments at m/z 107 and below are very likely $HNCSe^{+\bullet}$ and $NCSe^{+}$ ions.

In analogy to the oxygen and sulphur homologues the six molecular ions expel CSe to form the single fragment at m/z 68.

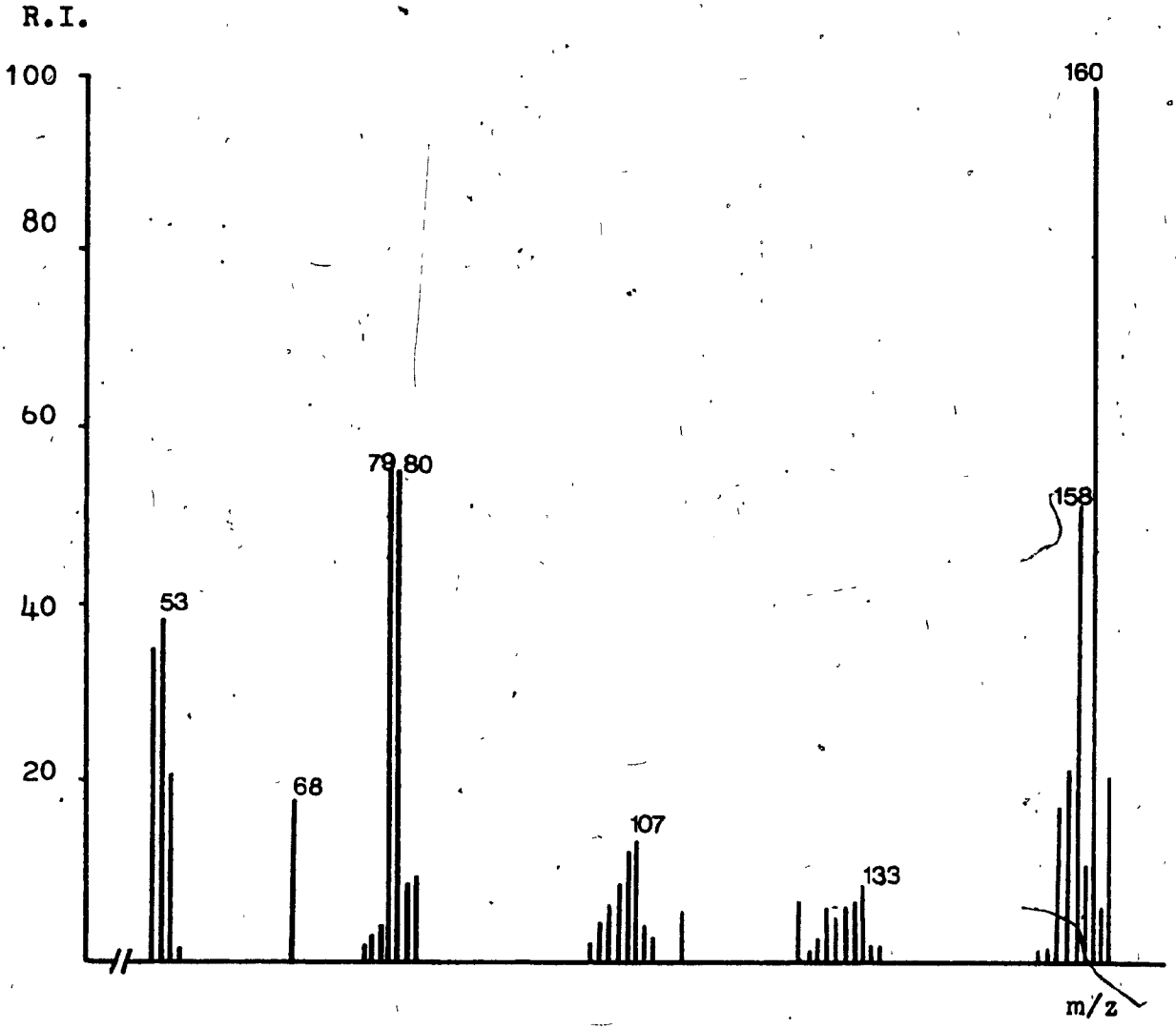

Fig. V-11 Mass spectrum of 2-pyrimidinselenone

The main fragmentation pathways are the following:

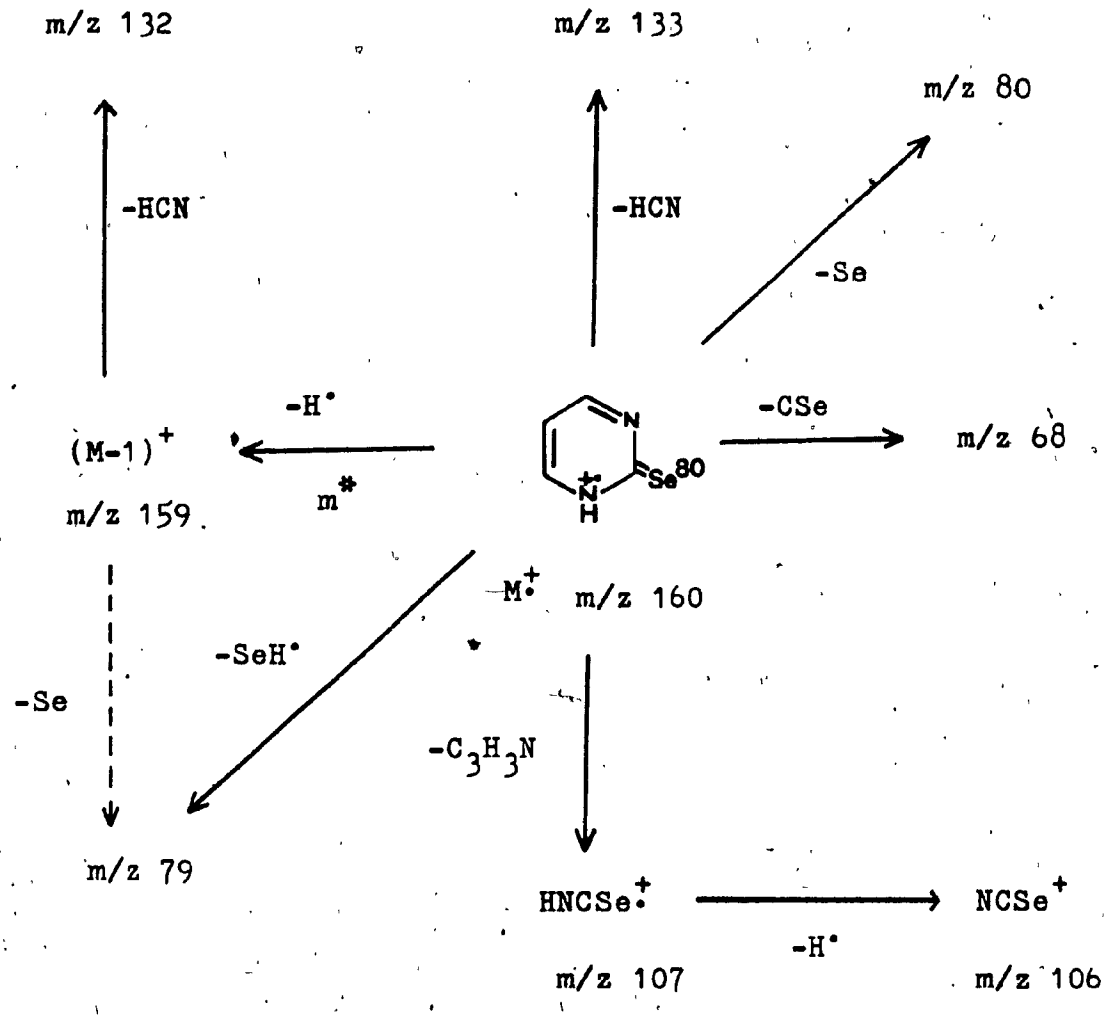

Scheme V-11. Fragmentation pattern for 2-pyrimidinselenone

3/ DISCUSSION ON THE STRUCTURE ELUCIDATION OF THE M-1 IONS

a/ M-1 ions in general

It has been proposed[11] that, in contrast to the fragmentations of the oxygen homologues, the N-methyl and N-ethyl pyrimidinthione molecular ions expel a hydrogen atom from the N-alkyl substituent to form the cyclic daughter ions I and II, respectively.

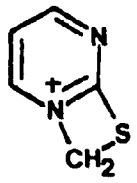

I

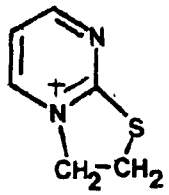

II

This proposal is consistent with earlier work[55,59] and with the well known greater nucleophilicity of sulfur relative to oxygen. The fragmentation patterns of the unlabelled N-methyl and N-ethyl pyrimidinthiones have been discussed previously[11]. The mass spectra of the analogous compounds with deuterium labelled N-alkyl substituents demonstrate that the N-substituents are involved in the hydrogen atom loss.

Comparative metastable peak abundances and measured kinetic energy releases($T_{0.5}$) for H(D) loss from the molecular ions of seventeen N-substituted pyrimidinones and pyrimidinthiones are given in Tables V-1a and V-1b. Although metastable peak abundances were all measured under comparable

Relative m^* Abundances and $T_{0.5}$ for Loss of H°(D°) From the Molecular Ions of N(1)-substituted 2-pyrimidinones:

SUBSTITUENT	INTENSITY		$T_{0.5}$(eV)[b]	
	$M^+ - 1$	$M^+ - 2$	$M^+ - 1$	$M^+ - 2$
Methyl	-	-	-	-
Methyl-d_3	-	-	-	-
Ethyl	v.wk.	-	(a)	-
Ethyl-d_5	v.wk.	v.wk.	(a)	(a)
Phenyl	m	-	0.260	-
Phenyl-d_3	m	w	0.167	0.524
Isopropyl	s	-	0.260	-
Isopropyl-d_6	s	s	0.240	0.350
Isopropyl-d_1	s	-	0.230	-
Benzyl	s	-	0.240	-
Benzyl-$\alpha\alpha' d_2$	s	-	0.240	-

(a) Metastable peak too weak for reliable measurement of $T_{0.5}$

(b) Measured on Hitachi RMU-7 mass spectrometer

Table V-1a

Relative m^* Abundances and $T_{0.5}$ for Loss of $H^\bullet(D^\bullet)$ From the Molecular Ions of N(1)-substituted 2-pyrimidinthiones:

SUBSTITUENT	INTENSITY		$T_{0.5}$(eV)[b]	
	$M^{+\bullet}-1$	$M^{+\bullet}-2$	$M^{+\bullet}-1$	$M^{+\bullet}-2$
Methyl	m	-	0.087	-
Methyl-d_3	v.wk	m	(a)	0.200
Ethyl	s	-	0.150	-
Ethyl-d_5	v.wk	s	(a)	0.430
Phenyl	s	-	0.471	-
Phenyl-d_3	m	s	0.623	0.527

(a) Metastable peak too weak for reliable measurement of $T_{0.5}$

(b) Measured on Hitachi RMU-7 mass spectrometer.

Table V-1b.

experimental conditions, any numerical comparison would be inappropriate because of a significant isotope effect (cf.p.131). Kinetic energy releases were calculated as described previously.

Loss of H$^{\bullet}$ from the molecular ions of N-methyl or N-ethyl-2-pyrimidinone is associated with a very weak (or absent) metastable peak. The absence of a strong metastable peak may be interpreted in terms of a fast simple bond cleavage mechanism[60] occuring mainly in the ion source. The molecular ion of 1-(ethyl-d_5)-2-pyrimidinone loses both H$^{\bullet}$ and D$^{\bullet}$, with a weak metastable peak observed for both processes, whereas 1-(methyl-d_3)-pyrimidinone loses H$^{\bullet}$ and D$^{\bullet}$ without an observed FFFR metastable peak. We conclude from these observations that, in these compounds, H$^{\bullet}$ loss occurs both from the pyrimidine ring and from the N-alkyl substituent. Loss of a ring hydrogen atom occurs, predominantly in the ion source, by a fast, simple bond cleavage. A similar process is involved in H$^{\bullet}$ atom loss from the methyl group attached to N(1), but with increasing length of the aliphatic chain, a slower rearrangement process involving terminal H atoms may be involved to a small extent.

These conclusions are supported by the results obtained when the N-substituents are phenyl, benzyl or isopropyl(cf. Table V-1a). The presence of intense metastable peaks for H$^{\bullet}$(D$^{\bullet}$) loss in the fragmentation of the molecular ions of these compounds indicates that a more complicated process than just simple bond cleavage is involved in the

formation of the M-1 ions.

The molecular ion of 1-phenyl-2-pyrimidinone loses $H^{\bullet}$ with an accompanying FFFR metastable peak of medium intensity. It has been suggested[11] that loss of a hydrogen from phenyl substituent in the fragmentation of this compound generates a fragment ion with the oxazolium structure, III. The process is dominant in the fragmentation pattern of 1-phenyl-2-pyrimidinthione, in agreement with the greater stability of thiazolium compounds(cf.p.119).

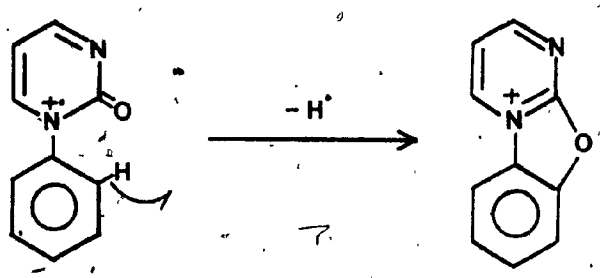

III

A metastable peak of medium intensity is observed for loss of $H^{\bullet}$ from the molecular ion of 1-(phenyl-2,4,6-d_3)-pyrimidinone. It is suggested that this process involves a hydrogen atom on the pyrimidine ring, via a rearrangement in which the phenyl hydrogen is transfered to the oxygen followed by loss of a heterocyclic ring hydrogen.

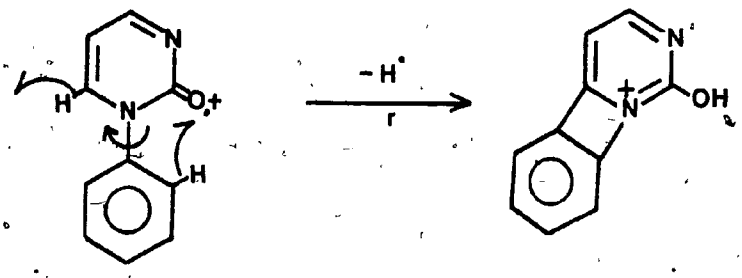

IV

A similar explanation can be postulated to rationalize the fragmentation of the 1-benzyl-2-pyrimidinone molecular ion. Deuterium labelling showed that the benzylic hydrogens are not involved in the formation of M-1 ions in the first free field region. It is suggested that loss of hydrogen atoms from the phenyl and pyrimidine rings give rise to daughter ions with structures V and VI, respectively.

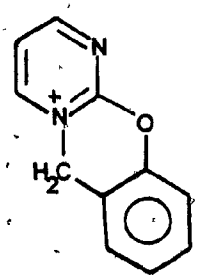

V

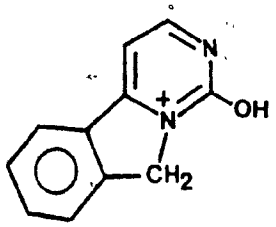

VI

Analogously, M-1 ions derived from the 1-isopropyl-2-pyrimidinone could have structures VII and VIII for hydrogen atom loss from the isopropyl group and the pyrimidine ring, respectively, although these structures are highly strained.

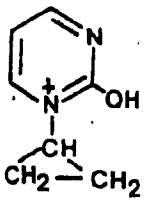

VII

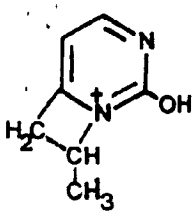

VIII

Deuterium labelling shows that the methine hydrogen of the isopropyl group is not involved in the formation of the M-1 ion.

b/ The M-1 ion of the N-ethyl-2-pyrimidinthione

Comparison of the data summarized in Tables V-1a and V-1b shows that the N-substituted pyrimidinthiones behave similarly as the N-substituted pyrimidinones with respect to loss of H· from the pyrimidine ring, if the substituents are methyl and ethyl groups. The differences are observed in the formation of the M-1 ions from N-methyl and N-ethyl substituents of the pyrimidinthiones; the observation of a moderately intense metastable FFFR peak suggests that, in addition to the fast simple cleavage process, a slower rearrangement pathway is participating to a significant extent. We now consider in some detail the formation of the M-1 ion from N-ethyl-2-pyrimidinthione, in attempt to substantiate the proposed[11,59] cyclic structure II for the daughter ion.

(i) Isotope Effects

In addition to the labelled pyrimidinthione V-9b, two more labelled species, V-9c and V-9d, were synthesized and the metastable transitions upon

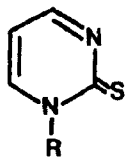

V-9a R = CH_2CH_3

V-9b R = CD_2CD_3

V-9c R = CH_2CD_3

V-9d R = CD_2CH_3

the formation of the M-H or M-D ions in the FFFR were examined for the four labelled compounds V-9a - d. Table V-2 shows the the results which indicate considerable isotope effects for the H°(D°) elimination processes.

$T_{0.5}$ for Loss of H°(D°) from the Molecular Ions of Differently Labelled N(1)-substituted 2-pyrimidinthiones:

	Substituent	(a) $T_{0.5}$	(b) $T_{0.5}$
I. Loss of H°	CH_2CH_3	0.15	0.29
	CH_2CD_3	0.08	0.12
	CD_2CD_3	(c)	(c)
	CD_2CH_3		0.21
II. Loss of D°			
	CH_2CD_3	0.38	0.48
	CD_2CH_3		(c)
	CD_2CD_3	0.43	0.47

(a) Hitachi RMU-7

(b) Kratos-AEL MS-902s

(c) Metastable peak too weak for accurate measurement of $T_{0.5}$

Table V-2

In experiments such as those reported here, a discussion of the isotope effect on T values and m^* abundances is complicated by the fact that two different molecular ions, with different internal energy distributions and different zero point energies, are involved.

Effect on $T_{0.5}$

In the case of R = CD_2CH_3 (T_H = 0.21 eV), and R = CH_2CD_3 (T_D = 0.48eV) the T_H/T_D ratio is $\approx$0.5. This implies (assuming the same partitioning in each case) that zero point energies in the product ions differ more than zero point energies in the transition state:

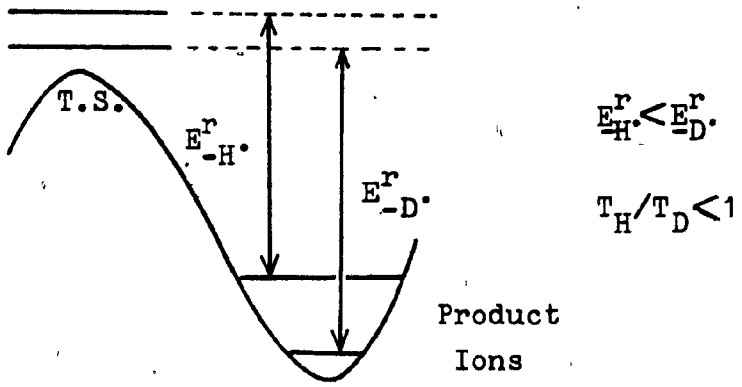

Fig. V-12

The isotope effects upon kinetic energy release have been reported in the literature [21b] and it has been suggested that H· loss should give $T_H/T_D \approx 1$ (cf. p. 32). Such a situation occurs for N-phenyl and N-(phenyl-d_3)-2-pyrimidinthione, where T_H/T_D ratio is much closer to unity than in the

N-ethyl compounds, suggesting that zero point energy differences in the product ions are close to those in the transition state(assuming again that partitioning is not affected by isotopic substitution):

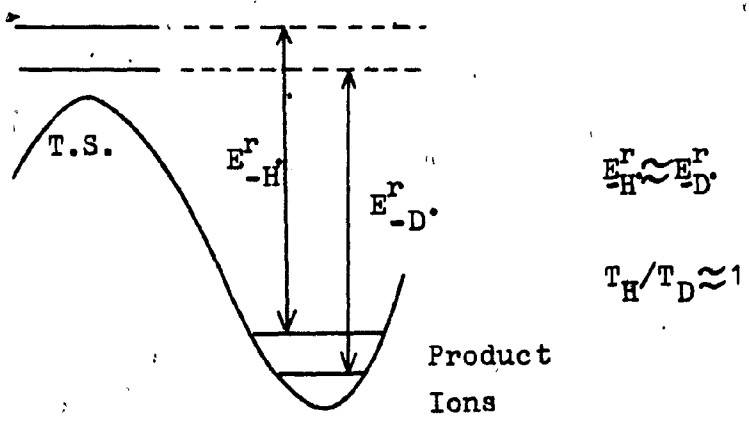

Fig. V-13

Effect on m^* abundances

The isotope effect on metastable peak abundances has been reported a number of times, and is discussed by Cooks et al.[21a]. The authors discuss H° and D° loss from the same molecular ion(cf.Fig.III-7,p. 32) while in our case different molecular ions are involved for H° and D° loss.

The metastable peak for loss of D° from N-CD_2CH_3-2-pyrimidinthione was too weak to observe on either Hitachi RMU-7 or the Kratos-AEI MS-902s. H° loss from the analogous N-CH_2CD_3 gave a readily observable metastable peak ($T_{0.5}$ = 0.12eV). A large isotope effect on metastable peak can be rationalized for this type of experiment in terms of

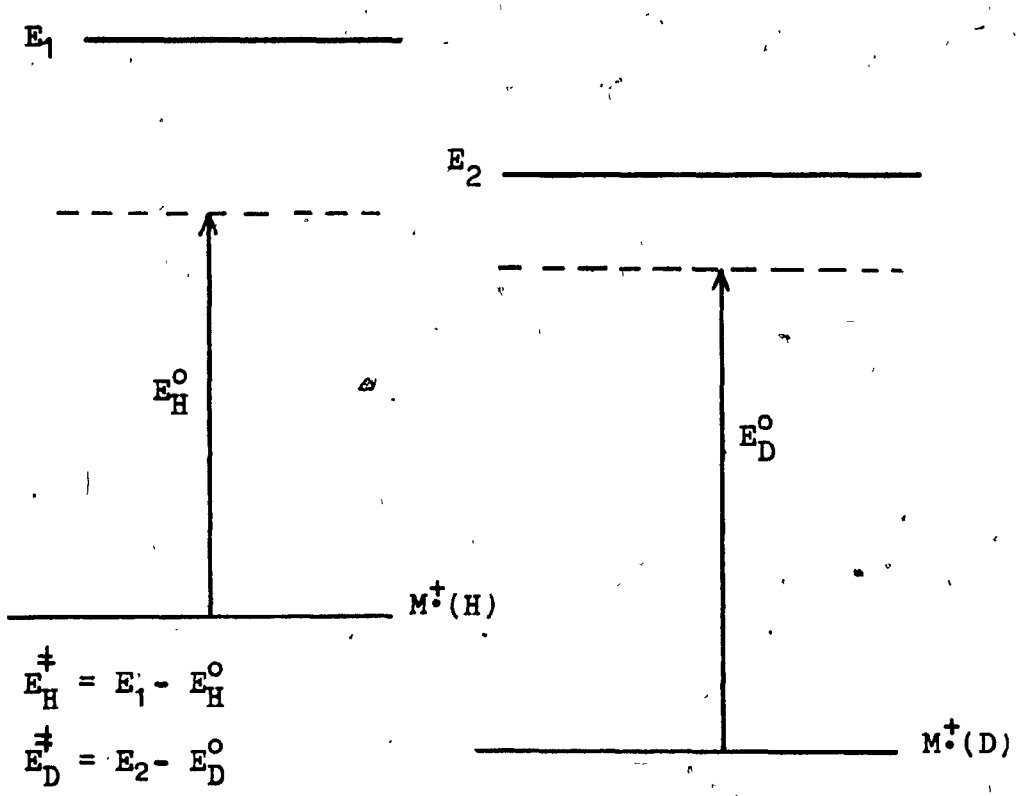

If $E_D^\circ > E_H^\circ$, then $E_H^\ddagger > E_D^\ddagger$, (note that $E_1 = E_2$ = energy deposition, E).

Fig. V-14

Fig. V-14 and Fig. III-8a, p.34 . If the zero point energy difference is less in the transition state than in the reactant (in this case, $M^{+\cdot}$), then the threshold (activation) energy will be lower for loss of H· from the $(M-H)^+$ activated complex than for loss of D· from $(M-D)^+$. If the energy deposition function is essentially unaffected by the isotopic substitution, then for a given amount of energy deposited, E, the excess energy will be greater for $(M-H)^+$ then for $(M-D)^+$, i.e. $E_H^* > E_D^*$ (cf. Fig. V-14).

The second factor to be considered is the variation of k with the internal energy, E. If k rises rapidly with E, then isotopic substitution may lower k_d to a value which puts it outside the metastable region(log $k \approx 4.5$-5.5), and the metastable peak will be weak or absent(cf.Fig. III-8a, p.34). Alternatively, if k increases slowly with E, the isotope effect k_H/k_D will be considerably smaller, and the metastable peak for the isotopically labelled compound will be observed(cf.Fig. III-8b, p.34).

Cooks et al.[21a] point out that

(a) The magnitude of the isotope effect may be independent of the difference in activation energies involved.

(b) The slopes of the log k vs. E curves is related to the entropy of activation for the process; reactions in which H° is lost by a low-frequency factor process (including rearrangements) will be associated with a small k_H/k_D and vice versa.

If we apply these considerations to the N-ethyl-2-pyrimidinthiones we may draw the following conclusions.

(a) $T_{0.5}$ for H° loss from N-CH_2CD_3 is significantly lower than that observed for loss of H° from N-CD_2CH_3 (0.12eV and 0.21eV, respectively) and comparable to that observed for H° loss from N-CH_3(0.09eV, but different instrument).This suggests two different processes.

(b) The large k_H/k_D for H° and D° loss from the methylene group of N-ethyl-2-pyrimidinthione indicates a

steep log k vs. E curve. This in turn, points to a process with high frequency factor, i.e. cleavage, rather than rearrangement.

(c) Loss of H° and D° from the methyl group of N-ethyl-2-pyrimidinthione shows a much smaller isotope effect upon m^* abundances, consistent with rearrangement. The large $T_{0.5}$ values indicate a large reverse activation energy.

In summary we conclude that

1. Loss of a methylene hydrogen is probably a cleavage reaction, with little rearrangement. The same is true of H° loss from N-CH_3-2-pyrimidinthione.

2. Loss of H° from methyl group of N-ethyl-2-pyrimidinthione is probably a rearrangement process.

(ii) <u>Fragmentation of the M-1 ions</u>

A slow process is a necessary condition for the thiazolium ring formation, after a hydrogen atom is lost from the molecular ion of N-ethyl--2-pyrimidinthione. However, it is not a sufficient condition, because any structure resulting from a loss of the methyl H° would require some rearrangement, r.

e.g.

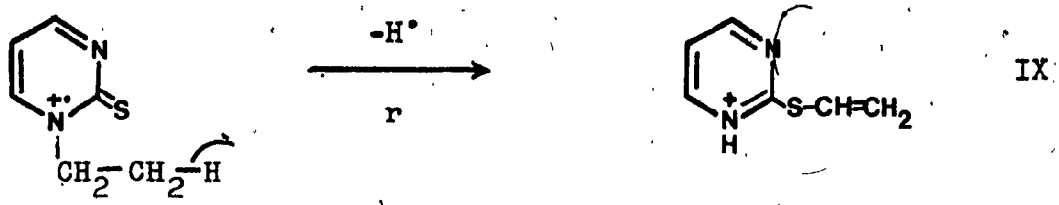

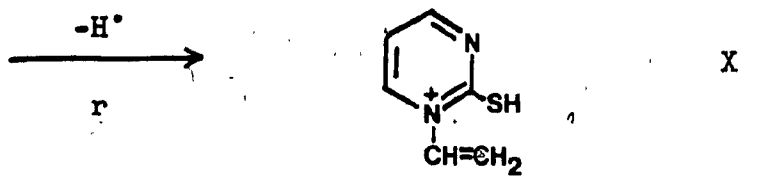

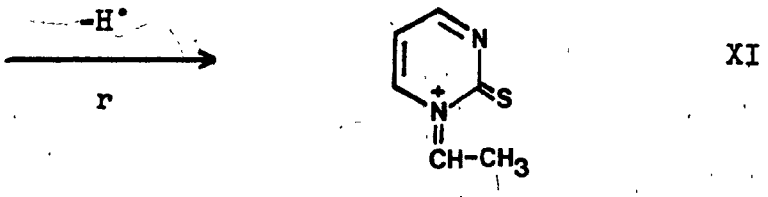

We believe, however, that if the cyclic M-1 ion was formed, it would not fragment further by loss of C_2H_4:

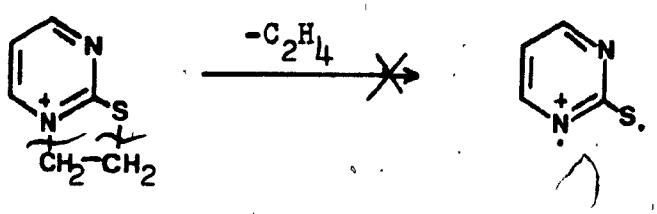

Such process would involve a rupture of the thiazolium ring, which might be energetically unfavorable process. On the

other hand if the structure of the M-1 ion is such that the N-substituent maintains the chain form, as in the structures IX, X, and XI(cf.p.139); it could fragment easier by loss of C_2H_4, CH_4, etc.

Further studies of the transitions in the FFFR showed that loss of 28 m.u. occurs from the M-1 ions of N-ethyl-2-pyrimidinthione and N-ethyl-2-pyrimidinone. The labelling studies helped to determine which hydrogen is lost from the molecular ion to form the M-1 ion that loses 28 m.u., presumably C_2H_4. The following schemes illustrate the relevant fragmentations. These were the only fragmentations of the M-H(D) ions in question, detected by a metastable transition in the FFFR.

$M^{+\bullet}$ =

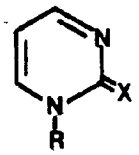

$$M^{+\bullet}\ (R = CH_2CH_3,\ X = S) \xrightarrow[m^*]{-H^\bullet} (M-1)^+ \xrightarrow[m^*]{-(C_2H_4)} m/z\ 111$$

m/z 140 m/z 139

$$M^{+\bullet}\ (R = CD_2CH_3,\ X = S) \xrightarrow[m^*]{-H^\bullet} (M-1)^+ \xrightarrow[m^*]{-(C_2D_2H_2)} m/z\ 111$$

m/z 142 m/z 141

$$M^{+\cdot}\ (R = CH_2CD_3,\ X = S) \xrightarrow[m^*]{-H^\cdot} (M-1)^+ \xrightarrow[m^*]{-(C_2H_2D_2)} m/z\ 112$$

m/z 143 m/z 142

$$M^{+\cdot}\ (R = CD_2CD_3,\ X = S) \xrightarrow[m^*]{-H^\cdot} (M-1)^+ \xrightarrow[m^*]{-32(C_2D_4)} m/z\ 112\ ^{\#}$$

m/z 145 m/z 144

$$\xrightarrow{-32(S)}$$

#The high resolution mass measurement showed that the peak at m/z 112 contains two ions, in the ratio 5:1. The smaller peak is due to the loss of sulfur, while the more abundant ion is due to the loss of C_2D_4 from M-1 ion.

$$M^{+\cdot}\ (R = CH_2CH_3,\ X = O) \xrightarrow[m^*]{-H^\cdot} (M-1)^+ \xrightarrow[m^*]{-(C_2H_4)} m/z\ 95$$

m/z 124 m/z 123

$$M^{+\cdot}\ (R = CD_2CD_3,\ X = O) \xrightarrow[m^*]{-H^{\cdot}} (M-1)^{+} \xrightarrow[m^*]{-(C_2D_4)} m/z\ 96$$

m/z 129 m/z 128

The above schemes show that the relatively unstable M-1 ion, which further expels ethylene, originates from the molecular ion by loss of the ring hydrogen atom. This process is identical for oxygen and sulfur homologues and proceeds probably by a pseudo McLafferty rearrangement:

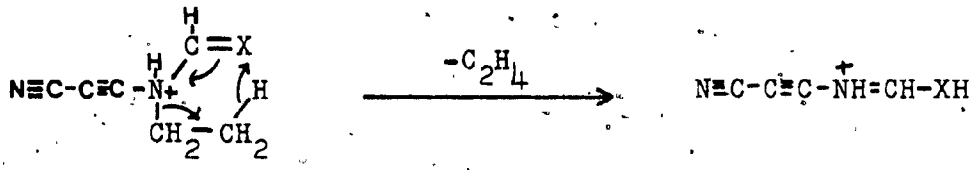

$(M-1)^{+}$ X = S,O

It should be noted, that the above discussion does not include any possible fragmentation of the M-H(D) ions that could occur only in the source. Therefore we conclude that there is no evidence against a formation of the proposed thiazolium ring structure.

(iii) Thermochemical Considerations

Requirements for ion thermochemistry.

The assignment of ion structure on the basis of thermochemical measurements is a well-developed method[62,63], where heats of formation of ions are measured and compared with heats of formation of similar ions in order to draw conclusion about ion structures (cf. p.38).

In order to substantiate the proposed cyclic structure II for the M-1 ion of 1-ethyl-2-pyrimidinthione, its heat of formation has to be compared with heats of formation for those ions, where similar structure could be expected(i.e. the M-1 ion of 1-ethyl-2-pyrimidinone), or where such structure cannot be formed(i.e. the M-1 ions of 1-methyl-2-pyrimidinthione, 1-methyl-2-pyrimidinone, 2 (1H)-pyrimidinthione and 2(1H)-pyrimidinone).

The situation is complicated by the fact that there might be three structurally different M-1 ions of 1-ethyl-2-pyrimidinthione, since the molecular ion expels the hydrogen atom from three sites,i.e. from the pyrimidine ring, from the methylene group and from the methyl group.

However, satisfactory results could be obtained, assuming that, if elimination of the methyl hydrogen atom resulted in the formation of the thiazolium ion II, it would be the most abundant ion, since it would have the lowest energy.

The appearance energy AE may be considered as an energy of reaction ΔE_r,

$$AE = \Delta E_r = \Delta H_r + \Delta(PV). \qquad (V-1)$$

Within the tolerance of most measurements of appearance energy, $\Delta(PV)$ is neglected and the appearance energy equated to ΔH_r, the heat of reaction. Further, it is sometimes possible to measure the excess translational energy(cf.p.23) with which an ion is formed and to correct the appearance energy for it.

In general, for the reaction (V-2) where M is the N-substituted or unsubstituted pyrimidinone or pyrimidinthione, the appearance energy AE may be considered as the heat of reaction ΔH_r, which is equal to:

$$M \longrightarrow (M-1)^+ + H^\cdot + E_{excess} \qquad (V-2)$$

$\sum \Delta H_f$products - $\sum \Delta H_f$reactants.

$\therefore$

$$AE = \Delta H_r = \Delta H_f(M-1)^+ + \Delta H_f H^\cdot + E_{excess} - \Delta H_f M(g)$$

or

$$\Delta H_f(M-1)^+ = AE + \Delta H_f M(g) - \Delta H_f H^\cdot - E_{excess} \qquad (V-3)$$

Thus, in order to obtain the heat of formation for the M-1 ions, it is necessary to obtain

(a) ΔH_f of the neutral molecule M

(b) AE of the M-1 ion

(c) $\Delta H_{sublimation}$ for the process $\Delta H_f M(s) \longrightarrow \Delta H_f M(g)$, since the examined compounds are solids.

The literature value for ΔH_f H° is 52 kcal/mole[67] and the E_{excess} is important only in high accuracy measurements and will not be considered at this stage.

Heats of formation of neutrals.

(a) Literature values.

Heats of formation for some heterocyclic compounds related to our study are given in Table V-3[64,65]. The heats of formation for these compounds were derived from their corresponding heats of combustion, which were determined by calorimetric methods. This method is well established for compounds containing carbon, hydrogen oxygen and nitrogen and is capable of giving results of high accuracy. In order to calculate the heats of formation of these compounds from their corresponding heats of combustion only the heats of formation of $CO_2(g)$ and $H_2O(liq)$ are needed[66]. Organic nitrogen compounds form $N_2(g)$ as the product in the combustion reaction, which by definition has a heat of formation of zero.

Thus, for example, the heat of formation for uracil, $C_4H_4O_2N_2(s)$, was calculated from the heat of

Literature Data for Heats of Formation of some Compounds related to our Study:

Compound		ΔH_f^o 298° (kcal/mole)[64]
$C_4H_4N_2$	pyrimidine(liq)	+35.04
"	" (g)	+46.99
"	pyridazine(liq)	+53.74
"	pyridazine(g)	+66.52
$C_4H_4N_2O_3$	barbituric acid(s)	-152.2
$C_5H_6N_2O_2$	6-methyluracil(s)	-109.2
$C_5H_6N_2O_2$	thymine, (5-methyluracil)(s)	-111.9
$C_4H_4O_2N_2$	uracil(s)	-101.4
$C_4H_5ON_3$	cytosine(s)	-52.89
CH_4N_2O	urea(s)	-79.71
C_4H_4O	furan(liq)	+14.84
CH_4N_2S	thiourea(s)	-21.13
$C_3H_7NO_2S$	L-cysteine(s)	-124.6
$C_6H_{12}N_2O_4S_2$	L-cystine(s)	-245.7
C_4H_4S	thiophene(liq)	+19.24

Table V-3

combustion ΔE_c^o, which refers to the idealized combustion reaction at 298°K represented by the following equation[65]:

$$C_4H_4O_2N_2(s) + 4O_2(g) = 4CO_2(g) + 2H_2O(liq) + N_2(g)$$

The application of the bomb calorimetric method to compounds that also contain sulfur involves many specific difficulties which have delayed the developement of an accurate method for determination of heats of combustion and formation of organic sulfur compounds.

One of the main problem is the quantitative conversion of sulfur to the hexavalent state during the combustion process. The heat of combustion for the sulfur compounds given in the Table V-3, was determined with a rotating bomb calorimeter, which works on the principle that all the sulfur is converted by combustion, and subsequent stirring, into a sulfuric acid solution of a uniform concentration[69].

The experimental results showed that under the same conditions of the combustion experiment, the final concentration of sulfuric acid is $x(H_2SO_4.115H_2O)(liq)$, where x is number of sulfur atoms in the original organic compound. The value of -212.192 kcal/mole at 298.15°K for $\Delta H_f(H_2SO_4.115H_2O(liq))$ was used for calculation of the respective heats of formation of the above compounds containing sulfur.

Thus, for example, the heat of formation of thiophene, $C_4H_4S(liq)$ was calculated from the heat of combustion

ΔE_c°, which refers to the idealized combustion reaction at 298.15°K represented by the following equation[64]:

$$C_4H_4S(liq) + 114H_2O(liq) + 13/2\ O_2(g) = 4CO_2(g) + H_2SO_4 \cdot 115H_2O(liq)$$

(b) Experimental measurements.

An adiabatic combustion calorimeter(Parr series 1200 with 1101 static bomb) was used in our laboratory in an attempt to determine the heat of combustion of 2(1H)-pyrimidinone and 2(1H)-pyrimidinthione.

Theory[69,70].

The standard enthalpy of combustion for a substance is defined as the enthalpy change, ΔH_c°, which accompanies a process in which the given substance undergoes reaction with oxygen gas to form specified combustion products(such as $CO_2(g)$, $H_2O(liq)$, $N_2(g)$), all reactants and products being in their respective standard states at the given temperature T.

The enthalpy of combustion can be calculated from the temperature rise which results when the combustion reaction occurs under adiabatic conditions in a calorimeter.

In the actual calorimeter process, the final and initial temperatures, T_2 and T_1 respectively, are not equal and the reactants and products are not in their standard states(cf.Fig.V-15).

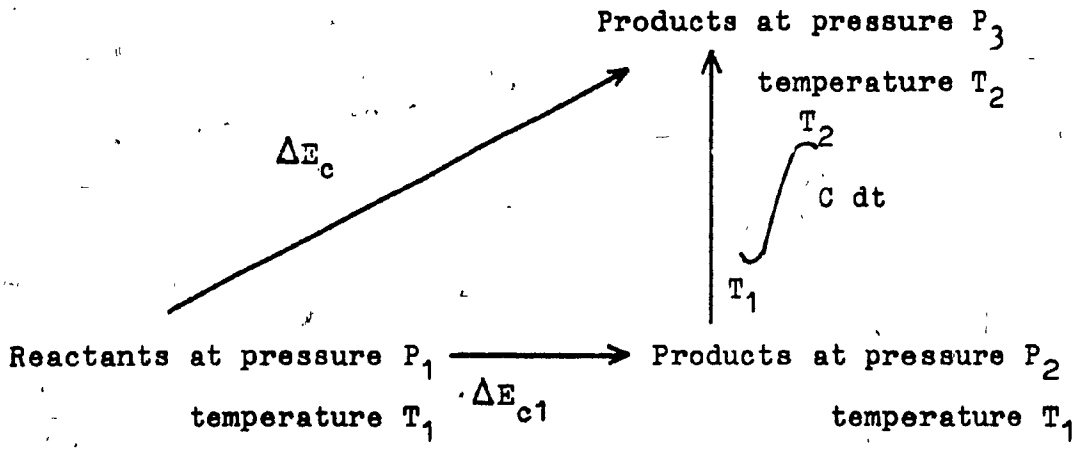

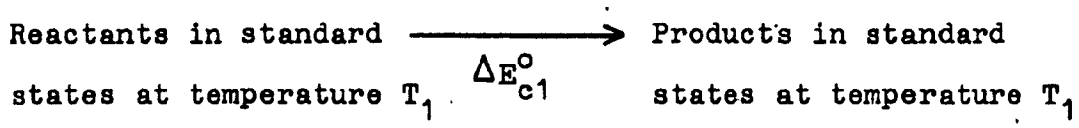

Fig. V-15

ΔE_c is the energy change for the actual calorimeter process, while ΔE_{c1} is the energy change for an imaginary process in which the final state is at T_1 rather than T_2. The heat capacity C is that for the can(in the adiabatic-jacket bomb calorimeter the bomb is immersed in a can of water, fitted with a thermometer and this assembly is placed in a water-filled outer jacket), and its contents under the conditions of the experiment.

Since

$$\Delta E_c = \Delta E_{c1} + \int_{T_1}^{T_2} C_v dt, \qquad (V\text{-}4)$$

and since, from the first law of thermodynamics considering the adiabatic conditions,

$$\Delta E_c = 0, \qquad (V\text{-}5)$$

it follows that

$$\Delta E_{c1} = -C(T_2 - T_1).$$

C is considered a constant, which is equal to the heat capacity or energy equivalent of the calorimeter.

To calculate ΔE°_{c1} from ΔE_{c1} requires a correction to standard states, called the Washburn correction, which is important only in work of high accuracy.

The standard enthalpy change ΔH°_{c1}, may be calculated from the definition of H as follows.

$$\Delta H^{\circ}_{c1} = \Delta E^{\circ}_{c1} + \Delta(PV) \qquad (V\text{-}7)$$

The contributions to $\Delta(PV)$ for reactions in which both reactants and products are solids or liquids is generally negligible; $\Delta(PV)$ may be significant in combustion calorimetry where some of the reactants and products

are gases.

Following the procedure[70] approximately 1g of the sample was formed into pellet by means of a pellet press. The pellet was weighed and placed in the sample pan. The fuse wire, of measured length about 10cm and known heat of combustion per unit length was attached to the two terminals and adjusted to give firm contact with the pellet. Water (1.0 ml) was added to the bomb and then the cover with the sample was assembled with the bomb and tightened. The bomb was slowly filled with oxygen until the pressure was ~30atm.. About 2000ml of water was weighed in the calorimeter can and placed in the adiabatic jacket. The bomb was immersed in the water and the ignition leads were connected. The stirrer was started and when the equilibrium temperature was reached, it was recorded as the initial temperature T_1. The ignition switch was then closed until fusion of the wire was indicated by glowing of the lamp. After a successful ignition, the temperature of the calorimeter rose quickly. The final steady temperature of the can was then recorded as T_2.

For sulfur compounds, the oldest method, developed by Huffman and Ellis(H-E) in 1935[71], was tried. The H-E method employs a static bomb calorimeter for a combustion experiment, but no water is added to the bomb. Otherwise, the same procedure, as outlined above was followed, using the adiabatic bomb calorimeter.

Before one uses a calorimeter it must be standardized. The term "standardization" denotes operation of the calorimeter on a standard sample from which the energy equivalent factor of the system can be calculated. This factor represents the combined heat capacity of the water bucket, of the water itself, of the bomb and its contents and of the parts of the thermometer, stirrer and supports for the bucket.

The procedure for a standardization test is exactly the same as for testing any sample. A pellet of standard benzoic acid weighing approximately 1g, accurately weighed, was submitted to the adiabatic combustion. The temperature rise, t, from the observed test data was determined and the energy equivalent, C, was calculated from the following equation(cf.p.150).

$$C = - \frac{(\Delta E_{c1}\ \text{B.A.} \times m) + e_1}{t} \quad \text{cal/ } ^{\circ}\text{F} \qquad \text{(V-8)}$$

where

ΔE_{c1} B.A. = heat of combustion of standard benzoic acid in calories per gram

m = mass of standard benzoic acid sample in grams

t = corrected temperature rise in degrees F

e_1 = correction for heat of combustion of firing wire, in calories.

After standardization the heat of combustion of the sample, ΔE_{c_1} SA, was calculated from the following equation.

$$\Delta E_{c1} \text{ SA} = - \frac{tC - e_1}{m} \text{ cal/g} \qquad \text{(V-9)}$$

where

t = temperature rise in degrees F

C = determined energy equivalent of the calorimeter in calories per degrees Fahrenheit

e_1 = correction in calories for heat of combustion of fuse wire

m = mass of the sample in grams.

Results.

The calorimeter was calibrated using benzoic acid (N.B.S. sample, heat of combustion -6318 cal/g). The energy equivalent of the calorimeter as the average of two calibration runs was 1754 $\pm$ 20 cal/^{o}F. Using this value, the heat of combustion, ΔE_{c1}, for 2(1H)-pyrimidinone, $C_4H_4N_2O$, was -561.8 kcal/mole. This value refers to combustion reaction at 298^{o}K represented by the equation:

$$C_4H_4N_2O(s) + 9/2\ O_2(g) = 4CO_2(g) + N_2(g) + 2H_2O(liq)$$

The standard heat of formation for the neutral molecule of

1(H)-2-pyrimidinone, $\Delta H_f^o n$, was then calculated from the values -94.05 and -68.32 kcal/mole for the standard enthalpy of formation of $CO_2(g)$ and $H_2O(liq)$, respectively, as follows:

$$\Delta E_{c1} = -561.8 = 4(-94.05) + 2(-68.32) - \Delta H_f^o n$$

$$\therefore \quad \Delta H_f^o n \ 2(1H)\text{-pyrimidinone(s)} \simeq 49 \text{ kcal/mole}$$

The attempt to obtain heat of combustion for the sulfur compounds by calorimetric measurements was not successful(cf.p.147). The H-E method[71] was tested, using l-cystine(heat of combustion -996.4 kcal/mole) as the test substance. Following the procedure and the described correction for sulfuric acid[71], the heat of combustion for l-cystine according to the equation

$$C_6H_{12}O_4N_2S_2(s) + 10O_2(g) = 6CO_2(g) + N_2(g) + 2(H_2SO_4 \cdot 2.7H_2O)(liq) - 1.4H_2O(liq),$$

resulted in high value of -8837.6kcal/mole. A similar high result was obtained when a platinum crucible was used in the combustion experiment. The results are in accord with Moore[74], who states that "another source of error is the corrosion of parts of bomb by H_2SO_4 resulting in unknown heat effect".

Since neither platinum-lined static bomb, nor the appropriate rotating bomb calorimeter, used today for combustion of organic sulfur compounds(cf.p.147) was available, no further calorimetric experiments were performed on the sulfur containing compounds.

(c) Estimation methods and results.

In some cases estimation methods can be used to determine the standard heat of formation for a neutral compound, $\Delta H_f^o n$. There exist five such methods that give comparable $\Delta H_f^o n$ to values determined experimentally,when simple aliphatic and alicyclic compounds containing C,H,O, and N are examined[72]. All the methods involve some form of group-estimation based on the structure of the molecule. The most successful is the method of Benson[73], where atoms or molecular groups are chosed and allowance is made for next-nearest neighbors to this atom or group.

For example the experimental standard heat of formation for ethylbenzene(g) is 7.12 kcal/mole[64]. The standard heat of formation for ethylbenzene estimated by Benson is 7.07 kcal/mole, as illustrates the following example:

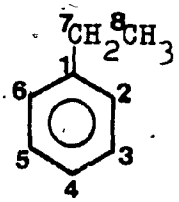

	ΔH°_{f298}, kcal/mole [73]
$5(C_B^{2\text{-}6}-(H))$	+5(3.30)
$C_B^{1}-(C^{7})$	+5.51
$C^{8}-(C^{7})(H_3)$	-10.08
$C^{7}-(C_B^{1})(C^{8})(H_2)$	-4.86

ΔH°_{f}n ethylbenzene estimated by Benson: 7.07 kcal/mole

To obtain reliable estimates for the ΔH°_{f}n of the examined pyrimidinones and pyrimidinthiones would be convenient since the estimated properties of the molecules refer to a gaseous form. In such case it would not be necessary to determine the heat of sublimation, which is needed for the determination of $\Delta H_f(M-1)^+$, if ΔH°_{f}n of a solid compound is obtained from a combustion experiment.
e.g.

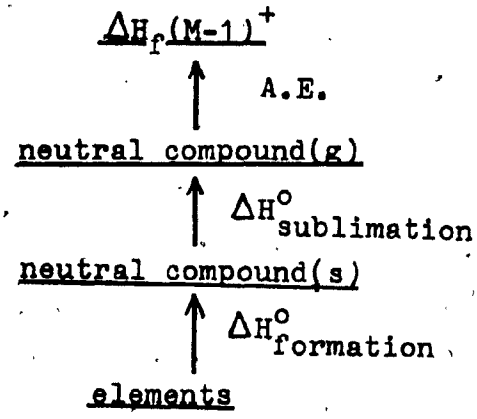

Of the five methods for estimating ΔH_f^o, the method of Benson[73] is the most accurate. It is also the most complete because it is applicable to many types of organic compounds. The bond energy group technique is easy to use, but is less accurate. The other three group-contribution methods (Franklin, Verma-Doraisway and Anderson-Beyer-Watson) are reasonably accurate and general. However, none of the five methods is reliable for heterocyclic nitrogen compounds[73].

Nevertheless, attempts were made to estimate the heats of formation of the examined pyrimidines in order to find out how accurate the estimates would be. For that purpose, the Benson's group-contribution technique could not be used, since not enough data are available. Therefore, the bond-energy technique was employed, which works well if compounds containing benzene rings are examined.

e.g.

The theoretical value for heat of formation of mercapto-benzene was calculated according to the equation

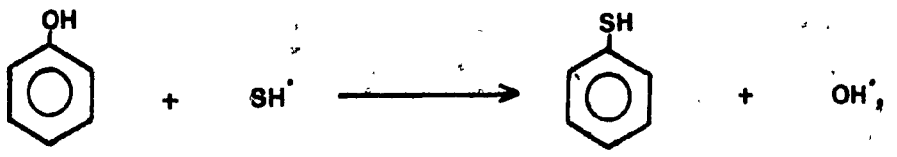

using the following literature data[67,68]:

	ΔH_f°, kcal/mole
phenol(g)	-23.03
SH•	35.0
OH•	9.0

	bond energy, kcal/mole
C—O	86
C—S	65

$$\Delta H_{reaction} = \sum E_{bonds\ formed} - \sum E_{bonds\ broken} = 21\ kcal/mole,$$

$$= \Delta H_f^\circ mercaptobenzene + \Delta H_f^\circ OH^\bullet - \Delta H_f^\circ phenol - \Delta H_f^\circ SH^\bullet$$

$\therefore$

$\Delta H_f^\circ mercaptobenzene(g) = 24$ kcal/mole

$\Delta H_f^\circ mercaptobenzene(g)$, lit. value[66] = 26.6 kcal/mole

The same method was used to calculate the heat of formation for cytosine, formed from 2(1H)-pyrimidinone,

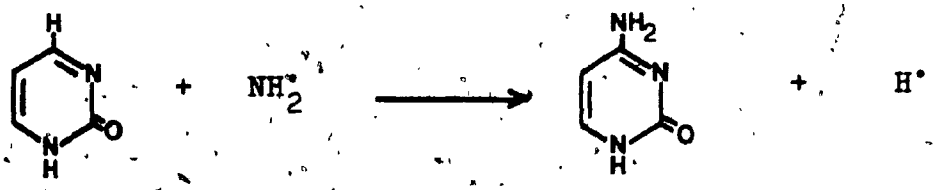

using the following literature data[67,68]:

	ΔH_f°, kcal/mole
$NH_2^\bullet$	41
$H^\bullet$	52
2(1H)-pyrimidinone(s)	49 (p.154)
	bond energy, kcal/mole
C-N	73
C-H	99

$\Delta H_{reaction}$ = 26 kcal/mole

$= \Delta H_f^\circ cytosine + \Delta H_f^\circ H^\bullet - \Delta H_f^\circ 2\text{-pyrimidinone(s)} - \Delta H_f^\circ NH_2^\bullet$

$\Delta H_f^\circ cytosine$ = 64 kcal/mole (estimated value)

$\Delta H_f^\circ cytosine(s)$ = -52.89 kcal/mole (literature value[65])

For appropriate comparison the heats of sublimation for 2-pyrimidinone and cytosine should be considered, since bond energy calculations refer to gaseous species (cf.p.156). Both heats of formation for cytosine(the estimated and the literature value) would be higher, the former depending on ΔH_fsublimation for 2-pyrimidinone. However, the error is probably insignificant, judging from the thermochemical data for other heterocyclic species[64].

Due to the large discrepancy between the estimated and measured value of ΔH_f° for cytosine, the estimates, based upon the identical method, and represented by following equations, cannot be used for further thermochemical calculations:

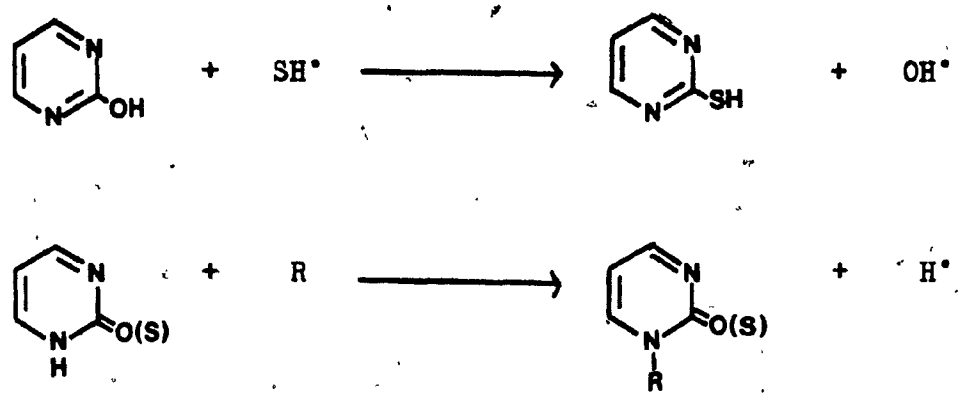

R = $^{\bullet}CH_3$ (ΔH_f = 33 kcal/mole)[67]

$^{\bullet}CH_2CH_3$ (ΔH_f = 29 kcal/mole)[67]

	ΔH_f, estimated, kcal/mole
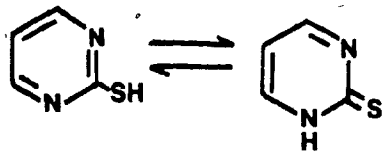	95
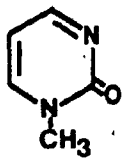	50
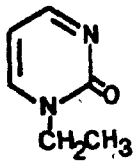	46
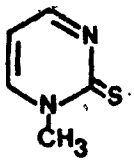	97
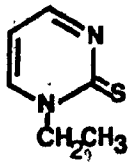	93

IE and AE measurements.

The procedure used in our laboratory for the measurement of IE and AE is described in the experimental section(p.61). Table V-4 shows the results together with the differences between the individual AE's and IE's. The values are an average of two measurements with accuracy ± 0.5eV. Xenon was the reference gas and the semi-log plot was used for interpretation of the results.

Table V-5 shows the AE and IE values of the same compounds measured by KRATOS-AEI MS-902S at the University of Ottawa.These values are also averages of two measurements with accuracy ±0.05eV.The method of initial onset ionization current was used for interpretation of the results. However, these values are relative, since no standard was used as a reference.

The literature data[65] for IE's of 2(1H)-pyrimidinone and 1-methyl-2-pyrimidinone are given in Table V-6. The values are the average of three determinations, the deviation being ±0.05eV. The ionization efficiency curves were recorded with AEI-902 mass spectrometer and interpreted by the semi-log plot. Xenon was the reference gas.

Considering the literature IE's as the most reliable values, the MS 902S results are probably more convincing than ours. This is also apparent from the IE's obtained in our laboratory for the sulfur compounds. Such low IE's in the range of 5-6 eV are reported rarely and

usually only for radicals e.g. $SH^{\bullet}$ [67].

From the combined results it can be concluded roughly that, AE-IE for $S_{compounds}$ < AE-IE for $O_{compounds}$, for R = H, and, AE-IE for $S_{compounds}$ ≈ AE-IE for $O_{compounds}$, for R = CH_3 and C_2H_5.

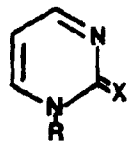

IE and AE Values for 1-R-2- Pyrimidinone and Pyrimidinthione Molecular Ions and M-1 Ions, measured on Hitachi-RMU 7:

X	R	IE(eV)	AE(eV)	AE-IE(eV)
O	H	8.8	12.8	4.0
O	CH_3	8.4	12.7	4.3
O	CH_2CH_3	8.6	11.5	2.9
S	H	8.4	11.3	2.9
S	CH_3	7.9	10.9	3.0
S	CH_2CH_3	5.9	9.9	4.0
S	CH_2CD_3	6.8	8.8	2.0
S	CD_3CH_2	5.9	8.3	2.4

Table V-4

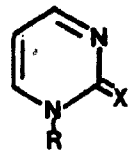

IE and AE Values for 1-R-2- Pyrimidinone and Pyrimidinthione Molecular Ions and M-1 Ions, measured on Kratos-AEI MS-902S:

X	R	IE(eV)	AE(eV)	AE-IE(eV)
O	H	9.9	12.9	3.0
O	CH_3	9.6	11.4	1.8
O	CH_2CH_3	7.8	10.3	2.5
S	H	9.1	11.2	2.1
S	CH_3	8.6	11.1	2.5
S	CH_2CH_3	9.2	11.1	1.9
S	CH_2CD_3	8.8	9.7	0.9
S	CD_2CH_3	8.6	9.8	1.2

Table V-5

Literature Data[65] for IE Values of 1-R-2-Pyrimidinone Molecular Ions:

X	R	IE(eV)
O	H	10.06
O	CH_3	9.31

Table V-6

Determination of IE and AE by electron impact technique with accuracy suitable for thermochemical consideration is in general a difficult task. The difficulties associated with the measurements and with the interpretation of the results are discussed in the theory section(p.36). Another source of error arises when solid samples are measured, because of an uneven rate of evaporation of the sample in the source.

$\Delta H_f M^{\cdot+}$ and $\Delta H_f (M-1)^+$ reported in the literature[67] are obtained mainly by photoionization or photoelectron methods. However, in some cases, different values from different laboratories for the same compound are reported even if the same technique of ionization is employed. Thus, for example, for N,N-dimethylaniline five different values for IE's are indicated[67], which fluctuate between 7.14-9.8 eV when a photoionization method was used.

Finally it should be emphasized that the heats of formation of ions presented in the literature[67] do not represent equilibrium thermochemical properties. They are the results of measurements on isolated molecules, and were arrived at by employing known heats of formation of neutral species in conventional thermochemical equations using the measured appearance energy as the heat of reaction(cf.p.144). Furthermore, the temperature at which the measurements were made is not usually known. Fortunately, the temperature effect is not large, and

accordingly all the reported ionization and appearance energies were treated as heats of reaction at 298°K.

In order to obtain reliable heats of formation of ions, search for improved techniques is constantly in progress. Today, probably, the photoionization technique and the electron impact ionization with an electrostatic monochromator and a quadrupole mass spectrometer are the most satisfactory methods.

Conclusion drawn from above.

The major problems associated with the determination of heats of formation of the M-1 ions arise because their corresponding neutral molecules are all heterocyclic solid compounds containing nitrogen and further, some contain sulfur.

From the experimental results and studied literature it implies that ΔH_f° of the neutral oxygen compounds can be determined using a static bomb calorimeter. To determine ΔH_f° of the neutral sulfur compounds the rotating bomb calorimeter method is required with a platinum lined bomb. Since the estimation methods proved to be unreliable, it is not sufficient to determine ΔH_f° for the unsubstituted pyrimidinone and pyrimidinthione, but ΔH_f° for all N-substituted pyrimidinones and pyrimidinthiones has to be measured separately, each five times with a reasonable accuracy. If necessary, the heat of sublimation can be obtained from the slope of a plot of the

vapor pressure vs. $1/T$ for each solid sample[70].

The RMU-7 mass spectrometer can be employed for IE and AE measurements only after reproducible results with adequate accuracy are obtained on a solid compound of the accurately known IE value.

Since an enormous amount of work is involved in such measurements, and further since the appropriate calorimeter for the determination of $\Delta H_f^o n$ of the sulfur compounds is not available, we cannot evaluate the heats of formation of the M-1 ions at this stage.

However, we believe that it will be an interesting topic for another research project.

(iv) Kinetic energy distribution.

In many cases isomeric daughter ions arising from the fragmentation of identical precursor ions by competitive fragmentation pathways are responsible for different energy releases which cause differences in metastable peak widths and thus could give rise to composite metastable peaks[12a,58].

The profiles of metastable peaks observed in the FFFR of a mass spectrometer consist of range of kinetic energies, T. Holmes and Osborne[61] developed a method of obtaining the T-distribution, n(T), directly from the observed metastable peaks. The n(T) can be used to identify composite metastable peaks(i.e. to identify the presence of two components) and to evaluate the average value of the re-

leased kinetic energy, $T_{(av)}$. As the authors point out,

(a) the most easily measured parameter for the kinetic energy, $T_{(0.5)}$, corresponding to the width of the peak at half-height, is not necessarily characteristic of a given process;

(b) the relationship $T_{(0.5)} : T_{(av)} = 1 : 2.16$ can be used to estimate $T_{(av)}$ from $T_{(0.5)}$ only for metastable peaks of exactly Gaussian shape.

The outlined method[61] was tried in the present study in an attempt to identify the presence of the two components in the metastable peak arising in the FFFR due to the loss of H° from the molecular ion of 1-ethyl-2-pyrimidinthione.

A least squares, non-linear parameter estimation routine[75] was used to fit the measured peak profiles to the 5-parameter equation derived by Holmes and Osborne[61]. The equation was then used to generate the analytical function for the T-distribution, n(T), and to evaluate $T_{(av)}$, as described by the authors. All metastable processes involved in the loss of H°(D°) from the molecular ions of the variously labelled 1-ethyl-2-pyrimidinthione were analyzed.

However, standard errors of the produced parameters exceeded in some cases 25%. The large errors were caused by attempting to fit a 5-parameter equation to the steep sides of the experimental peaks.

Because of the large inaccuracy we did not have any confidence in the obtained results.

VI - SUMMARY

The fragmentation patterns showed that for both series of compounds(X = O or S), loss of CX and HCN from the molecular ion or M-1 ion occurs to some extent. Intensities of the resulting daughter ions depend mainly on the N-substituents.

Thus, for the 1(H)- 2-pyrimidinone and 2-pyrimidin--thione the loss of CX and HCN belongs to the main fragmentation pathways, while the different N-substituents alter the fragmentation patterns by giving rise to new ions of high stability, which result in a suppression of the two above mentioned fragmentation routes. With increasing size of the N-alkyl substituent more fragments appear in the spectra, while the reverse holds for the N-phenyl substituent, where delocalization contributes to the stability of the molecular ion, and the relatively stable M-1 ions preclude certain fragmentations.

The difference between the two series of compounds is that loss of S and SH$^{\bullet}$ from the 2-thiones is quite evident, while loss of O or OH$^{\bullet}$ from the oxygen analogues is not apparent.However, the main fragmentations of 1(H)-2-pyrimidinselenone are loss of Se and SeH$^{\bullet}$. These observations are in accord with the increasing size of the three heteroatoms (O<S<Se) and the decreasing strength of the carbonyl, thiocarbonyl and selenocarbonyl bonds, respectively.

Studies based upon deuterium labelling and metastable transitions in the FFFR showed that the molecular ions of both series of compounds lose a hydrogen atom partly from the pyrimidine ring and partly from the N-substituents.

In the case of pyrimidine ring it is the 4 or 6 position that is involved in the loss of H$^{\bullet}$ and proceeds probably by simple bond cleavage mechanism if the N-substituents are methyl or ethyl. In the case of a larger N-substituent the loss of pyrimidine H$^{\bullet}$ could be associated with a rearrangement.

The intensities of those M-1 ions that originate by expulsion of H$^{\bullet}$ from an N-substituent depend upon the heteroatom(S or O) and on the character of the substituent.

Considerable attention has been given to the M-1 ion of 1-ethyl-2-pyrimidinthione. The metastable transition studies for loss of H$^{\bullet}$ and D$^{\bullet}$ from the four differently labelled molecular ions showed that the hydrogen atom is expelled from three sites, namely from the pyrimidine ring, the methylene group and the methyl group. Cleavage of the methylene hydrogen probably proceeds by a simple bond rupture, while the loss of methyl hydrogen atom is accompanied by a rearrangement.

This unexpected observation plus the problems associated with determination of the ΔH_fn for heterocyclic compounds containing nitrogen and sulfur, did not allow us to obtain more information about the postulated thiazolium

ring structure which could result when a methyl hydrogen atom is expelled from 1-ethyl-2-pyrimidinthione.

However, the approach to this difficult task, based upon the experimental measurements and the literature study has been outlined which, we hope, will lead to future research projects in the field of mass spectrometry and thermochemistry.

The latter might be of interest especially for physical chemists, since relatively little research work has been associated with thermochemistry of heterocyclic nitrogen compounds containing sulfur.

APPENDIX I

2-Pyrimidinone.(V-1a)

m/z	Rel. Int.	% Σ_{30}
96	100.0	13.88
95	31.8	4.42
69	27.3	3.79
68	93.2	12.93
67	18.2	2.52
54	5.1	0.70
53	23.9	3.31
52	43.2	5.99
51	20.5	2.84
44	23.9	3.31
43	10.5	1.45
42	75.0	10.41
41	72.7	10.09
40	70.5	9.78

1-d_1-2-Pyrimidinone (V-1c)

m/z	Rel. Int.	$\%\Sigma_{30}$
97	99.1	9.18
96	76.1	7.06
95	12.4	1.15
70	25.2	2.34
69	100.0	9.27
68	79.4	7.36
67	13.8	1.28
54	12.4	1.15
53	37.6	3.49
52	56.0	5.19
51	39.4	3.66
45	25.7	2.38
44	19.3	1.79
43	56.9	5.27
42	78.0	7.23
41	71.6	6.63
40	71.6	6.63

5-Deuterio-2-pyrimidinone (V-1d)

m/z	Rel. Int.	$\%\Sigma_{30}$
97	100.0	14.37
96	46.2	6.64
95	7.5	1.08
70	23.6	3.39
69	94.3	13.56
68	37.7	5.42
67	6.6	0.95
54	10.4	1.49
53	28.3	4.07
52	18.9	2.71
51	20.8	2.98
44	15.1	2.17
43	43.9	6.31
42	64.2	9.22
41	54.2	7.80
40	28.3	4.07

1-Methyl-2-pyrimidinone (V-2a)

m/z	Rel. Int.	$\%\Sigma_{30}$
110	100.0	17.55
109	79.3	13.91
83	6.2	1.09
82	58.7	10.31
81	29.4	5.15
80	4.5	0.79
69	7.1	1.24
68	16.0	2.80
67	6.0	1.06
55	18.7	3.29
54	22.5	3.94
53	8.6	1.52
52	17.4	3.05
42	64.3	11.29

1-(Methyl-d_3)-2-pyrimidinone (V-2b)

m/z	Rel. Int.	$\%\Sigma_{30}$
113	100.0	14.62
112	86.6	12.66
111	2.8	0.41
85	71.1	10.40
84	20.8	3.04
83	19.7	2.88
71	9.9	1.44
69	12.7	1.85
68	7.0	1.03
58	23.2	3.40
57	12.3	1.80
56	13.0	1.90
45	77.5	11.32

5-Deuterio-1-methyl-2-pyrimidinone (V-2c)

m/z	Rel. Int:	$\%\Sigma_{30}$
111	100.0	15.93
110	84.9	13.52
109	12.2	1.94
83	67.3	10.72
82	45.1	7.18
81	9.3	1.48
69	17.6	2.80
68	7.8	1.24
67	8.5	1.35
56	17.1	2.72
55	16.1	2.56
54	13.7	2.18
53	15.1	2.41
42	74.1	11.81

1-Ethyl-2-pyrimidinone (V-3a)

m/z	Rel. Int.	$\%\Sigma_{30}$
124	100.0	12.36
123	12.0	1.49
109	55.0	6.80
97	11.1	1.38
96	60.3	7.45
95	42.7	5.27
82	48.4	5.98
81	36.5	4.51
80	11.0	1.36
79	5.1	0.63
69	24.0	2.96
68	75.2	9.30
67	12.0	1.49
66	10.9	1.34
56	27.3	3.37
55	10.3	1.27
54	41.3	5.11
53	17.0	2.10
52	27.3	3.37
42	27.1	3.34
41	32.6	4.02
49	41.3	5.11

1-(Ethyl-d_5)-2-pyrimidinone (V-3b)

m/z	Rel. Int.	$\%\Sigma_{30}$
129	100.0	9.43
128	8.0	0.75
127	4.0	0.38
111	80.0	7.54
101	4.0	0.38
97	60.0	5.66
96	46.7	4.40
87	8.0	0.75
84	40.0	3.77
83	53.3	5.03
82	2.0	0.19
69	86.7	8.17
68	12.7	1.19
67	9.3	0.88
58	10.7	1.01
57	14.0	1.32
56	23.3	2.20
55	22.0	2.07
54	12.0	1.13
53	17.3	1.63
52	22.0	2.07
40	46.7	4.40

1-Isopropyl-2-pyrimidinone (V-4a)

m/z	Rel. Int.	$\%\Sigma_{30}$
138	93.4	14.83
137	8.7	1.39
123	41.3	6.55
97	100.0	15.87
96	24.6	3.90
95	28.4	4.51
82	12.8	2.04
80	8.7	1.39
68	44.3	7.03
54	14.8	2.34
43	37.7	5.98

1-(Isopropyl-2-d_1)-2-pyrimidinone (V-4b)

m/z	Rel. Int.	$\%\Sigma_{30}$
139	56.3	5.32
138	8.8	0.83
124	40.3	3.81
98	34.6	3.27
97	100.0	9.46
96	40.9	3.87
95	22.3	2.11
83	20.1	1.90
81	26.1	2.47
69	18.9	1.78
68	72.6	6.87
44	92.5	8.74
42	88.7	8.39

1-(Isopropyl-1,1,1,3,3,3-d_6)-2-pyrimidinone
(V-4c)

m/z	Rel. Int.	$\%\Sigma_{30}$
144	100.0	11.59
143	5.7	0.66
142	5.7	0.66
126	64.2	7.44
99	84.1	9.74
98	55.7	6.45
97	29.5	3.42
96	21.0	2.44
82	23.9	2.76
80	11.4	1.32
69	33.5	3.88
49	38.6	4.48
45	39.2	4.54

1- Benzyl-2-pyrimidinone (V-5a)

m/z	Rel. Int.	$\%\Sigma_{30}$
188	100.0	25.3
185	18.8	4.7
157	14.0	3.5
144	12.5	2.9
130	6.5	1.6
92	10.3	2.6
91	87.9	22.2
81	16.1	4.1
80	10.1	2.5
77	3.7	0.9
65	17.2	4.3
64	1.7	0.4
39	5.7	1.4

1-Benzyl-$\alpha,\alpha-d_2$-2-pyrimidinone (V-5b)

m/z	Rel. Int.	$\%\Sigma_{30}$
188	48.3	10.9
187	11.0	2.7
186	11.0	2.7
159	3.4	0.8
158	3.4	0.8
146	6.8	1.7
132	5.9	1.5
131	4.2	1.1
94	13.5	3.4
93	100.0	24.8
92	7.6	1.9
91	22.0	5.6
83	12.7	3.1
82	10.2	2.5
81	12.7	3.1
80	63.0	15.6
77	4.2	1.0
68	9.3	2.3
67	10.2	2.5
66	5.1	1.2
65	25.4	6.3

1-Phenyl-2-pyrimidinone (V-6a)

m/z	Rel. Int.	$\%\Sigma_{30}$
172	100.0	19.40
171	41.7	9.10
144	31.7	6.14
143	7.3	1.42
130	6.0	1.16
117	13.3	2.59
104	13.3	2.59
90	3.8	0.74
78	8.3	1.62
77	83.3	16.17
51	38.3	7.44

1-(Phenyl-2,4,6-d_3)-2-pyrimidinone (V-6b)

m/z	Rel. Int.	$\%\Sigma_{30}$
175	100.0	17.44
174	58.5	10.20
173	19.5	3.40
147	32.3	5.64
146	13.6	2.37
133	4.6	0.81
132	1.5	0.27
120	9.5	1.65
119	5.6	0.98
107	7.7	1.34
106	5.4	0.94
80	47.9	8.36
79	18.5	3.22
53	14.9	2.59
52	14.4	2.50

2-Pyrimidinthione (V-7a)

m/z	Rel. Int.	$\%\Sigma_{30}$
112	100.0	20.93
111	13.5	2.15
85	17.2	3.48
84	10.0	1.99
79	7.8	1.45
68	33.3	6.81
59	38.9	7.97
58	23.3	4.98
53	30.6	6.31
52	30.0	6.40
32	28.3	5.81

5-Deuterio-2-pyrimidinthione (V-7b)

m/z	Rel. Int.	$\%\Sigma_{30}$
113	100.0	13.54
112	35.2	4.76
111	5.6	0.75
86	14.8	2.01
85	13.0	1.76
80	8.9	1.20
69	35.6	4.81
60	13.0	1.76
59	34.8	4.71
54	23.3	3.16
53	32.2	4.36
32	54.4	7.37

1-Methyl-2-pyrimidinthione (V-8a)

m/z	Rel. Int.	$\%\Sigma_{30}$
126	100.0	23.58
125	22.2	5.24
110	2.2	0.52
98	5.6	1.31
93	2.5	0.59
80	10.8	2.55
68	22.2	5.24
66	16.1	3.80
42	30.6	7.21
32	30.6	7.21

5-Deuterio-1-methyl-2-pyrimidinthione (V-8b)

m/z	Rel. Int.	$\%\Sigma_{30}$
127	100.0	25.47
126	38.6	9.84
125	3.4	0.87
99	5.7	1.45
94	2.3	0.58
81	11.4	2.89
69	22.7	5.79
68	10.8	2.75
67	10.8	2.75
42	24.4	6.22

1-(Methyl-d_3)-2-pyrimidinthione (V-8c)

m/z	Rel. Int.	$\%\Sigma_{30}$
129	100.0	31.54
128	13.4	4.23
127	9.8	3.08
99	3.7	1.15
98	4.3	1.35
95	3.7	1.15
94	4.3	1.35
81	9.8	3.08
71	23.2	7.31
70	6.1	1.92
69	9.1	2.88
45	20.1	6.35

1-Ethyl-2-pyrimidinthione (V-9a)

m/z	Rel. Int.	$\%\Sigma_{30}$
140	100.0	10.61
139	19.4	2.06
125	13.3	1.42
112	77.8	8.25
111	24.4	2.59
107	32.2	3.42
98	18.3	1.95
85	18.3	1.95
84	12.8	1.36
82	40.0	4.25
81	18.9	2.00
80	40.0	4.25
79	15.6	1.65
68	36.7	3.89
53	32.2	3.42
42	23.3	2.48

1-(Ethyl-d_5)-2-pyrimidinthione (V-9b)

m/z	Rel. Int.	%Σ_{30}
145	100.0	18.55
144	7.1	1.32
143	11.0	2.04
127	8.7	1.62
113	44.7	8.28
112	12.6	2.34
111	14.2	2.64
100	4.5	0.84
87	17.5	3.24
83	12.0	2.22
69	17.2	3.18

1-(Ethyl-2-d_3)-2-pyrimidinthione (V-9c)

m/z	Rel. Int.	$\%\Sigma_{30}$
143	100.0	14.97
142	8.0	1.20
141	8.0	1.20
125	10.0	1.50
113	40.8	6.11
112	12.8	1.92
109	10.4	1.56
85	33.6	5.03
82	14.4	2.16
81	12.4	1.86
80	14.4	2.16
69	20.8	3.11

1-(Ethyl-1-d_2)-2-pyrimidinthione (V-9d)

m/z	Rel. Int.	$\%\Sigma_{30}$
142	100.0	14.07
141	19.6	2.75
140	4.3	0.61
127	8.7	1.22
113	14.1	1.99
112	56.5	7.95
111	15.2	2.14
109	17.4	2.45
84	39.1	5.50
68	21.7	3.06
53	19.6	2.75

1-Phenyl-2-pyrimidinthione (V-10a)

m/z	Rel. Int.	$\%\Sigma_{30}$
188	55.3	13.82
187	100.0	24.99
77	36.3	9.06
51	21.6	5.39
39	9.8	2.45

1-(Phenyl-2,4,6-d_3)-2-pyrimidinthione (V-10b)

m/z	Rel. Int.	$\%\Sigma_{30}$
191	47.9	7.4
190	39.8	6.8
189	100.0	17.1
188	23.0	3.9
80	42.7	7.3
79	21.7	3.7
53	27.9	4.8
52	27.1	4.6
40	16.2	2.8
39	15.8	2.7

2-Pyrimidinselenone (V-11a)

m/z	Rel. Int.	$\%\Sigma_{30}$
160	100.0	14.89
159	10.0	1.49
158	52.8	7.86
157	22.2	3.31
156	20.0	2.98
133	10.0	1.49
132	7.2	1.08
131	6.7	0.99
130	5.6	0.83
129	6.1	0.91
107	14.4	2.15
106	13.3	1.99
105	10.0	1.49
104	8.9	1.32
80	58.3	8.68
79	58.3	8.68
68	18.3	2.73
53	42.2	6.29
52	36.7	5.46

BIBLIOGRAPHY

1. A. Albert, Heterocyclic Chemistry, 2nd edition, The Athlone Press(1968).

2. a/ D. J. Brown, The Pyrimidines, Vol. 16 of Chemistry of Heterocyclic Compounds, (A. Weisberger ed.), Interscience, N. Y.(1962).

   b/ D. J. Brown, The Pyrimidines, Supplement I, (as above), (1970).

   c/ Chemical Abstracts, 9th Collective Index (1972-76), Index of Ring Systems Formulas.

3. K. Bieman and J. A. McCloskey, J. Am. Chem. Soc., 84, 2005(1962).

4. J. M. Rice, G. O. Dudek and M. Barber, J. Am. Chem. Soc., 87, 4569(1965).

5. T. Kato and H. Yamanaka, Org. Mass Spectrometry, 9, 981(1974).

6. T. Nishiwaki, Tetrahedron, 23, 1153(1967).

7. K. Bieman, Mass Spectrometry, McGraw-Hill, N. Y.(1962).

8. T. Nishiwaki, Tetrahedron, 22, 3117(1966).

9. K. Undheim and G. Hvistendhal, Org. Mass Spectrometry, 5, 325(1971).

10. E. Wyrzykiewicz, M. Stobiecki and K. Golankiewicz, Org. Mass Spectrometry, 14, 405(1979).

11. E. M. Kazdan, M. Sc. Thesis(1976).

12. a/ R. G. Cooks, J. H. Beynon, R. M. Caprioli and G. R. Lester, Metastable Ions, Elsevier Scientific Publishing Company, N. Y.(1973).

    b/ R. G. Cooks in Organic Structural Analysis, (A. Streitwieser ed.), MacMillan Publishing Company, Inc., N. Y.(1976).

c/ E. F. Brittain, W. O. George and C. H. Wells, Introduction to Molecular Spectroscopy, Academic Press, London and New York(1970).

d/ F. W. McLafferty, Interpretation of Mass Spectra, 2nd ed., W. A. Benjamin, Inc.(1973).

13. J. A. Hipple,and E. V. Condon, Phys. Rev., 68, 54(1945).

14. Ref. 12b, p. 408.

15. Ref. 12d, p. 208.

16. T.W. Shannon and F.W. McLafferty, J. Am. Chem. Soc., 88, 5021(1966).

17. J. H. Beynon, R. M. Caprioli and T. Ast, Org. Mass Spectrometry, 5, 229(1971).

18. E. G. Jones, L. E. Bauman, J. H. Beynon and R. G. Cooks, Org. Mass Spectrometry, 7, 185(1973).

19. J. H. Beynon, M. Bertrand and R. G. Cooks, ibid., 7, 785(1973).

20. R. G. Cooks, J. H. Beynon and M. Bertrand, ibid., 7, 1303(1973).

21. a/ ibid., 7, 193(1973).
b/ ibid., Int. J. Mass Spectrom. Ion Phys., 9, 346(1972).

22. O. S. Tee and E. M. Kazdan, unpublished results.

23. D. G. Lister, J. K. Tyler, J. H. Hog and N. W. Larsen, J. Mol. Structure, 23, 255(1974).

24. R. L. Frank and P. V. Smith, Org. Synthesis, Collective Volume 3, 735, J. Wiley and Sons, Inc., N. Y.(1955).

25. R. F. Nystrom, J. Am. Chem. Soc., 69, 2548(1947).

26. W. R. Kirner and W. Windus, Org. Synthesis, Collective Volume 2, 136(1943).

27. G. C. Hopkins, J. P. Jonak, H. Tieckelmann and H. J. Minnemeyer, J. Org. Chem., 31, 3969(1966).

28. M. L. Moore and F. S. Crosley, Org. Synthesis, Collective Volume 3, 599, J. Wiley and Sons, Inc., N. Y.(1955).

29. T. L. Davis and K. C. Blanchard, J. Am. Chem. Soc., 51, 1795(1951).

30. F. D. Popp and H. P. Schulz, Organic Chemical Preparations, W. B. Saunders, Philadelphia(1964).

31. A. I. Vogel, Practical Organic Chemistry, 3rd edition, Longmans(1958).

32. A. H. Sommers, J. Am. Chem. Soc., 73, 5749(1957).

33. Personnal communication with Dr. T. Adley., Chemistry department, Concordia University.

34. a/ Instruction for Hitachi model ME-1010C double focus attachment, Hitachi Ltd., Tokyo, Japan.
b/ Instruction manuel for model MD-3050 ion detector system, Hitachi Ltd., Tokyo, Japan.

35. Variable Leak, Granville-Phillips Company, Colorado.

36. R. W. Kiser, R. E. Sullivan and M. S. Lupin, Analytical Chemistry, 41, 1958(1969).

37. K. R. Jennings, J. Chem. Phys., 43, 4176(1965).

38. T. K. Davies, D. L. McGillivray and T. W. Wiley, Int. J. Mass Spectrom. Ion Phys., 15, 350(1974).

39. Ref. 12b, p. 471.

40. F. P. Lossing, A. W. Tickner and W. A. Bryce, J. Chem. Phys., 19, 1254(1951).

41. D. J. Brown and R. V. Foster, J. Chem. Soc., 4911(1965).

42. J. J. Fox and D. Van Praag, J. Am. Chem. Soc.,486(1960).

43. J. F. McOmie, J. Chem. Soc., 3716(1952).

44. Ref. 2a, p. 371.

45. Ref. 2b, p. 294.

46. A. Albert and G.B. Barlin, J. Chem. Soc., 3129(1962).

47. D. G. Crosby, R. V. Berthold and H. E. Johnson, Org. Synthesis, Coll. Vol. V, 703(1973).

48. A. R. Katritzky, M. Kingsland and O.S. Tee, J. Chem. Soc. B, 1484(1968).

49. T. V. Protopova and A.P. Skoldinov, Zhur. Obschei. Khim., 57, 27(1957).

50. P. Beak, F. S. Fry,Jr., J. Lee and F. Steele, J. Am. Chem. Soc., 98, (1), 171(1976).

51. A. R. Katritzky and J. M. Lagowski, Adv. Het. Chem., 1, 339(1963).

52. J. Van Thuijl, K. J. Klebe and J. J. Van Houte, Org. Mass Spectrometry, 7, 1165(1973).

53. J. H. Beynon, Mass Spectrometry and its Application to Organic Chemistry, p. 78, Elsevier, Amsterdam(1960).

54. H. Budzikiewicz, C. Djerassi and D.H. Williams, Interpretation of Mass Spectra of Organic Compounds, Holden-Day, Inc., San Francisco(1964), p.p. 240,163.

55. R. Lawrence and E. S. Waight, J. Chem. Soc., B, 1(1968).

56. M. C. Hamming and N. G. Foster, Interpretation of Mass Spectra of Organic Compounds, Acad. Press, N. Y.(1972).

57. L. A. Paquette, Principles of Modern Heterocyclic Chemistry, W. A. Benjamin, Inc., N. Y.(1968).

58. J. L. Holmes, R. T. B. Rye and D. Yuan, Org. Mass Spectrometry, 12, 254(1977).

59. K. Undheim and G. Hvistendhal, Org. Mass Spectrometry, 5, 325(1971).

60. Ref. 12d, p. 209.

61. J. L. Holmes and A. D. Osborne, Int. J. Mass Spectrom. Ion Phys., 23, 189(1977).

62. a/ F.P. Lossing, J. Am. Chem. Soc., 99, 7526(1977).

62. J. L. Franklin in G. A. Olah and P. von R. Schleyer, Carbonium Ions, Vol. 1., Interscience, N. Y.(1968), p. 77.

63. A. G. Harrison in A. L. Burlingame, Topics in Organic Mass Spectrometry, Wiley-Interscience, N. Y.(1970).

64. E. S. Domalski, J. Phys. Chem. Ref. Data, Vol. 1(2), 222(1972).

65. S. R. Wilson, I. D. Watson and G. N. Macolm, J. Chem. Thermodynamics, 11, 911(1979).

66. ICSU-CO data Task Group, Report on Key Values for Thermodynamics, J. Chem. Thermodynamics, 8, 603(1976).

67. U. S. National Bureau of Standards, NSRD Series 26(1969).

68. Selected Values of Chemical Thermodynamic Properties, U. S. National Bureau of Standards(1961).

69. F. D. Rossini, Experimental Thermochemistry, Interscience Publishers, Inc., N. Y.(1956).

70. F. Daniels, J. W. Williams et al., Experimental Physical Chemistry, 6th edition, McGraw-Hill, N. Y.(1962).

71. H. M. Huffman and E. L. Ellis, J. Am. Chem. Soc., 57, 46(1935).

72. R. C. Reid, J. M. Prausnitz and T. K. Sherwood, The Properties of Gases and Liquids, McGraw-Hill, N. Y. (1977).

73. S. W. Benson et al., Chem. Reviews, 69, 279(1969).

74. G. E. Moore in ref. 69, p. 173.

75. D.W. Marquardt, J. Soc. Indust. and Applied Math., 11, 431(1963).

76. D. J. Brown and T. C. Lee, Aust. J. Chem., 21, 243 (1968).

77. The Merck Index, 8th edition, Merck & Co. Inc., N.J., U.S.A.,1968.